UNIVERSITY OF CALIFORNIA,

IRVINE

Carefully Constructing Circuits in the Developing CNS: How DSCAM Intricately Modulates Visual Circuit Assembly *In Vivo*

DISSERTATION

submitted in partial satisfaction of the requirements
for the degree of

DOCTOR OF PHILOSOPHY

in Biological Sciences

by

Rommel Andrew Santos

Dissertation Committee:
Professor Susana Cohen-Cory, Chair
Professor Karina Cramer
Professor Kim Green

2020

Dedication

This dissertation is dedicated to my mom, dad, and brother,
who have always told me ‘kaya mo yan’ a Tagalog expression which translates to –
‘you can do it.’

Table of Contents

List of Figures

Acknowledgements

I am grateful for the scientific advising and personal mentorship Susana Cohen-Cory has provided me throughout my academic career. Susana has been the catalyst for launching my research career and firmly believing in me, especially when I was applying for graduate schools. I am very fortunate for her unwavering support and for the many letters of recommendation she has written for undergraduate and graduate awards. When I think about the times working with Susana as an undergrad, which I cherish the most, she not only worked alongside me to teach me molecular techniques and wet bench work, but she also demonstrated, through example, how making a scientific discovery can be exhilarating. As undergraduate at the time, I am very lucky to have had that intellectual freedom and creativity to explore many new techniques in the lab – which still, currently to this day, has constantly been a motivating factor and drive for me to go to lab and see my experimental results. As a graduate student, she still provided me the intellectual freedom and creativity I thrived in the lab, but carefully showed me, through many discussions, that good science has to be directed and have a meaningful purpose – which I has forever been instilled in me as budding scientist. As I approach anything science-related, I critically think about how my work, whether big or small, has genuine impact in the field.

I am thankful for a supporting team of undergraduate students who have all helped me with my projects throughout the years – Brandon Vu, Gaby Romero, Rodrigo Jr. Del Rio, Eduardo Munoz, and Alex Alvarez. I would also like to thank past members of the lab – Rosa Serrano, Ariel Fuertes, Ginger Short, Kevin C. Donohue, Hanjuan Shao, Julian Quintanilla, Parinaz Malakzadeh, Nathan Cruz, Ana Nagel, Sarah Mortero, Arseny Bechay, Marc Piercy, and Jayne Hobin.

I want to also thank current and past members of my thesis committee – Dr. Karina Cramer, Dr. Kim Green, and Dr. Sunil Gandhi. Thank you for being so accommodating and many thanks for the feedback on directing the work I have done throughout graduate school. I also want to thank Dr. Ian Parker, Dr. Marcelo Wood, and Dr. Mike Mulligan for advising me during the last years of my graduate work and being there to lend support.

Financial Support was provided by the National Eye Institute (EY-011912), the National Science Foundation (GRFP, DGE-1321846), Department of Neurobiology and Behavior, and the School of Biological Sciences.

Curriculum Vita

Rommel Andrew Santos

Education

University of California, Irvine – PhD. Biological Sciences
University of California, Irvine – BS. Neurobiology

Journal Publications

[1] Igarashi M, **Santos RA**, Cohen-Cory S. Impact of Maternal n-3 Polyunsaturated Fatty Acid Deficiency on Dendritic Arbor Morphology and Connectivity of Developing Xenopus laevis Central Neurons In Vivo. *Journal of Neuroscience*, 35; 6079-6092, (2015).

[2] Nagel AN, Marshak M, Colleen Manitt, **Santos RA**, Piercy MA, Mortero SD, Shirkey-Son NJ, Cohen-Cory S. Netrin-1 directs dendritic growth and connectivity of vertebrate central neurons in vivo. *Neural Development* 10:14, (2015). doi:10.1186/s13064-015-0041-y.

[3] Xu X, Ikrar T, Sun Y, **Santos R**, Holmes T, Walter F, Berton F. High-resolution and cell-type-specific photostimulation mapping shows weak excitatory versus strong inhibitory inputs in the bed nucleus of the stria terminalis. *J Neurophysiol. 2016;115(6):3204-16.*

[4] Lazaro MT, Taxidis J, Shuman T, Bachmutsky T, Ikrar T, **Santos R**, Marcello G, Myalavarapu A, Chandra S, Foreman A, Goli R, Tran D, Azhdam M, Goli R, Tran D, Sharma N, Azhdam M, Dong H, Choe K, Peñagarikano O, Masmanidis S, Racz B, Xu X, Geschwind D, Golshani P. Reduced Prefrontal Synaptic Connectivity and Disturbed Oscillatory Population Dynamics in the CNTNAP2 Model of Autism. *Cell Rep*. 2019;27(9):2567-2578.e6.

[5] **Santos RA**, Fuertes AJC, Short G, et al. DSCAM differentially modulates pre- and postsynaptic structural and functional central connectivity during visual system wiring. *Neural Dev*. 2018;13(1):22.

Teaching/ Pedagogy Experience

CIRTL Scholar Researcher – Pedagogical Research in Undergrad Education

- Conducted a study, where I surveyed over 182 biology students enrolled in a neurobiology lab (across two quarters). This current study is under the mentorship of Dr. Audrey Lew.
- Assessed how many hours these biology students put into outside work commitments and the amount of time spent studying for the neuro-lab course, then determine whether these variables had a significant impact on their final course grade. Data is currently being analyzed.

Think-On Summer Camp Mentor – Da Lat, Vietnam

- Mentored underrepresented students in Central Vietnam (Da Lat City), providing a liberal arts education for 20 Vietnamese high school students.
- Collaborated with a colorful cast of instructors from around the world. I was working with instructors from Nepal, the Philippines, South Korea, Malaysia, Taiwan, and Bangladesh
- Developed a neurobiology workshop at the camp; I had students build a paper microscope called the foldscope. I had brought with me mice brain samples where individual neurons were Golgi stained. Students would examine these neurons through the foldscope they built.
- Had students dissect a raw pork brain to examine anatomical brain structures.

Pueblo Science Instructor

- Worked with Pueblo Science for over three years developing educational science experiments as part of their initiative to advance STEM education across developing countries.
- Traveled with Pueblo to the Philippines, Jamaica, and Guyana (South America). In each country, we worked with over 100 to 200 science teachers to incorporate hands-on science lesson plans for their students.

Graduate Teaching Assistant (TA) – Bio 93, Neurobiology Lab N113L, N152
Department of Neurobiology and Behavior

- Taught three quarters of N113L presenting weekly lectures and running the lab experiments with 20 undergraduate students. Made exams and graded assignments (i.e. lab reports, quizzes, and midterms).
- Final Instructor Evaluation Grade by the students (Mean 3.98)
- TA for Developmental Neurobiology N152 for one quarter. I led a lecture as a journal club discussion, used active learning to engage students on how to read primary literature and critical think about results presented from the paper. Student enrollment was 130 students. Made exams and graded assignments

Undergraduate TA –
UCI Bio Sci Undergraduate Peer Tutoring Program

- Three academic quarters of holding weekly office hours; presented exam review sessions to 200+ students. Mentored by Dr. Berkelhamer, Associate Dean of Undergraduate Education UC Irvine at the time, who helped improved my teaching and presentation skills.
- Organisms to Ecosystems (Bio 94) - Went over topics in Darwinian evolution, phylogeny trees – tree of life, biodiversity in ecosystems, etc.
- Molecular Biology (Bio 99) **-** Went over topics in central dogma of molecular biology, groundbreaking experiments that pioneered the understanding of DNA and mRNA, famous molecular biologists, etc.

Research Fellowships & Awards

NSF Graduate Research Fellowships Program*
National Science Foundation (NSF GRFP)
*3 years fully funding my research stipend and graduate student tuition at UC Irvine

Edward Steinhaus Teaching Award*
UC Irvine – School of Biological Science. Dept of Neurobiology and Behavior
*Given to only one Graduate Student in the department each year

Chancellor's Award for Excellence in Undergraduate Research
UC Irvine – Undergraduate Research Opportunities Program (UROP)
*Given to only one Undergrad Student in the School of Biological Sciences each year

Excellence in Undergraduate Research Award
UC Irvine – School of Biological Science

Undergraduate Research Opportunities Program Fellowship
UC Irvine - UROP

Summer Research Undergraduate Program (SURP) Fellowship
UC Irvine – UROP

Undergraduate Student Researcher of the Month UROP - June
UC Irvine - UROP

Abstract of the Dissertation

Carefully Constructing Circuits in the Developing CNS: How DSCAM Intricately Modulates Visual Circuit Assembly *In Vivo*

By Rommel Santos

Doctor of Philosophy in Biological Sciences

University of California, Irvine, 2020

Professor Susana Cohen-Cory, Chair

The wiring of functional neural circuits during embryonic development requires coordinated organization between developing axon and dendritic arbors, a process that is dependent on an array of molecular guidance cues including neurotrophins, chemoattractants, repulsive cues, cell adhesion molecules, etc. These molecules work in concert to direct and establish precise, topographically organized synaptic connections which are all necessary for the formation of specific neuronal circuits and, ultimately, for proper brain function. For my dissertation, I explore the role of Down Syndrome Cell Adhesion Molecule (DSCAM), a multifaceted cell surface protein implicated in Down Syndrome and Autism. DSCAM is most prominently known for shaping the self-avoidance pattern of dendritic arbors in Drosophila neurons and mouse retinal cells, but how it modulates the interconnectivity between axons and dendrites of "central" visual neuronal circuits in developing vertebrates remains unclear. To examine how DSCAM mediates pre- and postsynaptic circuit development, we utilized the *Xenopus laevis* retinotectal circuit as an accessible model to study events in real time and within the in-tact animal brain *in vivo*. This model also provides us a unique

temporal and spatial understanding of how central circuits are dynamically shaped. DSCAM gene expression was altered using a targeted knockdown approach aimed at individual RGCs and tectal neurons; subsequent changes in the morphology of RGC axons and dendritic arbors of tectal neurons were observed through confocal imaging. As RGC axons innervate the tectum, retinal axons remained relatively simple when DSCAM expression was decreased. Conversely, downregulating DSCAM in tectal neurons exhibited abnormally increased dendritic growth and branching rates while also inducing dendrites to take on convoluted directional pathways. Changes in dendritic morphology of tectal neurons by DSCAM knockdown corresponded with functional deficits in visually guided behavior of freely swimming tadpoles. Together, our observations implicate DSCAM in the control of both pre- and postsynaptic structural and functional connectivity in the developing retinotectal circuit, where it primarily acts as a neuronal brake to limit and guide postsynaptic dendrite growth of tectal neurons while it also facilitates arborization of presynaptic RGC axons cell autonomously. I also observe how DSCAM coordinates the topography of retinal axons as bundles of axons project and arborize into the tectum. Additionally, I demonstrate that DSCAM plays a role in a subset of retinotectal synapse, by stabilizing their connections in the developing tadpole central nervous system. Together, my observations implicate DSCAM in the control of both pre- and postsynaptic structural and functional connectivity in the developing retinotectal circuit. These crucial developmental instructions mediated by DSCAM are necessary for normal visual system function.

Chapter 1

General Introduction

1.1. Background and Significance

Neurons differentiate from neural progenitor cells and migrate to a specific site in the nervous tissue. At this point, mature neurons begin to grow out neurites which allows cells to connect with other neurons. Multiple synaptic connections are made possible due to specialized fiber-like processes that neurons develop called axons and dendrites. Dendrites are processes protruding from the neuronal cell body. Since ribosomes, smooth and rough endoplasmic reticulum, and Golgi elements are found in the cytosol of dendrites, dendrites have been thought to be an extension of the cell body [1]. In comparison, axons are long protruding processes that can travel distances to make long-range communication possible with neurons located away from the cell body. Axons meet dendrites to form a synapse where neuronal communication between neurons can be facilitated, ultimately forming a neural circuit. Important electrochemical information is relayed between circuits to execute complicated cognitive and regulatory functions, which are essential for an animal's survival.

Neuronal circuits throughout the CNS are built with structural specificity and pattern, which influences the potential function of the circuit. Patterning of neuronal wiring in the nervous system sets up the framework for how circuits will function in the CNS. Circuit patterns are established by a diverse series of carefully guided events orchestrated during

development [1, 2]. For this dissertation, I discuss three primary events that shape neuronal circuit connectivity: (1) guiding axons to correct target sites, (2) axons and dendrites arborizing into a defined zone, and finally (3) axons forming functional synaptic connections at distinct regions on post-synaptic neurons [3]. Guiding the connections of millions of maturing neurons in the vertebrate central nervous system (CNS) is by far a remarkably complex sequence of events coordinated during development. What makes this process even more outstanding is a neurons' specialized ability to make synaptic contact with thousands of neurons locally or across the nervous tissue [4]. This astonishing feature continues in humans; by the time at birth, the human brain has a functional neuronal network made of trillions of synaptic connections.

The construction of neuronal circuits is not facilitated by a top-down control system overseeing assembly; for example, axons and dendrites do not make a direct bee line towards each other to form a synaptic connection. But what instead occurs is a constructive process mediated by multiple complex cellular and molecular interactions occurring between neurons and other cell types (i.e. glia) or its environment. The diverse range of interactions that takes place during circuit assembly, collectively results in an emerging major nerve tract. For instance, pioneering axonal growth cones navigate by exploring potential directions and physically encountering multiple target sites, until an appropriate region along the nervous tissue is found. The events underlying circuit formation raises a fundamental question – what are the mechanisms that wire structural connectivity of millions of neurons during development?

Key findings throughout the field, using a range of developmental animal models and cutting-edge imaging techniques, have revealed a key repertoire of molecular and cellular mechanisms shaping the steps in circuit assembly [5]. The molecular cues and signaling events that shape the pattern and connectivity of circuits are evolutionarily conserved throughout species. A fundamental concept found is that a single molecular cue is not limited to a specific step in circuit assembly; but instead, an individual molecular cue is multifaceted and reused at multiple steps in assembly [6]. Insight to the cellular events underlying circuit formation and how a single molecule is involved during circuit development is key to understanding the cause of numerous devasting neurodevelopmental pathologies. It is interesting to note that failure in cellular differentiation or migration, events that occur prior to circuit wiring, give rise to developmental defects at a global brain level i.e. microcephaly and lissencephaly. More subtle disorders such as autism, schizophrenia, or neuropsychiatric intellectual disabilities result from mishaps, in relatively small but crucial steps, in neural circuit wiring [7].

This dissertation explores the role of an important developmental protein called Down Syndrome Cell Adhesion Molecule (DSCAM) in wiring neuronal connectivity. Much of our understanding of DSCAM is derived from the invertebrate fruit fly model. In Drosophila, DSCAM acts as a contact-dependent adhesion molecule with over 38,000 alternatively spliced isoforms coordinating the self-avoidant patterning of neuronal dendritic and axonal arbors [8-11]. While genetic conservation appears to exist between vertebrate

DSCAM and Drosophila DSCAMs, emerging roles for vertebrate DSCAM are beginning to be uncovered. In DSCAM knockout mice, retinal ganglion cells (RGCs) have severe defects in dendritic self-avoidance phenotypes [12-14]. Studies in the chick retina have shown that DSCAM plays a role in synapse formation by promoting the targeting of RGC dendrites and bipolar cell axons to the same layer [15]. Additionally, recent evidence has demonstrated that DSCAM actively regulates circuit level plasticity by inhibiting dendritic arbor growth and receptive field size of mature retinal bipolar cells [16]. These findings suggest that DSCAM has a prominent role in wiring and maintaining the intricate arbor connections of retinal circuits in the eye. Its role, however, in orchestrating the interconnectivity between pre- and post-synaptic arbors of circuits in the brain, particularly at higher visual centers, remains largely unknown.

The developing vertebrate visual system has been a powerful model to observe basic underlying mechanisms organizing neuronal connectivity. The visual pathway is a sensory system that is made of remarkably precise connections that are tuned to respond to an array of features in the surrounding visual scene (mechanisms underlying development of visual maps and receptive fields). When photons of light enter the eye, photoreceptors transduce light stimulus into an electrochemical neural signal. This neural signal is then sent to the retina of the eye which further relays the signal to higher centers in the visual system, including the lateral geniculate nucleus, the superior colliculus (a midbrain structure homologous to the amphibian or fish optic tectum), and the primary visual cortex [17]. The mechanisms facilitating visual circuit development have largely been discovered

using the Xenopus retinotectal circuit. This model allows for a range of developmental studies to explore nearly all phases of circuit formation in vivo using the intact Xenopus tadpole brain [18-21]. For this dissertation, I use the Xenopus laevis embryo as an in vivo model to explore the underlying molecular mechanism of DSCAM in circuit assembly. Because the epidermis of the Xenopus embryo is translucent, imaging of the retinotectal circuit at the midbrain is optically accessible. Work from my dissertation involved observing the development of axons, dendrites, and synapse formation of the retinotectal circuit in real time using fluorescence confocal microscopy.

In the following sections, I will introduce fundamentals concepts outlining the development of neural circuits. I will also discuss how coordination of complex neurodevelopmental events in circuit assembly are mediated by molecular cues with an emphasis exploring the current known function of DSCAM.

1.2. Axon Pathfinding

During embryonic eye development, maturing postmitotic RGCs project axons that take on a lengthy journey to reach a suitable target in the visual system. The navigational behavior of pioneering axons is primarily led by their growth cone, a versatile structure that is motile and dynamic. Growth cones are equipped with receptors that are sensitive to the molecular cues in their environment. Pathfinding depends on the expression of receptors on the axon and growth cone surface, and the distribution of relevant cues in the environment [22] or membrane-bound cues expressed on neighboring cells. Because

guidance receptors on axons are expressed differently, either spatially along the axon or temporally expressed at a point in development, subpopulations of retinal projections make certain navigational decisions that differ from other projections. Additionally, axon guidance cues are potent signals that have differential effects depending the developmental contexts in which they act [22]. These molecular cues can act as an ‘attractive’ or ‘repulsive’ molecule that regulate the cytoskeletal dynamics within the growth cone – steering an axon to either advance or withdraw from a specific direction. These cues can act over long distances, at a local spread, or in a contact-dependent manner. Also present in the pathway are ‘modulators’ that do not directly guide growth, but instead, influence a growth cone’s response to a coincident signal by altering receptor expression on the axon surface [23]. The formation of the retinotectal circuit is dependent on the dynamic response of the RGC growth cone to a surrounding environment that is rich with a diverse set of molecular guidance cues.

The major anatomical nerve tract that emerges from pathfinding is consistently similar within a given species. For example, RGC axons of fish and amphibians will always exit the retina via the optic nerve – this nerve travels contralaterally to cross the midline at the optic chiasm and arrive at the contralateral side of the midbrain called the optic tectum. Axons continue to grow along the contralateral surface via the optic tract and terminate in the neuropil of the optic tectum. In contrast, mammalian RGC axons make the decision to travel either ipsilaterally or contralaterally at the midline point of the optic chiasm.

Despite anatomical tract differences among species, axon projections of all vertebrates are arranged in an orderly manner that creates a topographic map of the visual world.

Topography refers to the degree of spatial relation between cells and the cells their axon projects to, in other words, neighboring sets of cells in proximity project and connect to a clustered set of cells at the receiving end. For example, in the visual system, RGC axons continuously map across the tectum in a manner that mirrors the relative positioning of RGCs across the retina – effectively constructing a point-to-point representation of visual space in the brain [24-26]. Topographic organization is a shared fundamental property found in nearly all vertebrate species, this property is exemplified in other sensory systems (i.e. auditory or somatosensory) which generally preserves the topography of stimuli by forming “maps” within the central nervous system [27]. As stimulus information move towards higher processing centers in the brain, neighboring projections carrying the stimulus information remain together in proximity – creating an ordered representation of the stimulus-rich environment [28].

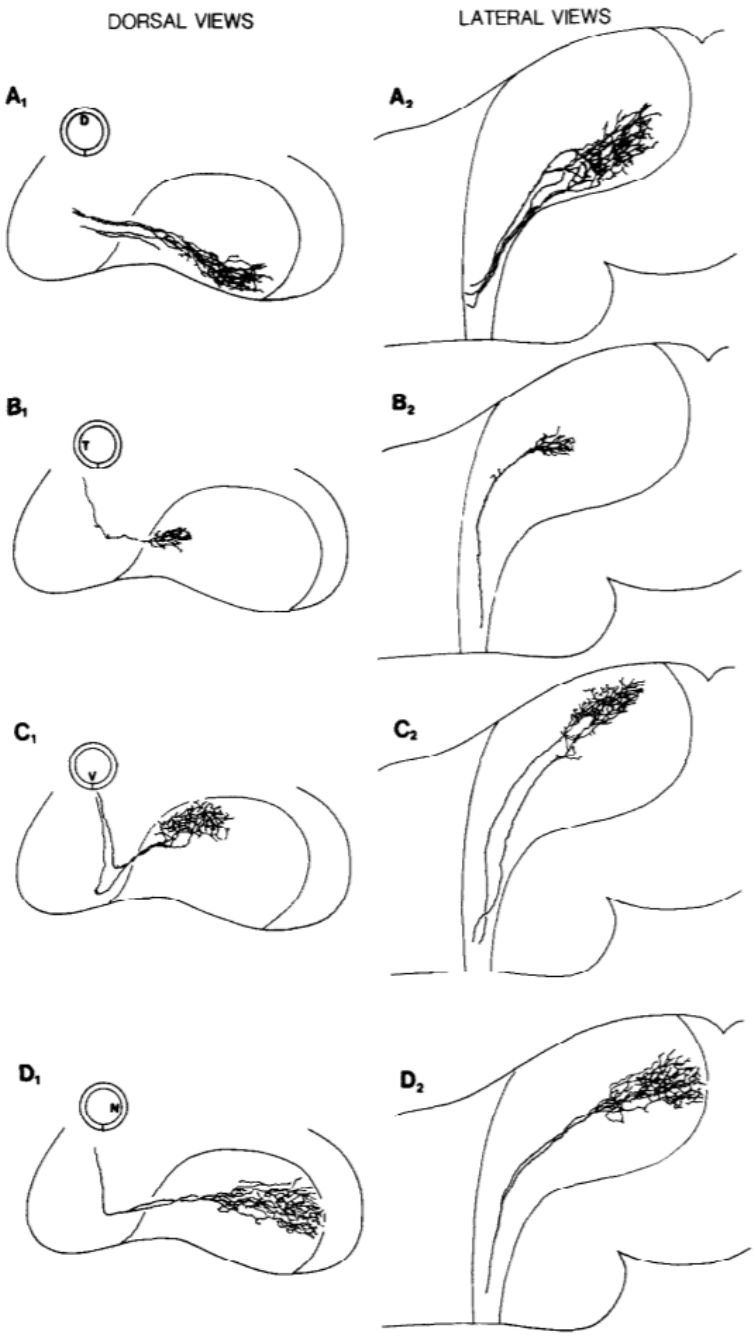

Figure 1.1. Schematic representation of retinal projection depicting topographic organization in the Xenopus tadpole as described by Sakaguchi and Murphey [27]. A to E shows the terminal arborization of individual retinal ganglion cells in the dorsal view (A1 to E1) and lateral view (A2 to E2) from whole mount brains following cobalt injections at various positions around the contralateral eye (drawn as a circle). Projections of retinal axons of the right eye of tadpoles staged at 47 to 48 are as follows:

A1 Dorsal (D) retinal axons project ventrolaterally.

B1 Temporal (T) retinal axons project rostrally (anteriorly).

C1 Ventral (V) retinal axons project dorsomedially.

D1 Nasal (T) retinal axons projected caudally (posteriorly).

1.3. Topographic Organization of the Xenopus Retinotectal Circuit

Classical work done by Dr. Sakaguchi and Murphey carefully outlined the trajectory of retinal axons as they project into optic tectum of the Xenopus tadpole [27]. As depicted in the schematic in Fig 1.1, the authors showed that the retinotectal circuit is organized topographically, where the dorsal-ventral axis of the retina maps respectively on to the ventral-dorsal axis of the tectum; the nasal-temporal axis of the retina project respectively to the caudal-rostral axis of the tecum [18, 27, 29]. During eye development, new retinal ganglion cells are generated at the ciliary margin located at the peripheral edges of the eye [29, 30]. Older cells are pushed towards the central portion of the retina and a gradient of maturing cells is created along the retina radius. Because of the temporal pattern of early eye development, the deployment of emerging RGC axons via the optic tract is set to a defined temporal sequence. Dorsal retinal fibers exit the eye first, navigate the optic pathway, and reach the tectum 6 hours ahead of ventral retinal axons. The newest axon fibers exiting the eye travel along the most ventral portion of the optic nerve as innervation takes place [29, 31]. The timing of retinotectal projections was thought to generate topographic mapping in the optic tectum, with the argument that pioneering dorsal fibers innervate ventral areas in the tectum simply for arriving first at the available sites. Ventral fibers of the retina would later follow and would be forced to occupy the next available sites at the dorsal area of the tectum, due to the constraints of existing dorsal axons [29]. Studies, however, have shown that disrupting timing of retinal axon deployment, by heterochronic transplantation of early age RGCs into older embryos, does not seem to affect the topographic mapping formed during development [29].

Studies throughout the last two decades have shown that rudimentary mechanisms involving molecular recognition of proper termination domains are at work guiding topographic organization. Such studies have shown that gradient distribution of molecular cues is important for topographic mapping. For example, topographic mapping of mice retinal axons along the anterior-posterior axis of the mouse SC (equivalent to the tectum in lower vertebrates) rely heavily on repulsive-mediated signaling between EphA receptors and their Ephrin-A ligands [32-34]. EphA receptors are expressed in a gradient in the retina, while Ephrin-A ligands are expressed in a complimentary gradient in the SC. Retinal axons with successively higher levels of EphA receptors map onto successively lower levels of Ephrin-A ligands expressed along the SC [32-34]. The relative difference between EphA receptors and Ephrin-A ligands, in part, establishes the topographic ordering of retinal axons along the SC. Mice studies have shown that disrupting the signaling gradient either by knocking out the receptor or the ligand does affect topographic ordering, but not entirely [32]. Axonal fibers, to a certain degree, shift posteriorly and others anteriorly, suggesting that graded ephrin signaling does not exclusively shape topography and additional key molecules are involved [35]. Furthermore, retinal axon fibers are already topographically sorted along the optic tract prior to reaching the tectum [36-40]. Investigating molecular cues expressed along the developing optic nerve is crucial to understanding the underlying mechanisms organizing topography.

DSCAM's role as a receptor for axon growth is evident [8-11, 41], but whether the molecule is involved in the topographic organization of retinal fibers remains unknown. Multiple studies have confirmed DSCAM expression in RGCs and retinal projections along the developing mouse optic nerve [9, 14, 42, 43]. Erskine and colleagues found that knocking out DSCAM disrupted the timing at which mouse retinal axons arrived at the thalamus, suggesting that DSCAM acts as a permissive signal and mediates growth-promoting interactions that help facilitate retinal axon growth towards their target [9]. In another relevant study, DSCAM was shown to be involved in segregating contralateral retinal projections from ipsilateral fibers in the dLGN [42]. Though these two studies did not directly test DSCAM's involvement in retinal topography, the implication of this work is that DSCAM may contribute to the specificity of axonal wiring at appropriate target sites. Additionally, histology data gathered for this dissertation showed high DSCAM expression along the ventral and posterior regions of the optic nerve (data shown in Chapter 1), indicating that a subpopulation of retinal fibers utilizes DSCAM during optic pathway development. As previously mentioned, newer axon fibers exit the eye via the most ventral portion of the optic nerve [29, 31]. Based on preliminary data and the current findings from the literature, we wanted to test whether DSCAM is a candidate for organizing topographic order of axons in retinotectal mapping.

Based on zebrafish development (which closely resembles Xenopus), dorsal fibers normally reach the optic tectum via the lateral branch, while ventral axons project via the medial branch. Disrupting mechanisms that organize topographic ordering causes dorsal

axons to aberrantly enter and project ectopically into the medial branch, where ventral fibers are located [36]. We followed a similar experimental design in the Xenopus embryo to study the effects of DSCAM knockdown on the establishment of retinotopic maps. We traced the projection of ventral and dorsal retinal fibers starting from the eye, followed the optic nerve into the chiasm, and into the Xenopus tectum. I will explain in the next following chapter how altering DSCAM levels, when arbors are mature and have arborized, does affect, to some degree, the topographic sorting of axonal arbors in the tectum.

1.4. Retinal Axon Arborization at the Tectum

Once bundles of axons innervate a specific part of the nervous tissue, tightly tethered axon bundles defasciculate and allow individual axons to respond to novel molecular cues in their new environment. Physical encounter with a specific modulator causes growth cones to change their surface receptors and prepare for the next stage of morphological trajectory – axonal arborization [44]. Presynaptic axon arbors take on many distinct forms over time due to the dynamic, active, and motile properties of individual axon branches. The branching properties of axonal arbors, observed *in vivo*, is a tightly regulated process that occurs in a stepwise sequence.

During retinotectal circuit wiring, retinal axons innervate the tectum. Interestingly, in the mouse visual system, RGC growth cones initially overshoot their respective termination zones, but this is not observed in the zebrafish larvae. During the events of axon

arborization, many transient dynamic branches are added, axons are further lengthened, and synaptic contact are made with numerous dendrites of postsynaptic tectal neurons – cells born in the tectum [45]. Synaptic connections are established at the preferred termination zone, where terminal branch arbors emerge. Overextended branches of the arbor are pruned and retracted, refining the terminal arbor to its mature form [46, 47]. It is interesting to note that the final pattern of a retinal axon arbor is much different than their initial appearance at the start of arborization. The maturation of retinal axonal arbors is mediated, largely in part, by a diverse set of molecular signals including DSCAM.

Locally secreted factors found at the axon termination site can act as a growth-promoting signaling cues to initiate and facilitate axon branching along the main retinal arbor. Brain derived neurotrophic factor (BDNF) and its high affinity receptor TrkB has been established as key signaling molecules involved in stimulating axon branch growth[48]. BDNF ligands are expressed uniformly throughout the tectum, with a sub-population of retinal axons expressing TrkB receptors. Studies from our lab have shown that injection of exogenous BDNF into the tectum increases the complexity and branching of retinal terminal arbor, while sequestering BDNF using neutralizing antibodies reduces axon arborization. Interestingly, not all RGC axons respond to BDNF growth-promoting effects due to a sub-population of axons not expressing the TrkB receptor [21], implying that additional signaling cues are also involved in directing specific axonal arborization.

While growth-promoting factors are at work, local inhibitory signaling cues are also present during axon development. Inhibition provides an important regulatory mechanism that restricts branching to a topographic-specific site. Several key studies have shown that the same ephrin and Eph signaling used for retinotopic mapping is also used to control specific arborization by restricting RGC axon branching [49-51]. However, an important note to understand is that ephrin signaling alone does not exclusively generate branching of RGC axons at a specific anatomical site. Current studies have suggested that ephrin signaling coordinates with BDNF to control retinal axon branching. Coupling of branch-promoting factors with regulatory mechanisms that restricts branching allows for precise retinotopic mapping.

Previous work from our lab has shown that netrin-1 signaling, mediated through its receptor Deleted in Colorectal Cancer (DCC), promote arborization of retinal axons in the developing Xenopus tectum [52, 53]. The effects of netrin-1 are similar to BDNF, where both ligands increase arbor complexity of retinal axon arbors. Netrin-1, in contrast, is a prominent chemoattractant that works with several receptors. Crosstalk between netrin-1 and its receptors allow for multiple roles to be performed, including axon guidance, arborization, and synapse maturation. This is generally a reoccurring theme that emerges in development where different combinations of neurotrophins, chemoattractants, and local inhibitory cues are all at work guiding the developing circuit pathway. Important crosstalk among these signaling cues orchestrate connectivity, which allows a single molecule to contribute to multiple events in circuit development.

Several emerging studies have revealed DSCAM as a novel netrin receptor mediating axon development [10, 54-57]. Previous work has shown that DSCAM, in collaboration with DCC, directs turning responses of spinal commissural axons to netrin-1 signaling [54]. These studies, performed on mice, originally identified DSCAM as an axon guidance cue but never explored DSCAM's role in the differentiation and arborization of retinal axons, events that occur after axon pathfinding. One of the key objectives for my dissertation addresses this unknown question on whether DSCAM modulates axon arborization. I will demonstrate in the chapters that follow that DSCAM acts as another relevant molecule that facilitates the maturation of retinal axon arbors in the tectum.

1.5. Dendritic Arbor Development of Post-Synaptic Tectal Cells

The maturation of RGC axons and dendritic arbors of tectal cells are two parallel events that are intimately linked during circuit assembly. The onset of dendritic arbor formation corresponds to the same timepoint tectal cells receive retinal axon input as depicted in the schematic drawn in Fig 1.2 by Zhenyu Liu and colleagues [18]. Axons of RGCs and dendritic arbors of tectal cells undergo an extensive growth period taking on additional new branches and extending dendrite length as the tadpole matures. As new branches emerge, selected dendrites are retracted and pruned [58-60]. Coordinated addition and retraction of dendrites allow gradual recognition between pre- and postsynaptic partners which, subsequently, allows synaptic connections to be formed [61, 62]. The growth rate

and branch dynamics of dendritic arbors eventually stabilizes as tectal cells reach maturity.

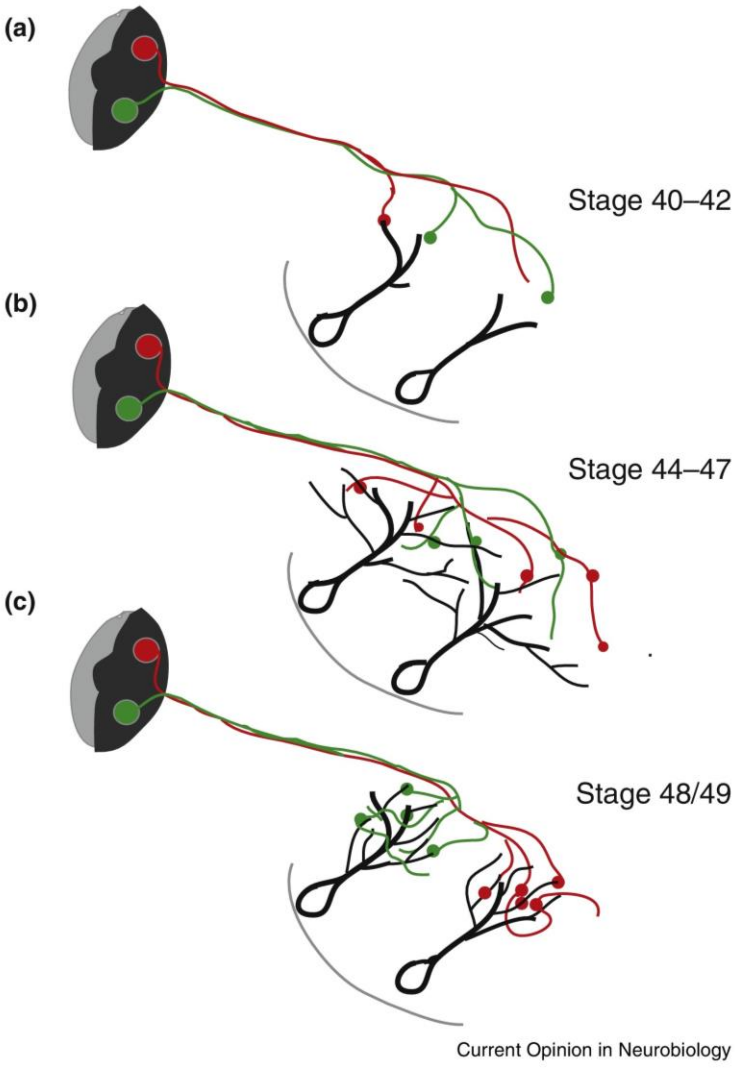

Figure 1.2. Schematic representation of the development of retinotectal circuits as described by Zhenyu Liu and colleagues [18]. (a) Stages 40–42: During this very early stage of circuit development, RGC axons have just begun forming immature synapses onto tectal cell dendrites. Morphology of both RGC axons and tectal neuron dendrites is simple, not yet complex. **(b)** Stages 44–47: The most dynamic phase of early retinotectal circuit development. This phase is characterized by high rates of synapse formation and loss as dendrites and axons extend and retract and overall grow more complex. Intrinsic excitability expressed by tectal neurons is at a high. Visual stimulation of RGC inputs is now able to drive action potential firing in most tectal neurons, thus supplying activity-dependent instruction. **(c)** Stage 48/49: As a result of activity-dependent mechanisms, the circuit has grown more stable and refined. RGC axons and tectal neuron dendrites are still complex but more focused in space. Any given tectal neuron is now receiving fewer different RGC axonal inputs, but the inputs it has kept have strengthened. Intrinsic excitability has significantly decreased.

Similar to axon development, maturing tectal cells rely on a diverse set of extracellular cues to shape the morphology of their dendritic arbors. Locally secreted cues used normally for axon arborization can elicit different effects on dendritic arbor development. This is a fundamental theme that emerges in circuit development that, for a developing neuron, signals in vivo are not one dimensional but rather multifaceted. For example, published work from our lab showed that treating RGC axons with exogenous netrin-1 significantly increased dynamic axon branching and total axon branch number [53]. The same netrin-1 treatment prunes dendritic branches of tectal neurons away from RGC axon arbors, suggesting that netrin-1 specifically influences the directionality of dendritic branch growth of tectal partners [63]. These results reveal that an individual signal can be differentially integrated to fine tune afferent and efferent circuit connectivity. Netrin-1, a versatile signaling cue, operates on several class of receptors, including DCC and uncoordinated-5 (Unc5). This allows the ligand to produce varying responses based on the receptors present on the cell surface. Additionally, its receptor DCC can act independently or as a co-receptor with Unc5. Whether a receptor acts alone or in collaboration with another receptor further adds another layer of signaling that can differentially regulate postsynaptic developing dendritic arbors from presynaptic axon development.

In contrast to diffusible ligands and their receptors that guide the directionality and growth of arborizing dendrites, additional cell surface molecules are being used as restrictive means to prevent inappropriate dendritic branching. Normally, dendritic neurites from the

same cell selectively avoid each other [64]. This common pattern called self-avoidance, emerges during dendritic arborization. Proper dendritic self-avoidance shapes a neuron's ability to receive, process, and transmit synaptic information. In addition to self-avoidance, dendritic branches from the same neuron avoid overlapping with neighboring neuronal arbors. This arrangement of arbors, known as tiling, typically occurs in a two-dimensional laminar space. Tiling minimizes branch overlap and allows arbors to efficiently innervate more territory and reduce redundant inputs [65-68]. Cell surface proteins are part of the underlying mechanism that facilitates proper tiling and self-avoidant patterning in developing dendritic arbors. These recognition molecules give cells a unique surface identity that, in turn, allows neurites of neurons to distinguish itself from other cells [64]. It is important to note that tiling occurs for Drosophila neurons and retinal neurons in the vertebrate retina, but I will discuss later how neurons, especially in the cortex of higher vertebrate animals, do not tile.

Our understanding of dendritic self-avoidance and tiling largely comes from the work done on Drosophila. The fruit fly can generate 38,016 different mRNA isoforms of DSCAM1 through alternative splicing [11]. Each unique cell surface isoform binds with a high affinity to itself, and poorly binds to other isoforms. Preferential binding, through homophilic interactions, between DSCAM1 isoforms contributes to neurite recognition and to the formation of self-avoidant patterns in dendritic arbors of Drosophila neurons [69-73]. Vertebrate DSCAM, in contrast to the fruit fly, does not undergo extensive alternative splicing and only two paralogs have been sequenced – DSCAM and DSCAM-

Like1 (DSCAML1) [74]. Even though mammalian DSCAM can undergo homophilic cell adhesion binding, it is apparent that the complexity of 38,016 isoform interactions cannot be achieved in the vertebrate model. It is still possible that DSCAM can function without molecular isoform diversity. As discussed previously, vertebrate DSCAM can signal through heterophilic ligands such as Netrin-1 [54] or with other cell adhesion molecules such as cadherins and protocadherins [75].

Research investigating DSCAM's function in dendrite development have been limited to a pool of cell types, specifically involving the visual and mechanosensory system in fruit flies, and the vertebrate retina of chick and mice models. Across these studies, the dendrites commonly featured in their work span a two-dimensional laminar plane and are localized on the same plane as the soma, or in close proximity to the soma. It is important to make the comparison that vertebrate neurons, in higher-order brain regions, project three-dimensional dendritic arbors that protrude away from the soma and traverse several neuropil layers. For example, in the zebrafish optic tectum, the neuropil contains nine synaptic sublayers, which includes the stratum griseum centrale (SGC) and the stratum fibrosum et griseum superficiale (SFGS). Periventricular tectal neurons project complex dendritic arbors, with an average depth of 30 μm, across the SGC and into the SFGS sublayers at late larval stages [76]. Additionally, these tectal arbors are not arranged in a tiled setup. Even though arbors are extensively overlapping, they still manage to exhibit dendritic self-avoidance with itself and other arbors [77]. It is beginning to become clear, based on work done in the zebrafish larvae, that there are several types of tectal cells in

the tectum, each carrying their own unique dendritic morphology. The molecular tools used to shape the unique dendritic features of these tectal neurons in the optic tectum have not been explored in vivo and during development. DSCAM, in particular, is likely a candidate that shapes the structural identity of such arbors.

For my next dissertation aim, I report DSCAM's function in dendritic arbors of Xenopus tectal neurons, which have a similar arbor morphology as periventricular neurons found in the early developing tectum of zebrafish larvae. The dendritic arbors of Xenopus tectal neurons develop three-dimensionally, but are far more complex, larger in total arbor length, and penetrate 50 to 80 μm depth of space in the neuropil. In the following chapters, I use time-lapse imaging to investigate how altering DSCAM levels influence the development of these complex dendritic arbors. Interestingly, my findings reveal that DSCAM modulates the dendritic arbors of tectal cells differently from developing RGC axons, indicating that differential signaling is involved.

1.6. Underlying Mechanisms Facilitating Synapse Formation

It is evident that molecular cues guide axon pathfinding, topographic ordering of axon projections, arborization of retinal axons and dendritic arbors of tectal cells. I have discussed that these events in development are orchestrated by an array of signaling molecules including neurotrophins, chemoattractant cues, local inhibitory molecules, etc. Cells surface proteins, notably cell adhesion molecules (CAMs), stand out during these events. Surface proteins take on a crucial role in helping neurites recognize their

surrounding environment and avoid collision with sister or neighboring neurites But paradoxically, these same cell surface proteins are used to help establish appropriate physical contact between potential pre- and postsynaptic neurite partners that eventually lead to synapse formation as depicted in Fig 1.3, a schematic drawn by Nikolaos Giagtzoglou and colleagues [78]. The contacts between the presynaptic and postsynaptic compartments are stabilized by recruitment of additional cell adhesion molecules such as N-cadherins and catenins; adhesional interactions activate downstream pathways that remodel the cytoskeleton and organize pre- and postsynaptic apparatuses [78]. What exactly makes the decision for neurites to generally avoid neurite collision, while making selective contact to initiate synapse formation?

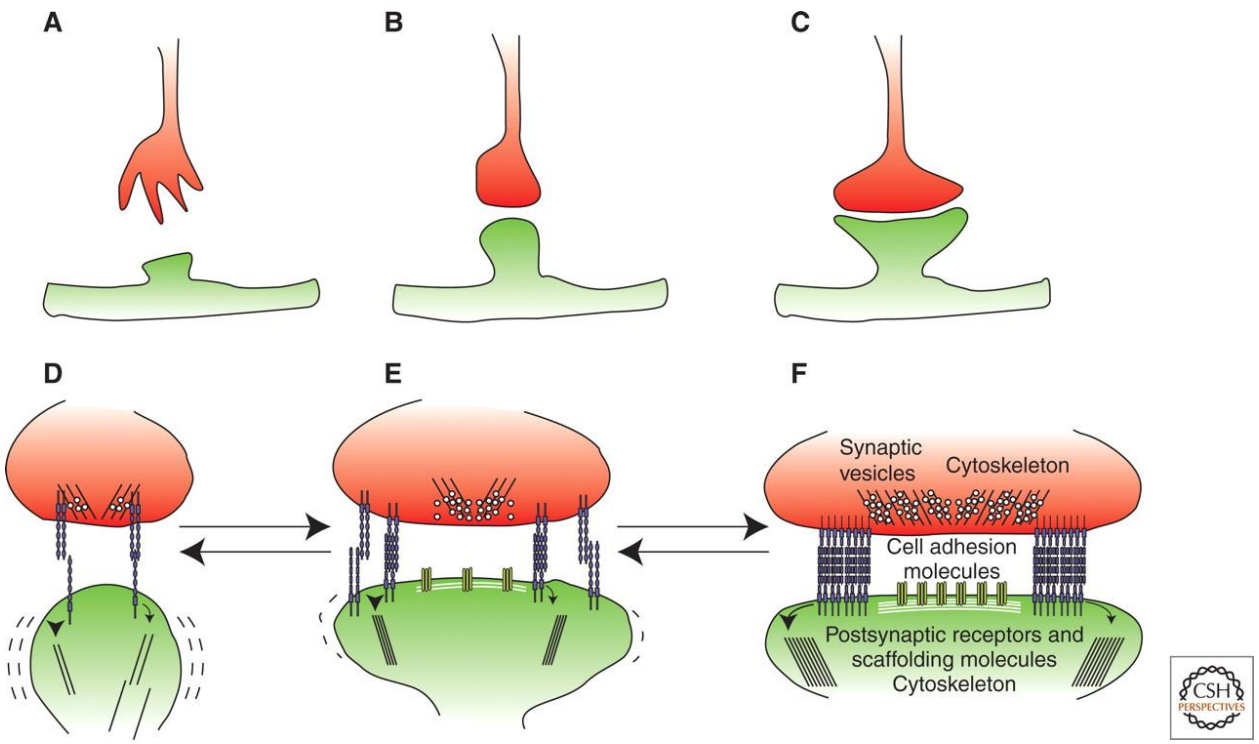

Figure 1.3. Schematic representation of the different stages of synapse formation as described by Giagtzoglou and colleagues [78]. **(A)** Target selection, **(B)** Synapse assembly, **(C)** Synapse maturation and stabilization. **(D–F)** The role of cell adhesion molecules in synapse formation is exemplified by the paradigm of N-cadherin and catenins in regulation of the morphology and strength of dendritic spine heads. **(D)** At an early stage the dendritic spines are elongated from motile structures "seeking" their synaptic partners. **(E)** The contacts between the presynaptic and postsynaptic compartments are stabilized by recruitment of additional cell adhesion molecules. Adhesional interactions activate downstream pathways that remodel the cytoskeleton and organize pre- and postsynaptic apparatuses. **(F)** Cell adhesion complexes, stabilized by increased synaptic activity, promote the expansion of the dendritic spine head and the maturation/ stabilization of the synapse. Retraction and expansion are dependent on synaptic plasticity.

Findings across several published research articles gives us insight to how cell surface molecules, such as DSCAM, mediate neurite avoidance, while facilitating physical contact between pre- and postsynaptic sites. Work done by Dr. Robert Burgess and colleagues has found that DSCAM can functionally interact with other CAMs, specifically cadherins and protocadherins, and "mask" their adhesive properties that, consequently, prevent neurite collision and fasciculation [75]. Their results, obtained in the mouse retina, reveal that DSCAM works in collaboration with other CAMs to modulate cell adhesion by acting as a "non-stick" signal. In comparison, studies have shown that DSCAM co-localizes with AMPA-like receptors during *de novo* synapse formation in Aplysia circuits. Blocking Aplysia DSCAM terminates synaptic transmission and clustering of AMPA-like receptors, suggesting that DSCAM mediates trans-synaptic interactions during developmental synapse formation. It is also been suggested that DSCAM collaborates with NMDA receptors to facilitate dendritic spine and synapse formation. Based on the studies discussed, it is possible that developing neurites use DSCAM, in collaboration with specific cell surface receptors, as a mechanism to distinguish areas that need to be avoided from specific areas where synapses can be established.

It is important to note that axon arborization, formation of dendritic arbors, and synaptic formation are all closely interdependent events. Synaptic connections formed between interacting axons and dendritic arbors are a major contributing factor to the arbors' growth, size and complexity [61, 62]. Work done in our lab has shown that the active branching dynamics of axonal arbors are closely related to the events of synaptogenesis

– where branches of more established synapses strengthen branch stability [61]. Based on these concepts, I investigate DSCAM's role in retinotectal synapse formation and correlate my results to axon arborization from my previous aim. Our experiments would, for the first time, show substantial in vivo evidence implicating DSCAM in synapse formation.

1.7. Visually-guided Behavior as a Means to Understand Synaptic Connectivity

The vast majority of inputs into the optic tectum are derived from RGCs in the eye [79]. Visual information from the surrounding environment is filtered and processed in the tectum. This information is then further relayed to motor systems, such as in the brainstem, where behavioral responses are produced. Retinotectal circuits in the tectum formulate the premotor commands that influence visual avoidance behavior – where moving visual stimulus perceived as a threat or "predator" triggers tadpoles to swim away from the object as demonstrated in Fig 1.4 representing the schematic drawn by Zhenyu Liu and colleagues [18]. Ablating the tectum abolishes motor visual avoidance [80]. While the bulk of my dissertation explores the work of DSCAM in the anatomical development of retinotectal circuits in the optic tectum, it is clear that proper structural development of the circuit affects how visually guided functions are executed. Part of my dissertation explores this physiological aspect of development and how premotor functions emerge from proper formation of dendritic arbors of tectal cells – the primary cells in charge of processing and relaying visual information to executive brainstem motor circuits. In my previous aims, I note how DSCAM plays a role in the structural development of dendritic

arbors of retinotectal circuits. I further address how perturbing this morphological development by DSCAM knockdown affects the performance of visually guided responses in freely swimming Xenopus tadpoles.

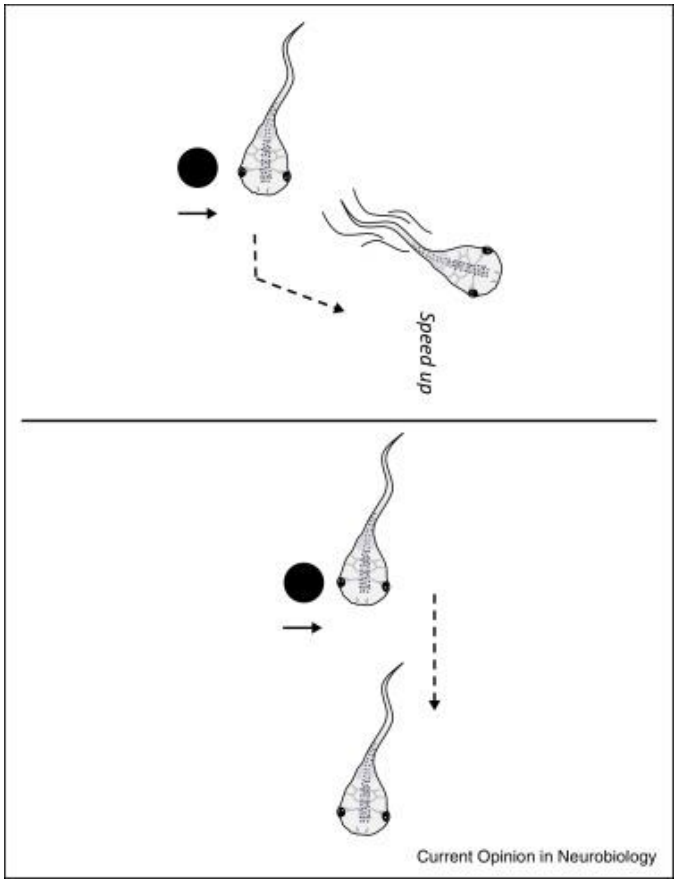

Figure 1.4. Visual avoidance behavior displayed by Xenopus laevis tadpoles in response to moving visual stimuli as described by Zhenyu Liu and colleagues [18]. Freely moving tadpoles are presented with a field of moving dots projected onto the floor of their tank. Solid black arrows indicate direction the dot is moving. Dashed arrows show direction tadpole swims. Top panel showing a tadpole displaying a visual avoidance response characterized by an obvious sharp turn and acceleration to avoid the approaching dot. Bottom panel showing a failure to dodge a moving dot as a result of tectal functional deficits. Note that the tadpole does not change swimming direction or speed upon encountering the moving dot

1.8. Summary and Objectives

As previously mentioned, abnormal wiring of neural circuits can disrupt proper physiological neural functions. It is interesting to note that circuit assembly is not a straightforward process; it is a complex ongoing process that requires many constructive steps. Each step heavily depends on an array of molecular signals to execute proper construction. Interestingly, a single type of molecule, such as DSCAM, plays reoccurring roles in many of the events that take place in development. Throughout my general introduction, I have explained how DSCAM can collaborate with many cell surface proteins and diffusible ligands to help construct many of the different wiring events that takes place in circuit assembly. It becomes increasingly apparent how disruption of this one heavily involved molecule can lead to the disruption of circuit connectivity – whether it would be by axons mistargeting, axonal or dendritic arbors aberrantly forming, or improper synaptic connections being made. If the majority of these key constructive events are not properly executed, disorders such as autism, schizophrenia, or neuropsychiatric intellectual disabilities can emerge and be a serious consequence of faulty neural circuits [7].

In summary, my dissertation focuses on understanding DSCAM's role in the many constructive steps that occur in circuit assembly. Using the Xenopus tadpole visual system as a model to study circuit formation, the work that I show captures key events that occur in real-time and in vivo. For my first chapter, I look into the branching mechanics of how axon and dendritic arbors of retinotectal circuits form. We will then see how

retinotectal connectivity gives rise to self-avoidant behavior, which I go in depth in the second chapter. In my third chapter, I explore the journey of RGC axons as they exit the tadpole eye, cross the optic chiasm, and enter into the tectum. We will see how RGC axons are topographically organized as they make their trajectory into the tectum and form synaptic connections with tectal partners. As I go through the events occurring in circuit assembly, I explain how DSCAM is involved and remarkably plays a multifaceted role in development.

Chapter 2

DSCAM Directs Growth and Directionality of Dendritic Arbors of Post-Synaptic Tectal Neurons In Vivo

2.1. Abstract

Proper patterning of dendritic is a critical step in the formation of functional neuronal circuits. Developing circuits rely on an array of molecular cues to shape arbor morphology, but the underlying mechanisms guiding the structural formation and interconnectivity of pre- and postsynaptic arbors in real time remain unclear. Here we explore how DSCAM shapes the dendritic morphology of tectal cells, which are central visual neurons found in the midbrain of the *Xenopus* tectum. Our first set of objectives was to examine DSCAM expression throughout the Xenopus visual system. We confirmed that DSCAM expression is present in RGCs, cells in the optic tectum and the tectal neuropil at the time retinotectal synaptic connections are made. The cell-autonomous role of DSCAM, in tectal neurons, was examined using targeted single-cell knockdown and overexpression approaches in developing tadpoles. Dendritic arbors of tectal neurons were visualized using real-time in vivo confocal microscopy imaging over the course of 3 days. Downregulating DSCAM in tectal neurons significantly increased dendritic growth and branching rates while inducing dendrites to take on tortuous paths. Overexpression of DSCAM, in contrast, reduced dendritic branching and growth rate. These results demonstrate that DSCAM primarily acts as a neuronal brake to limit and guide postsynaptic dendrite growth of tectal neurons.

2.2. Introduction

Wiring functional neuronal circuits during embryonic development involves a coordinated effort to spatially organize dendritic and axonal arbors into one cohesive circuit. The spatial pattern of dendritic arbors is critical to the neuron's input, so that incoming information from afferent axons is efficiently integrated [65]. Neuronal arbors can adopt an array of patterns to suit their connectivity. For a notable example, individual branches in a dendritic arbor avoid aggregating with neighboring sister branches stemming from the same neuron, a phenotype referred to as self-avoidance. Axon arbors also exhibit self-avoidance [66][2]. Extensive studies from the last decade have shown that Down Syndrome Cell Adhesion Molecules (DSCAMs) play a multifaceted role in shaping circuit connections. DSCAMs are key players mediating not only in self-avoidant dendritic patterning, but also neuronal arbor tiling, axon guidance, and neuronal fasciculation [8, 9, 16, 65, 67].

In Drosophila, DSCAM acts as a contact-dependent adhesion molecule with over 38,000 alternatively spliced isoforms coordinating the self-avoidant patterning of neuronal dendritic and axonal arbors [8-11]. While genetic conservation appears to exist between vertebrate DSCAM and Drosophila DSCAMs, emerging roles for vertebrate DSCAM are beginning to be uncovered. In DSCAM knockout mice, retinal ganglion cells (RGCs) have severe defects in dendritic self-avoidance phenotypes [12-14]. Studies in the chick retina have shown that DSCAM plays a role in synapse formation by promoting the targeting of RGC dendrites and bipolar cell axons to the same layer [15]. Additionally, recent evidence

has demonstrated that DSCAM actively regulates circuit level plasticity by inhibiting dendritic arbor growth and receptive field size of mature retinal bipolar cells [16]. These findings suggest that DSCAM has a prominent role in wiring and maintaining the intricate arbor connections of retinal circuits in the eye. Its role, however, in orchestrating the interconnectivity between pre- and post-synaptic arbors of circuits in the brain, particularly at higher visual centers, remains largely unknown. For this reason, we aimed to test the hypothesis that DSCAM directs retinotectal synaptic connectivity by guiding the structural arborization and development of pre- and postsynaptic arbors. Additionally, we addressed whether DSCAM gives rise to proper functional visual circuits.

To understand the cell-autonomous actions of DSCAM in the retinotectal circuit, we used targeted single-cell knockdown and overexpression approaches to alter DSCAM expression levels in Xenopus laevis tadpoles. Structural changes in the neuronal arbor in response to alterations in DSCAM levels were observed by in vivo confocal microscopy imaging. Our findings reveal that decreasing levels of DSCAM in tectal neurons surprisingly does not affect dendritic self-avoidant patterning. Instead, individual dendrites of neurons with DSCAM knockdown took on a tortuous meandering pathway. Additionally, tectal neurons exhibited exuberant dendritic arbor growth within 24 h of DSCAM knockdown, an effect that became more robust over a three-day period of imaging. Overexpression of Xenopus DSCAM in single tectal neurons, in contrast, resulted in stunted dendrite arbor development. Tectal neurons overexpressing DSCAM had a significantly shorter total dendrite arbor length and fewer branches compared to controls.

Our observations indicate that DSCAM can shape retinotectal connectivity by acting cell autonomously and limiting dendritic differentiation of postsynaptic central neurons.

2.3. Materials and Methods

Animals

Xenopus laevis tadpoles were obtained by in vitro fertilization of oocytes from adult females primed with human chorionic gonadotropin and raised in rearing solution [60 mM NaCl, 0.67 mM KCl, 0.34 mM Ca(NO3)2, 0.83 mM MgSO4, 10 mM HEPES, pH 7.4, and 40 mg/l gentamycin] plus 0.001% phenylthiocarbamide to prevent melanocyte pigmentation. Tadpoles were anesthetized during experimental manipulations with 0.05% tricaine methanesulfonate (Finquel; Argent Laboratories, Redmond, WA, USA). Staging was performed according to Nieuwkoop and Faber [81]. Animal procedures were approved by the Institutional Animal Care and Use Committee of the University of California, Irvine (Animal Welfare Assurance Number A3416–01).

Immunohistochemistry and western blot analysis

Stage 45 tadpoles were euthanized with tricaine methanesulfonate and fixed in 4% paraformaldehyde in PB, pH 7.5, for 2 h. For coronal sections, tadpoles were cryoprotected in 30% sucrose overnight and embedded in OCT compound (Sakura Finetek, Torrance, CA, USA), and 40-µm cryostat sections were obtained. Coronal sections at the level of the optic tectum were incubated with a rabbit polyclonal antibody against the middle region of human DSCAM (1:1000 dilution; Aviva System, San Diego,

CA, USA). DSCAM primary antibodies were visualized using goat anti-rabbit Alexa 488 secondary antibodies (1:500 dilution; Invitrogen, Eugene, OR, USA). The specificity of DSCAM antibodies (1:500 dilution) to recognize endogenous Xenopus DSCAM was further tested and confirmed by Western blot analysis: a band of ~ 220 kDa was detected by anti-DSCAM antibodies in stage 38, 41, 47 Xenopus brain lysates.

Immunohistochemistry was also used to confirm downregulation of DSCAM expression by lissamine-tagged morpholino anti-sense oligonucleotide (MO) treatment (300 nmol, Genetools, Philomath, OR, USA). Morpholino-injected embryos were raised until stage 38 or 42 (3 to 4 days-post fertilization) to be fixed and analyzed by immunohistochemistry for DSCAM as above. To obtain a relative change in DSCAM immunoreactivity, fluorescence intensity of Alexa 488 immunoreactivity was measured from at least five regions of interest (ROI = 30 × 30 μm) per brain hemisphere, or retina, where fluorescein-tagged DSCAM was localized and compared to the corresponding ROIs in the contralateral brain hemisphere, or adjacent retinal area, without MO label.

Transfection of Morpholinos or plasmids

Downregulation of DSCAM expression was performed using lissamine-tagged morpholino anti-sense oligonucleotides (300 nmol, Genetools, Philomath, OR, USA) to block protein translation. A morpholino (MO) against Xenopus laevis Dscam mRNA was designed with the sequence 5′-ACATATAAGACTTCGACAGAGACGT-3′. 10-nL volume of DSCAM MO was injected into the two light-shaded blastopores of a 4-cell stage embryo

using a pressurized microinjector (Picospritzer, General Valve). A standard lissamine-tagged control morpholino oligonucleotide with the following sequence 5′-CCTCTTACCTCAgTTACAATTTATA-3′ was used for control comparisons. Morpholino-injected embryos were raised until stage 38 or 42 (3 to 4 days-post fertilization) to be fixed and analyzed by immunohistochemistry for DSCAM as above. Targeted downregulation of DSCAM expression in developing tectal neurons or in RGCs was achieved using single-cell electroporation in developing Xenopus tadpoles [82]. Prior to electroporation, tadpoles were anesthetized with 0.05% tricaine methanesulfonate. A CUY-21 edit stimulator was used to electroporate and transfect individual tectal neurons or RGCs of stage 43 tadpoles (20 V, 1 ms pulse duration on, 1 ms pulse duration off, set to repeat 99 times). Tectal neurons or RGCs were electroporated with lissamine-tagged DSCAM MO (150 nM pipette concentration) and a cell-filling dye Alexa Fluor 488 Dextran, 3000 MW (2 mg/111 µl pipette concentration, Invitrogen, Eugene, OR, USA). Reagents were loaded onto an aluminosilicate electrode (AF100–64-10, 1.00 mm, 0.64 mm, 10 cm) with a pulled tapered-tip with an opening of about 0.5 µm. Neurons transfected with a standard lissamine-tagged control MO (150 nM pipette concentration) and 488 dextran were used as a control comparison with DSCAM MO transfected neurons. Co-transfections of lissamine-tagged morpholinos and Alexa 488 dextran was confirmed via fluorescence microscopy. For DSCAM downregulation in retina, Control or DSCAM MO was pressure injected into both the left and right eyes of anesthetized stage 42 tadpoles. Directly after the microinjection, tadpoles were electroporated with 20 V at both normal polarity and

reversed polarity with the CUY-21 edit stimulator. Tadpoles were then left in a 12-h light-dark cycle at 22 °C until stage 45 (~ 2 days later).

Overexpression of DSCAM in individual tectal neurons was conducted by co-electroporating pCALNL-TurboRFP and pCALNL-GFP-Dscam (both at 5 μg/μl pipette concentration) with pCAG-Cre:GFP (2 ng/μl pipette concentration) into the optic tectum of stage 43 embryos to sparsely label individual tectal neurons. The pCALNL-GFP-Dscam was constructed by amplifying the Xenopus laevis Dscam sequence from a pCMV-SPORT6-Dscam (pDONR223 vector, Source BioScience), with the following primers: forward Kpn-Dscam primer: 5'-CCGAGGTACCATGTTATATGACCTGCAGGA-3′, Reverse AgeI-DSCAM primer: The Dscam sequence was then ligated downstream of the GFP sequence of the pCALNL-GFP (Addgene plasmid # 13770), a gift from Connie Cepko [15]. The pCAG-Cre:GFP was also a gift from the Cepko lab (Addgene plasmid # 13776). The pCALNL-TurboRFP plasmid was generously provided by Yoshiaki Tagawa [16]. Co-transfections of sparsely labeled neurons with a pCS2-eGFP and the pCMV-SPORT6-Dscam plasmid were also performed by lipofecting the brain primordia of stage 22 tadpoles as before [83, 84]. Anesthetized tadpoles were imaged at stage 45 by laser-scanning confocal microscopy. Overexpression of DSCAM was further confirmed by immunohistochemistry after imaging (see Fig. 1j).

In vivo confocal microscopy imaging

Stage 45 tadpoles were anesthetized with 0.05% tricaine methanesulfonate prior to imaging, were mounted in a custom-made sylgard chamber during imaging, and were then allowed to recover in fresh rearing solution immediately after imaging. Neurons co-transfected with lissamine-tagged morpholinos and Alexa 488 dextran were imaged in real time using an LSM780 confocal microscope (Zeiss) over the course of 3 days, at 24-h intervals. The LSM 780 confocal microscope is equipped with a MaiTai Ti:Sapphire multiphoton laser system. A two-photon wavelength of 760 to 780 was used to image the Alexa 488 cell-filling dye in tectal neurons in the midbrain. Neurons co-transfected with pCALNL-TurboRFP and pCALNL-GFP-Dscam were imaged using a multiphoton LSM780 confocal microscope starting 48 h after electroporation over the course of 3 days, at 24-h time intervals. pCALNL-TurboRFP and pCALNL-GFP-Dscam co-transfected neurons were imaged with Argon and HeNe lasers simultaneously. For analysis of RGC and bipolar cell dendritic morphologies, tadpoles with retinal MO transfections were reared until stage 45 (48 h post-injection), euthanized with tricaine methanesulfonate, then fixed in 4% paraformaldehyde overnight at 4 °C and transferred to 30% sucrose for at least 1 h to overnight in 4 °C. Tadpoles were immersed in OCT embedding compound and 60 µm thick cryostat sections were obtained. Slides were then coverslipped with ProLong™ Gold Antifade Mountant with DAPI to label nuclei and differentiate between the retinal layers. For arbor analysis, images of the retina were taken with a 63× oil-immersion objective using a Zeiss Pascal laser scanning confocal microscope equipped with a HeNe laser.

Images were collected in a 0.5 μm interval throughout the extent of the dendritic arbor (z-axis).

Neuronal arbor analysis

In brief, three-dimensional images of fluorescently-labeled dendritic arbors were manually reconstructed using a Neuromantic tracing software blind to treatment. Each dendritic arbor was reconstructed plane-by-plane from the image stack and was then analyzed using the Neuromantic software. Branch tips were identified as the terminal ends of primary dendrites. Primary branches were identified as projections stemming from the soma. The total arbor lengths, branches, and branch tips of the cells were thresholded, binarized, and skeletonized with the Neuromantic software so that the soma perimeter and dendrites were represented as a single pixel width. Processes of more than 5 μm in length were considered branches, while processes less than 5 μm were categorized as filopodia. Statistical analysis was performed as described [63]. Additionally, ImageJ was used for three-dimensional Sholl analysis of reconstructed arbors to quantify the number of proximal and distal branches from a given neuron. A radius step size of 10 μm intervals were used for dendritic arbor measurements. For tectal neuron dendritic arbors, the number of intersections was quantified starting at the main branch point stemming from the soma. Sholl branch-tip distributions were compared across experimental groups and two-way ANOVA statistical analysis of data was performed. Neuromantic data and Sholl analysis results were considered significant in comparison to control as follows: $*p \leq 0.05$,

**p ≤ 0.005, ***p ≤ 0.001, unless otherwise indicated on the graph with bars marking additional significant comparisons.

2.4. Results

Patterns of DSCAM expression in the Xenopus retina and optic tectum during visual circuit development

Immunohistochemistry of coronal brain sections reveal that DSCAM is expressed both in the retina and optic tectum of Xenopus tadpoles at the time that RGCs differentiate and project their axons out of the eye and into the brain (stages 38–40; Fig. 2.1a, b, e). Western blot analysis of whole-brain lysates also confirmed expression of DSCAM in stage 38 to stage 47 tadpoles (Fig. 2.1c). Expression in the retina and optic tectum also occurs during the time when retinotectal synaptic connections begin to be made (stage 45; Fig. 2.1f, g). In the midbrain optic tectum DSCAM is expressed in the cell body layer where mature neurons localize as well as in the neuropil, where dendrites and axons establish functional synaptic connections (Fig. 2.1a, g). Expression of DSCAM in the ganglion cell layer (gcl), inner plexiform layer (ipl) and inner nuclear layer (inl) in the Xenopus retina (Fig. 2.1b, f, i) is consistent with expression patterns and roles for DSCAM in other vertebrate species [14-16, 85].

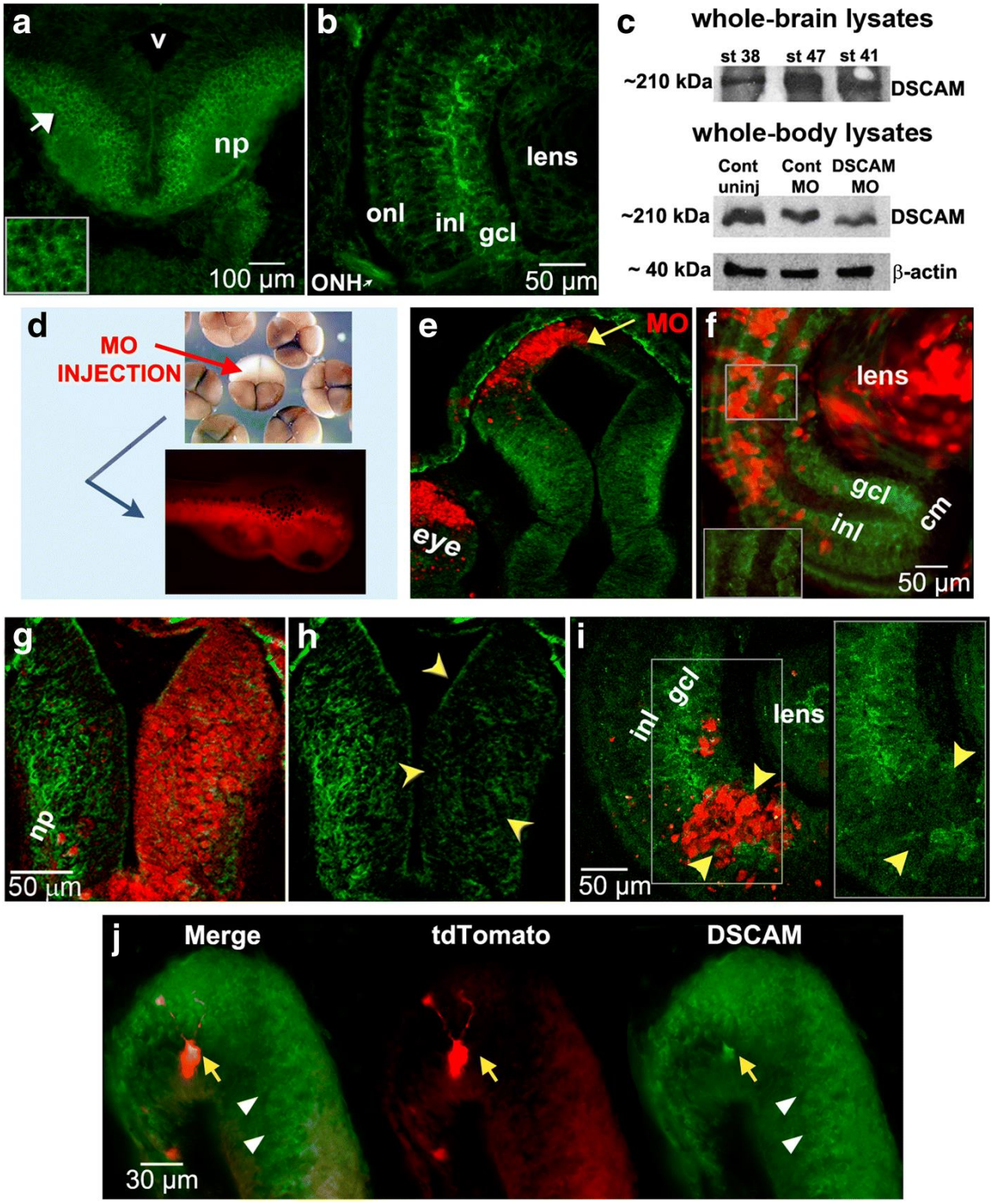

Fig 2.1. DSCAM expression in the developing *Xenopus* visual system and morpholino oligonucleotide-mediated knockdown. Caption on next page.

Fig 2.1. DSCAM expression in the developing *Xenopus* visual system and morpholino oligonucleotide-mediated knockdown. Immunostaining reveals patterns of DSCAM expression in the retina and tectum of developing *Xenopus* tadpoles. (**a**, **b**) DSCAM immunoreactivity (*green*) localizes to the midbrain (**a**) and retina (**b***)* of stage 40 tadpoles. In the midbrain optic tectum DSCAM immunoreactivity is localized to postmitotic cell bodies (white arrow and insert in **a**) and neuropil (np). In the developing retina (**b**), DSCAM immunoreactivity localizes to the inner nuclear layer (inl), ganglion cell layer (gcl) and optic nerve head (ONH). **c** Western blot analysis of whole brain lysates confirms DSCAM expression in stage 38, 41, and 47 tadpoles. Whole-embryo lysates at stage 30 show a 40% decrease in DSCAM expression after microinjection of DSCAM MO at the 2-cell stage. **d** Microinjection of lissamine-tagged DSCAM or Control MO into a light-shaded blastomere of 4-cell or 8-cell stage embryos localized the MO to cells in the eye and brain of developing tadpoles unilaterally. **e**, **f** Lissamine-tagged Control MO (*red*) did not alter DSCAM expression (*green*) in stage 38 tectum (**e**) or stage 45 retina (**f***;* see magnified insert) by injection at the 8-cell stage. **g-i** Decreased DSCAM expression (*green*) is observed in the tectal hemisphere of stage 45 tadpole (**g***, **h**; yellow arrowheads*) and portion of retina of stage 40 tadpole *(**i**; see magnified insert*; *yellow arrowheads*) with DSCAM MO lissamine tag (*red*). **j** DSCAM immunostaining of stage 45 tadpole brain lipofected with plasmids coding for *Xenopus Dscam* and tdTomato. Note the increased levels of DSCAM immunoreactivity in tdTomato-labeled neuron (*yellow arrow*). The white arrowheads denote endogenous DSCAM expression. *np,* neuropil; *v*, ventricle; *MO,* morpholino; *inl,* inner nuclear layer; *gcl,* ganglion cell layer; *onl*, outer nuclear layer; *ONH*, optic nerve head, *cm,* ciliary margin. Scale bars: 100 μm in (**a**); 50 μm in (**f**, **g**, **i**); 30 μm in (**j**)

To examine the impact of downregulating DSCAM levels during Xenopus visual circuit development, we utilized a morpholino (MO) anti-sense oligonucleotide targeted against endogenous Xenopus laevis Dscam mRNA to interfere with protein translation. To test for the specificity of the MO, we injected control or Xenopus-specific DSCAM MO into a single blastomere of 2-cell or 4-cell stage embryos and visualized changes in expression by western blot and by immunostaining tadpoles with antibodies to DSCAM at different developmental stages (Fig. 2.1c-i). Xenopus DSCAM morphants developed normally and were as healthy as controls. MO microinjections into a light-shaded blastomere of a 4-cell

stage embryo (or two light-shaded blastomere of 8-cell stage embryos) restricted the MO to only one side of the organism's body and resulted in tadpoles with MO localized to the eye and midbrain of stage 38 tadpoles (Unilaterally, Fig. 2.1d). DSCAM morphants showed significant changes in brain and retinal DSCAM expression (Fig. 2.1c, g, h, i). Tadpoles with DSCAM MO label (lissamine-tagged MO) localized to the neuropil, where retinotectal synaptic connections are formed, showed a 59.16% average fluorescence intensity reduction in DSCAM immunoreactivity (Fig. 2.1g, h). Similarly, DSCAM MO presence in the RGC layer of the retina correlated with a 59.6% reduction in DSCAM antibody fluorescence intensity (Fig. 2.1i, see insert). In contrast, injection of Control MO resulted in an 8.9% average fluorescence intensity reduction of DSCAM immunoreactivity in the RGC layer (Fig. 2.1f, see insert) and a 0% reduction within the tectal neuropil (data not shown). Consistent with these findings, western blot analysis of DSCAM morphant stage 30 tadpoles revealed a 40% decrease in DSCAM protein levels (Fig. 2.1c). These observations confirm our MO loss-of-function approach and indicate that DSCAM knockdown is specific and affects only DSCAM morphant neurons.

Developing tectal neurons exhibit exuberant dendrite growth and extend more proximal and distal branches in response to DSCAM downregulation

To define direct cellular actions of DSCAM on tectal neurons, single-cell electroporation of lissamine-tagged MOs together with Alexa 488 dextran in stage 43 tadpoles was used to acutely downregulate DSCAM expression cell-autonomously. Individual tectal neurons were imaged in vivo using two-photon confocal microscopy to visualize neuronal

morphology 24 h after MO transfection (stage 45 tadpoles). Tadpoles were imaged again 24 and 48 h after initial imaging. Single-cell DSCAM MO electroporation resulted in tectal neurons with exuberant dendritic arbor growth, an effect that was sustained over the entire imaging period (Fig. 2.2a-c). Three-dimensional reconstruction and quantitative analysis revealed that neurons transfected with DSCAM MO had significantly higher dendrite branch number at each imaging time point (Fig. 2.2c) and higher total dendrite arbor length by 48 h after initial imaging when compared to controls (Fig. 2.2d). Neurons with DSCAM MO-mediated knockdown also grew at a faster rate than controls (Fig. 2.2e). To further differentiate whether DSCAM downregulation increases branch and/or filopodia number, processes less than 5 μm were counted from each individual neuron at every imaging time point (filopodia marked red; Fig. 2.2b). This analysis revealed that tectal neurons with DSCAM knockdown possessed significantly more filopodia by 48 h after initial imaging (Fig. 2.2b, f), while the total number of branches was significantly increased at all imaging time points when compared to controls (stage 45: Control MO 19.53 ± 1.87, DSCAM MO 27.06 ± 2.63, $p = 0.024$; + 24 h: Control MO 23.78 ± 1.9, DSCAM MO 36.0 ± 3.78, $p = 0.0059$; + 48 h: Control MO 26.86 ± 2.5, DSCAM MO 48.5 ± 6.3, $p = 0.003$). These results indicate that the increase in total branching we observed from DSCAM downregulation is mostly a result from an increase in dendritic branch number and, to a smaller extent, an increase in filopodia number. In addition to the effect of DSCAM knockdown on dendrite number and length, we observed that the proportion of neurons that extended more than one axon was increased after DSCAM MO-mediated knockdown when compared with controls (Fig. 2.2g, h).

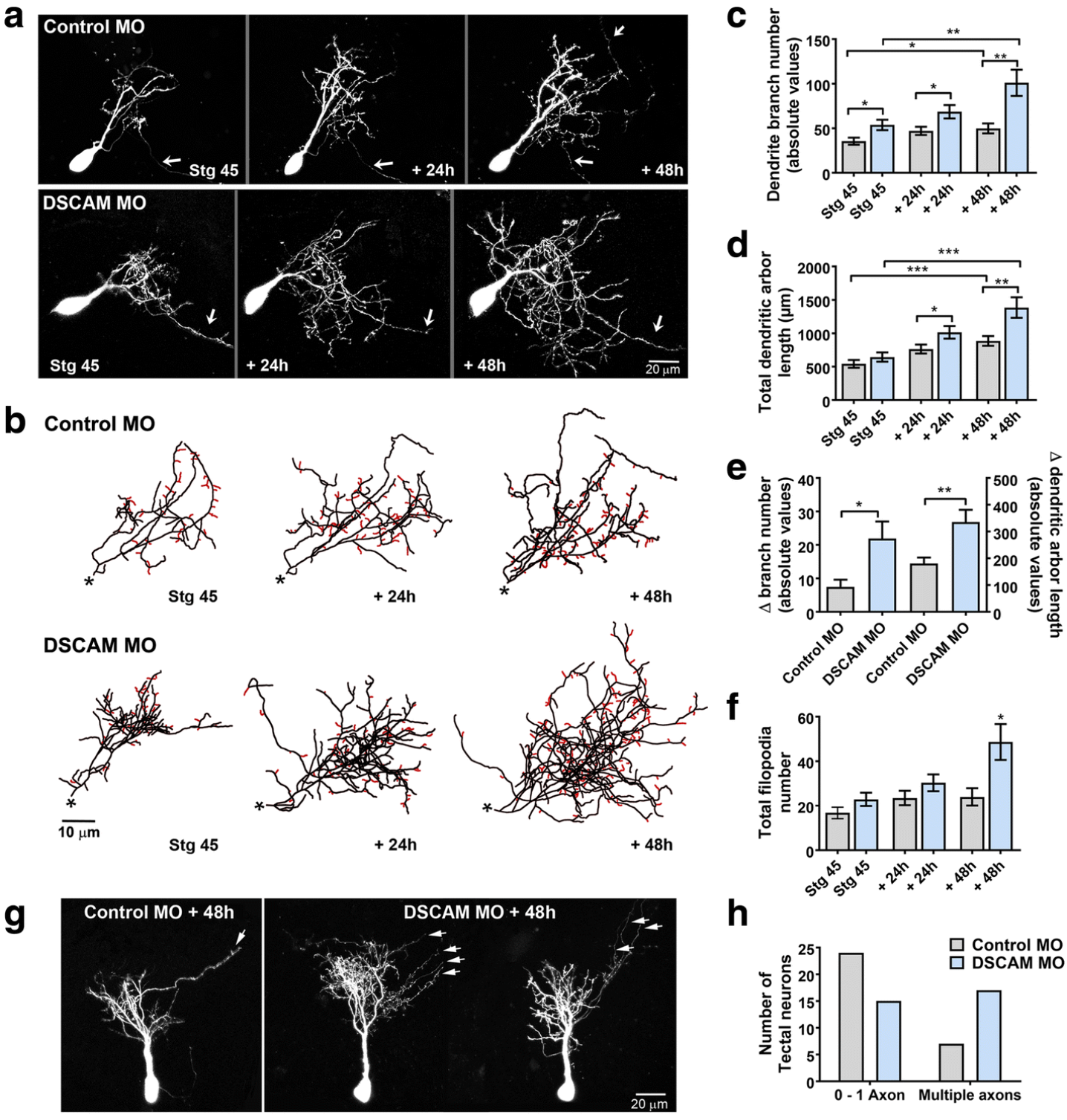

Fig 2.2. Single-cell DSCAM knockdown increases the branching and growth of tectal neurons in vivo. Caption on next page.

Fig 2.2. Single-cell DSCAM knockdown increases the branching and growth of tectal neurons in vivo. a Sample of neurons in stage 45 tadpoles transfected with Alexa 488 dextran and lissamine-tagged Control MO or DSCAM MO and imaged in vivo by two-photon confocal microscopy over the course of 3 days. b Dendritic arbors were digitally reconstructed in three-dimensions using the Neuromantic tracing software. Filopodia, processes of less than 5 μm were manually measured and highlighted in red. c Dendritic arbors of neurons with DSCAM MO had significantly a higher number of branches than controls at each imaging time point, (d) and a higher total arbor length at 28-h and 48-h after initial imaging compared to controls. e Quantifying the rate of branch addition and the increase in total dendritic arbor length reveals that tectal neurons with DSCAM MO grow at a more robust and faster rate than controls (Student's-t-test). b, f Tectal neurons had significantly more filopodia compared to controls by 48 h after initial imaging only. g, h Tectal neurons with DSCAM MO also extended significantly more axons (marked by the white arrows) than controls. Control MO (n = 31), DSCAM MO (n = 31). In c-e, comparisons are by Two-way ANOVA and Student's t-test. * $p \leq 0.05$, ** $p \leq 0.005$, *** $p \leq 0.001$. In h, statistical comparison was by Fisher's Exact Test, $p = 0.0192$. Scale bars: 20 μm in (a & g); 10 μm in (b)

Sholl analysis was used as an additional measure to understand the effects of DSCAM downregulation on dendritic arbor morphology and complexity of tectal neurons [86, 87]. Sholl analysis measured the number of dendrites, without considering filopodia, that intersected a series of spherical circles spaced at 10 μm ring intervals for each neuron analyzed in three-dimensions. Our analysis revealed that by 24 h after initial imaging, tectal neurons with DSCAM downregulation had significantly more distal branch intersections (70 to 110 μm from the soma) compared to controls (Fig. 2.3a, b). By 48 h after initial imaging, neurons with DSCAM MO-mediated knockdown had a significant increase in branch intersections both proximally and distally from the soma (20 to 110 μm) relative to controls. To ascertain that the increase in the proportion of distal dendrites was not a result of a primary dendrite growing longer rather than extending new branches, we measured the length of the primary dendrites of neurons treated with DSCAM MO and

control MO. There were no significant differences in primary dendrite length between neurons treated with DSCAM MO compared to controls (Fig. 2.3c). Together, these results indicate that knockdown of DSCAM positively regulates the branching and complexity of tectal neuron dendritic arbors.

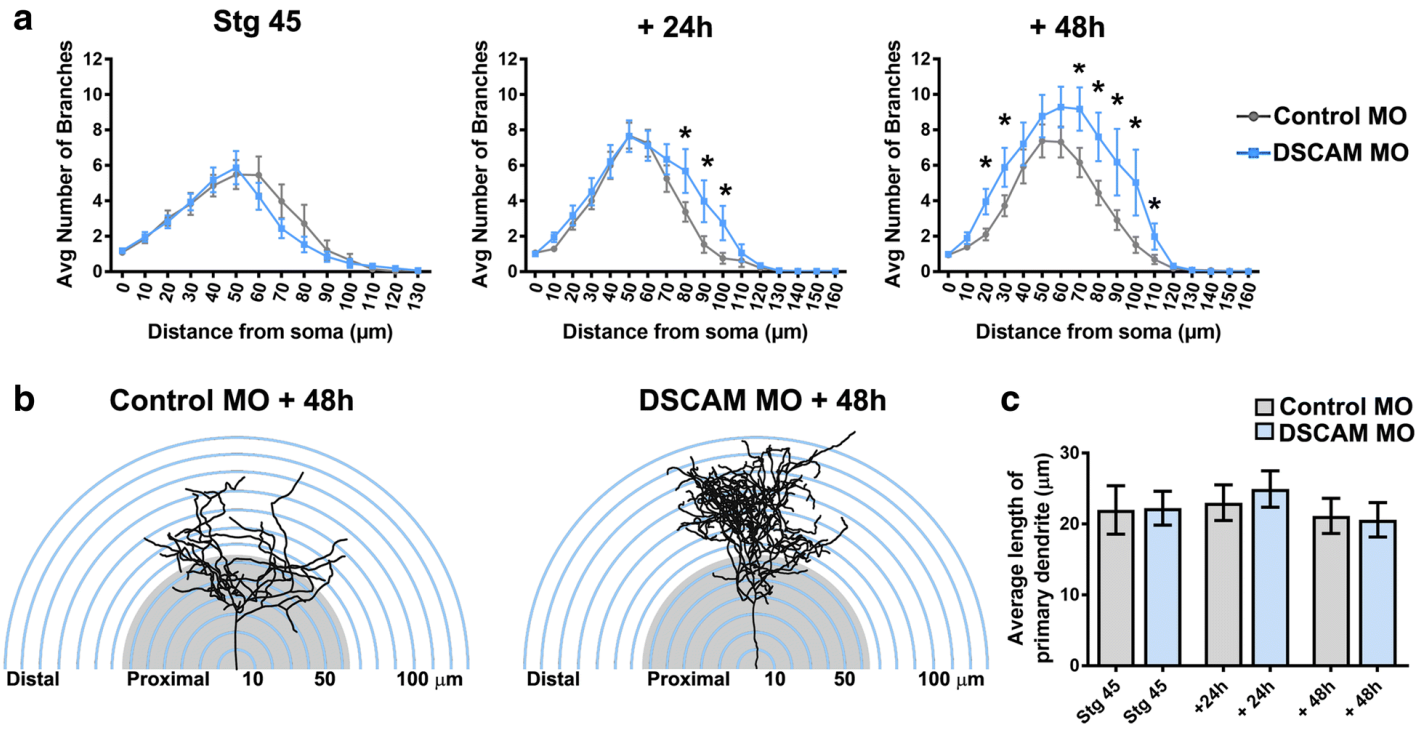

Fig 2.3. Exuberant dendrite arbor growth after DSCAM knockout. a Three-dimensional Sholl analysis of proximal and distal dendrites of tectal neurons transfected with either DSCAM MO or Control MO was used as a measure of dendritic arbor complexity. The number of proximal and distal branch intersections was measured for neurons in stage 45 tadpoles and 24 h and 48 h after initial imaging. b Tracings of representative neurons showing proximal vs distal branch distribution within a spherical Sholl-ring. c The length of the primary dendrite of neurons with DSCAM downregulation was similar to that of controls at each imaging time point. Control MO n = 31, DSCAM MO n = 31. Two-way ANOVA, error bars indicate mean ± SEM. *p < 0.05

Dendrites of neurons with DSCAM downregulation grow in highly tortuous meandering paths

Alterations in DSCAM expression result in errors in dendrite self-avoidance in Drosophila and in mature retinal neurons of DSCAM knockout mice [16, 65, 70, 73, 88]. We observed no perturbations in dendritic self-avoidance among Xenopus tectal neurons after MO-mediated DSCAM knockdown. Specifically, analysis of dendritic arbors in three-dimensional space using the Neuromantic software 3D viewer (where one can rotate and view tracings of reconstructed neurons at numerous angles through a 360° field of view) showed no fasciculation or crossing contact among sister dendrites of either Control MO or DSCAM MO transfected neurons (data not shown). We did notice, however, that individual branches of neurons with DSCAM downregulation took on a tortuous trajectory of growth within the dendritic arbor (Fig. 2.4a). Tortuous projections of arbors of neurons with DSCAM downregulation were observed in longer branches. To quantify the tortuosity of dendrites, we used the Neuromantic software contraction function to analyze the meandering of individual branches from 3D reconstructed neurons imaged in vivo. For this analysis, a dendritic branch that would take on an absolute straight path would score a value of 1, while dendrites that exhibit more "bending" or angled turns along their pathway receive lower values [89]. Dendritic pathways of the 1st and 2nd longest individual branches of reconstructed neurons were analyzed three-dimensionally and were combined to obtain an average value. Fig 2.4a illustrates the dendritic pathways of the 1st and 2nd longest individual branches of sample reconstructed neurons and their corresponding meandering scores. The 1st and 2nd longest individual dendrites of

neurons transfected with control MO had an initial average meandering value of 0.716 at stage 45, the initial imaging period, which then slightly decreased over the course of 2 days as dendrites grew and branched (Fig. 2.4a, b). In contrast, the individual branches of DSCAM MO transfected neurons showed a significantly lower meandering value of about 0.6 at each imaging time point compared to controls (Fig. 2.4a, b). This indicates that the growth directionality of individual dendrites is affected by DSCAM downregulation.

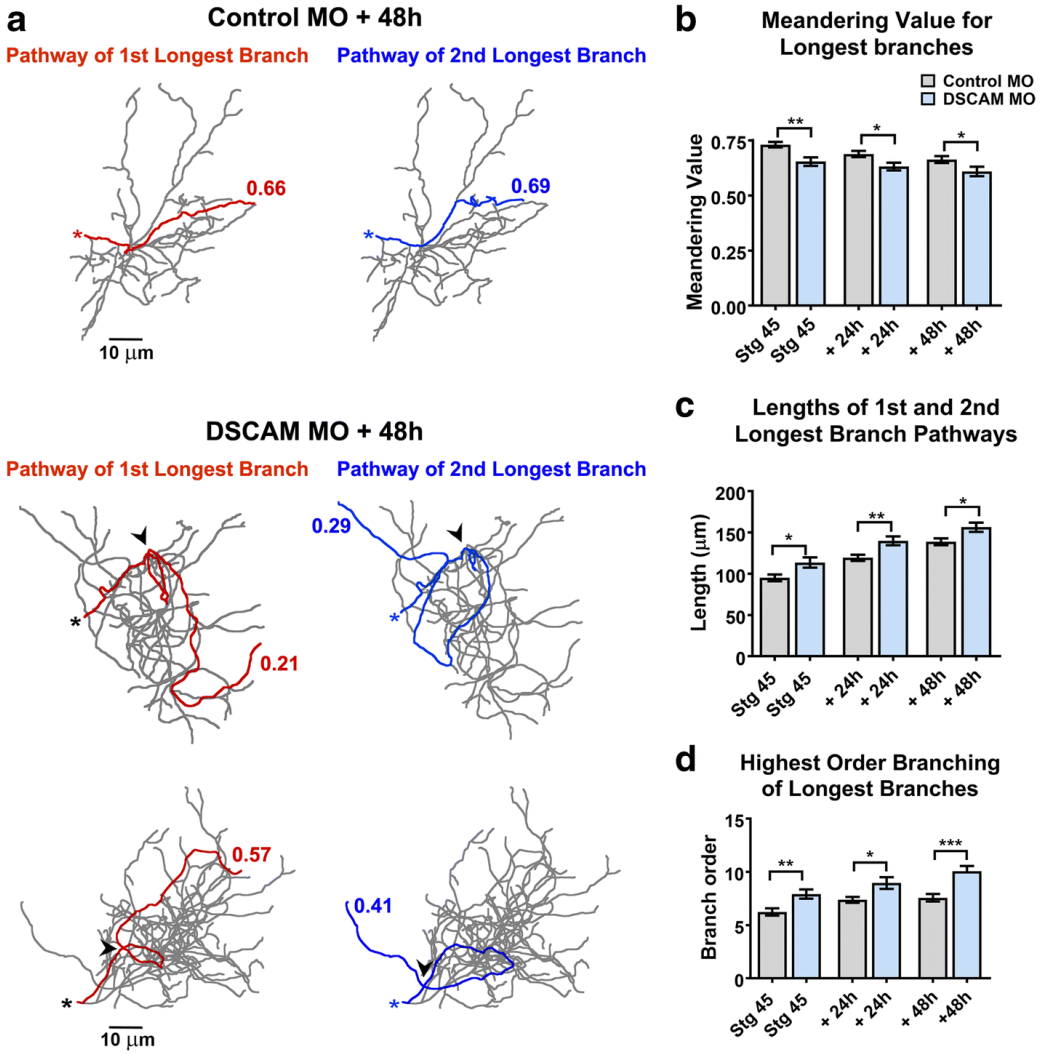

Fig 2.4. Dendrites of tectal neurons with DSCAM downregulation take tortuous meandering paths. Caption on next page.

Fig 2.4. Dendrites of tectal neurons with DSCAM downregulation take tortuous meandering paths. a Tracings of sample neurons transfected with Control or DSCAM MO and imaged 48 h after initial imaging. For the quantification of dendritic pathway turning the 1st and 2nd longest individual branches of reconstructed neurons were measured three-dimensionally (Control MO n = 62 dendrites, DSCAM MO n = 62 dendrites) using the Neuromantic software meandering contraction value which quantifies bends and turns in a scale from 0 to 1. Here, the pathways of the two longest branches for each sample neuron are highlighted in red and blue and their corresponding contraction values are shown. Note that dendrites of neurons with DSCAM MO take abnormal turns within the dendritic arbor. b Individual branches of neurons with DSCAM MO showed a significantly lower contraction value at each imaging time point when compared to controls. c A measurement of the lengths of the 1st and 2nd longest primary branches of each neuron reveal that dendrite branches were significantly longer in neurons with DSCAM MO than in those with Control MO. d The longest branches in neurons with DSCAM MO also bifurcated more than controls as shown by the significant difference in their branch order number. Scale bars: 10 μm in (a). Statistical comparisons are by Student's t-tests, error bars indicate mean ± SEM. *p ≤ 0.05, **p ≤ 0.005

We also quantified the total length and branch order for each neuron's 1st and 2nd longest individual branches. The tortuous meandering paths displayed by dendrites of DSCAM MO transfected neurons could have been a result of longer branches traversing longer distances and given a better chance to take angled turns. Additionally, the altered morphology displayed by the dendritic arbors of neurons transfected with DSCAM MO could result from dendrites splitting out to higher order branch number, which would also contribute to more angled turns. This analysis revealed that the 1st and 2nd longest individual branches of neurons with DSCAM MO were significantly longer than controls (Fig. 2.4c). Moreover, these dendrites also extended branches that split more relative to controls (Fig. 2.4d). Therefore, the bending of individual longer branches and their

splitting into higher order branches both contributed to the altered morphology and directionality we observed in the dendrites of neurons with DSCAM knockdown.

Cell-autonomous overexpression of DSCAM interferes with dendrite growth and differentiation of tectal neurons

Downregulating DSCAM levels in tectal neurons triggered exuberant growth, increasing branch number and total branch length, suggesting that endogenous DSCAM is part of cellular mechanism that controls tectal neuron arbor growth in a restrictive manner. To further test this possibility, we examined cell-autonomous effects of DSCAM overexpression on tectal neuron morphology. To manipulate DSCAM expression in individual tectal neurons, we co-electroporated a Cre driver plasmid with reporter plasmids – pCALNL-TurboRFP (cell-filling dye) and a plasmid coding for Xenopus Dscam tagged with GFP (pCALNL-Dscam-GFP) in stage 42 tadpoles, a manipulation that results in sparse expression of recombinant proteins in the midbrain. Tectal neurons transfected with the Cre driver plasmid driving only pCALNL-TurboRFP were used as controls. Individual neurons were imaged by confocal microscopy 48 h after transfection, at stage 45, to allow enough time for the tectal neurons to express the chimeric and reporter proteins. Tectal neurons were further imaged 24 and 48 h after initial imaging (Fig. 2.5a). Quantitative analysis of three-dimensionally reconstructed dendritic arbors revealed that while tectal neurons overexpressing DSCAM had similar branch number and length at stage 45, the initial imaging period (Control 18.5 ± 3.17, n = 22; DSCAM-GFP 14.9 ± 1.57, n = 20, p = 0.330, Fig. 2.5b), they had a significantly lower dendrite branch number when

compared to TurboRFP-only controls 24 h after initial imaging (Control 32.04 ± 4.26; DSCAM-GFP 19.4 ± 1.74, p = 0.0129, Fig. 2.5b), an effect that was maintained 48 h after initial imaging (Control 36.52 ± 5.007; DSCAM-GFP 24.58 ± 1.55, p = 0.0353, Fig. 2.5b). Similarly, total dendritic arbor length was significantly lower in DSCAM overexpressing neurons by 24 and 48 h after initial imaging (Fig. 2.5c). Quantifying the change in growth rate over the three imaging time points further demonstrates that dendritic arbors of DSCAM overexpressing neurons grew significantly slower than controls (Fig. 2.5d).

The effects of DSCAM overexpression on tectal neuron morphology were also examined in tadpoles co-transfected with plasmids coding for DSCAM only (rather than the chimeric construct) and GFP at stage 22, a manipulation that allowed us to alter DSCAM expression at the onset of neuronal differentiation (see Fig. 2.1j). Confocal microscopy imaging and analysis of neuronal morphology at stage 45 showed that tectal neurons overexpressing DSCAM had significantly fewer dendrite branches than controls (Control 20.0 ± 1.7, n = 11 neurons in 11 tadpoles; DSCAM 11.7 ± 1.6, n = 13 neurons in 13 tadpoles, p = 0.0024) confirming the specificity of the DSCAM overexpression effects. Together, our findings support a role for DSCAM during tectal neuron differentiation and indicate that endogenous DSCAM restricts dendritic arbor development of tectal neurons.

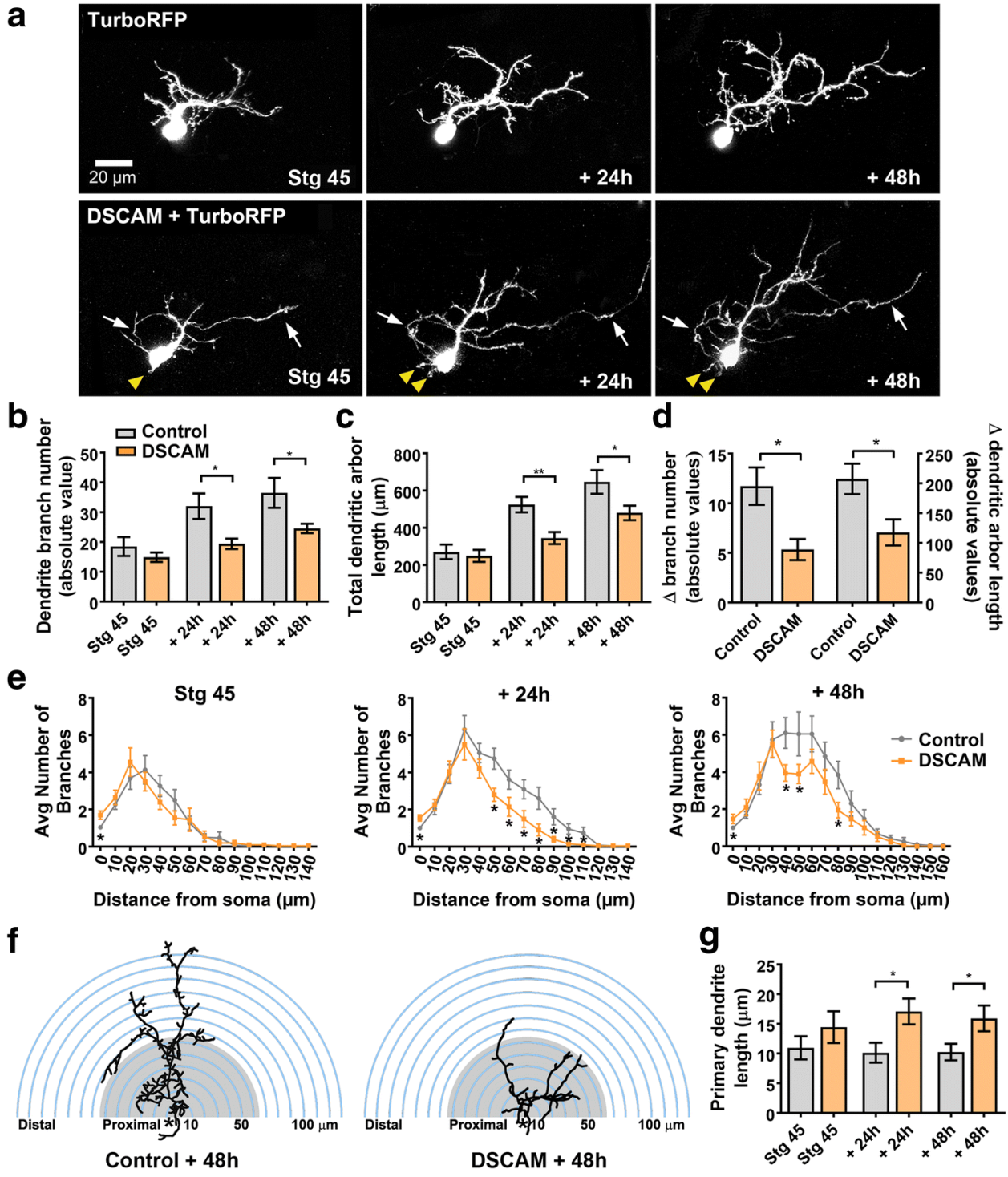

Fig 2.5. DSCAM overexpression decreases the branching and complexity of tectal neuron dendritic arbors. Caption on next page.

Fig 2.5. DSCAM overexpression decreases the branching and complexity of tectal neuron dendritic arbors. a Sample tectal neurons expressing TurboRFP or co-expressing TurboRFP and DSCAM-GFP plasmids at stage 45, and 24 and 48 h after initial imaging (arrows point to axons; yellow arrowheads point to neurites extending from soma). b-d The number of branches and total dendrite arbor length were measured for tectal neurons at stage 45, 48 h after plasmid transfection. Note that neurons overexpressing DSCAM had similar number of branches and total dendrite arbor length at the initial imaging time point but failed to increase their number of branches and their total dendrite arbor length at the rate of TurboRFP-only expressing controls. e, f Sholl analysis revealed a reduction in distal dendrite branches in neurons overexpressing DSCAM 48 h after initial imaging. g Note that while dendrites failed to branch, the length of the primary dendrite of neurons overexpressing DSCAM was significantly higher than controls. TurboRFP only (n = 22 neurons, one neuron per tadpole) or DSCAM + TurboRFP (n = 20 neurons, one neuron per tadpole) Comparisons are by Student's-t-test. Error bars indicate mean ± SEM. * $p \leq 0.05$, ** $p \leq 0.005$, *** $p \leq 0.001$. Scale bars: 20 μm in (a)

Sholl analysis was used as previously to assess the effects of overexpressing DSCAM on dendritic arbor morphology and complexity of tectal neurons. Overexpression of DSCAM in tectal neurons significantly reduced the number of dendritic branch intersections by 24 and 48 h after initial imaging (Fig. 2.5e, f). Interestingly, neurons overexpressing DSCAM had significantly more neurites extending from the soma than controls (Fig. 2.5a, yellow arrowheads), an effect that is reflected by the higher number of branch intersections close to the soma at stage 45 and 24 h after initial imaging (stage 45: Controls 1.045 ± 0.04545, $n = 22$, DSCAM 1.7 ± 0.2306, $n = 20$, $p = 0.0058$; at 24 h: Controls 1 ± 0, DSCAM 1.55 ± 0.1698, $p = 0.0012$). We also observed that despite having an overall simpler arbor morphology, the average length of the primary dendrite, where the dendritic tree predominantly arborizes, was significantly higher in tectal neurons overexpressing DSCAM compared to controls at 24 and 48 h after initial imaging (Fig. 2.5g). Together,

these results support our loss-of-function experiments and indicate that endogenous DSCAM restricts the overall structural growth of higher-order dendrites of developing tectal neurons.

2.5. Discussion

In this study, we examined whether DSCAM directs Xenopus retinotectal synaptic connectivity by guiding the structural development of post-synaptic arbors. To test cell-autonomous roles of DSCAM, we manipulated DSCAM expression in individual tectal neurons. Our results show that DSCAM restricts tectal neuron dendrite arbor growth. We also demonstrate that DSCAM plays a pivotal role in directing dendritic branch pathways of tectal neurons. The effects of altering DSCAM in tectal neurons suggest that the cell-adhesion molecule serves as a limiting factor that confines dendrite arbor growth during development. Overexpression of either a chimeric protein coding for DSCAM tagged with GFP or DSCAM protein alone in single tectal neurons in otherwise intact tadpoles significantly limited dendrite branching and growth, while MO-mediated knockdown of DSCAM expression resulted in exuberant arbor growth. Effects of DSCAM knockdown were unique and robust, as dendrites branched and took on a tortuous path of growth, significantly increasing arbor size and affecting their connectivity. It is therefore possible that restriction of dendritic arbor size and shape mediated by DSCAM is a result of potential repulsive mechanism [41, 72, 74, 90, 91] similar to that facilitated during neuronal tiling [92]. Tiling of arbors are mediated by homotypic repulsive interactions between neighboring cells, limiting arbors to a specific size and space to ensure that arbor

territories do not overlap [66]. This tiling arrangement of arbors typically occurs in a two-dimensional laminar space and is a mechanism that modulates neuronal arbor size [65-68]. For example, targeting DSCAM knockout to mature mouse retina has revealed that bipolar cells expand both their dendritic and axonal fields in the absence of DSCAM, suggesting that DSCAM acts as a signaling cue that restricts dendrite and axon outgrowth to preserve tiled arrangement [16]. In Xenopus, developing neurons do not tile within the tectal neuropil. Tectal neuron dendritic arbors are, however, quite elaborate in three dimensions (average 50–80 μm in depth) and overlap with neighboring arbor fields extensively. Our results therefore indicate that modulating the size of arbor fields developing three dimensionally within the brain may also be a mechanism by which cell surface proteins such as DSCAM control synaptic connectivity of developing neurons in the visual system.

One unexpected finding was that downregulation of DSCAM expression in tectal neurons did not result in perturbation of self-avoidant branch patterning of dendrites. No clear fasciculation of sister dendrite branches among arbors were observed in these neurons, although such phenotype was observed for dendrites of retinal bipolar cells with DSCAM knockdown. In the Drosophila peripheral nervous system, isoform-specific homophilic interactions of DSCAM trigger sister dendrite repulsion. This cellular organization occurs in a stereotypic manner and prevents the overlapping of neuronal dendrites from the same neuron while allowing dendrites from different cells to overlap in the neuropil [13, 70]. Dendritic self-avoidance is made possible due to the thousands of isoforms of

DSCAM that Drosophila can express and that is facilitated through mRNA alternative splicing [8]. Xenopus, as other vertebrate species, is known to express only two isoforms of DSCAM – DSCAM and DSCAML1 – that are coded by two distinct genes. We specifically altered expression of Dscam, the gene implicated in Down syndrome, to study its central function during vertebrate visual system development. Our real time imaging experiments demonstrate that while in Xenopus DSCAM does not mediate self-avoidant organization of dendritic and axonal arbors at retinotectal synapses, it differentially shapes both presynaptic RGC and postsynaptic tectal neuron arbors. In our studies, no clear fasciculation of sister dendrite branches among arbors were observed in tectal neurons with DSCAM knockdown.

2.6. Conclusion

Xenopus laevis was used as a model to examine developmental effects of down-regulating and overexpressing DSCAM in vivo and to provide a unique temporal and spatial understanding of how visual circuits are dynamically shaped. In the Xenopus visual system, endogenous DSCAM modulates arborization of dendritic arbors of tectal neurons by acting as a regulatory cue to restrict dendrite growth and controlling the directionality of individual dendrites.

Chapter 3

DSCAM Modulates Functional Connections in the Xenopus Optic Tectum

3.1. Abstract

Visual avoidance to moving light stimuli in Xenopus tadpoles is correlated with the maturation of visual responses in the optic tectum. Deficits in visually guided behavior, in turn, have been correlated with abnormal visual system wiring. The functionality of the Xenopus visual system can be assessed with behavioral tasks that focus on the animals' ability to avoid approaching visual stimuli, making it an ideal model to correlate the effects on neuron morphology with potential changes in visual functionality. In this study, we examined the behavior of tadpoles in a visual avoidance task after downregulating DSCAM levels in tectal neurons. Striking functional deficits mediated by tectal DSCAM knockdown were found using visually guided behavioral assays in swimming tadpoles, revealing significant deficits in normal visual circuit function. In addition to assessing visually guided behavior in tadpoles with DSCAM knockdown, we indirectly correlated structural dendritic changes to synaptic changes by examining VGLUT/VGAT expression as a proxy of synaptic changes in tectal neurons. We found that altering levels of DSCAM affects the balance of both VGLUT excitatory and VGAT inhibitory synapses in the optic tectum.

3.3. Introduction

Visual information from the surrounding environment is filtered and processed in the tectum. This information is then further relayed to motor systems, such as in the brainstem, where behavioral responses are produced. Retinotectal circuits in the tectum formulate the premotor commands that influence visual avoidance behavior – where moving visual stimulus perceived as a threat or "predator" triggers tadpoles to swim away from the object. Ablating the tectum abolishes motor visual avoidance [80]. While the bulk of my dissertation explores the work of DSCAM in the anatomical development of retinotectal circuits in the optic tectum, it is clear that proper structural development of the circuit affects how visually guided functions are executed. Part of my dissertation explores this physiological aspect of development and how premotor functions emerges from proper formation of dendritic arbors of tectal cells – the primary cells in charge of processing and relaying visual information to executive brainstem motor circuits. Results from the previous chapter demonstrate how DSCAM plays a role in the structural development of dendritic arbors of retinotectal circuits. I further address how perturbing this morphological development by DSCAM knockdown affects the performance of visually guided responses in freely swimming Xenopus tadpoles.

As previously mentioned, abnormal wiring of neural circuits can disrupt proper physiological neural functions. It is interesting to note that circuit assembly is not a straightforward process; it is a complex ongoing process that requires many constructive steps. Each step heavily depends on an array of molecular signals to

execute proper construction. Interestingly, a single type of molecule, such as DSCAM, plays reoccurring roles in many of the events that take place in development. DSCAM can collaborate with many cell surface proteins and diffusible ligands to help construct many of the different wiring events that takes place in circuit assembly. It becomes increasingly apparent how disruption of this one heavily involved molecule can lead to the disruption of circuit connectivity – whether it would be by axons mistargeting, axonal or dendritic arbors aberrantly forming, or improper synaptic connections being made. If the majority of these key constructive events are not properly executed, disorders such as autism, schizophrenia, or neuropsychiatric intellectual disabilities can emerge and be a serious consequence of faulty neural circuits [7].

In a study conducted by Dr. María Luz Montesinos and colleagues, the overexpression of DSCAM was shown to inhibit the branching of dendrites in the hippocampus' of Ts1Cje mice, a model of DS [93]. In wild type mice, DSCAM dendritic translation was induced by NMDA treatment, an excitatory neurotransmitter that activates glutamatergic synapses. However, in Ts1Cje mice, DSCAM translation was unaffected. An explanation for this effect is that the saturation signaling of the NMDA receptor (NMDAR) caused local DSCAM translation to be increased in wild type mice but not in mice with excess DSCAM. The authors from this specific study focused on understanding NMDA's role in regulating the translation of DSCAM in dendrites. Findings from this work suggest that DSCAM may be expressed at NMDAR excitatory synapses. It has yet to be shown whether altering DSCAM levels will affect the balance of excitatory and inhibitory

synapses in developing neurons. Nonetheless it has been shown in mouse models of DS that chromosome triplication led to faulty neurogenesis which causes a distorted imbalance of inhibition and excitation [94]. This chapter aims to explore and understand how the alteration in DSCAM expression in early development of the visual system of Xenopus laevis is involved in effecting the balance of inhibitory or excitatory synapses.

Here I show that Xenopus tadpoles alter their behavioral avoidance response to visual stimuli after downregulating DSCAM levels in tectal neurons, providing evidence that structural cell-autonomous changes in tectal neuron dendritic arbor morphology can impact their connectivity and in turn influence visual information processing in the developing retinotectal system, further confirming previous studies down in our lab [63]. This change in behavior and structural dendritic morphology is also correlated with a change in the balance of inhibitory and excitatory retinotectal synapses.

3.3. Methods

Immunohistochemistry

Immunohistochemistry of stage 45 tadpoles injected with fluorescein-tagged DSCAM or Control MO at the four-cell stage or electroporated at stage 43 was also used to determine synaptic changes by immunostaining with antibodies to vesicular glutamate transporter 2 (VGLUT2; 1:200 dilution, guinea pig polyclonal antibody; EMD Millipore, #AB2251) and vesicular GABA transporter (VGAT; 1:100 dilution, rabbit polyclonal antibody; Phosphosolutions, #2100-VGAT). Alexa 568 anti-rabbit and Alexa 633 anti-chick

secondary antibodies were used to visualize VGLUT and VGAT immunoreactivity respectively. To obtain a change in VGLUT or VGAT ratio, fluorescence intensity was quantified in individual cryostat sections imaged by confocal microscopy at the three wavelengths from at least five regions of interest (each ROI = 30 × 30 μm) per brain hemisphere where fluorescein-tagged MO was localized. Fluorescence intensity values for each wavelength were normalized for each brain section to compare fluorescence intensity in the area/hemisphere without MO label (contralateral side) with the corresponding area/hemisphere with the MO label (ipsilateral side). Specifically, to standardize fluorescence intensity across sections and animals, fluorescence intensity measures were normalized per brain section by averaging the pixel intensity values for all ROIs in the hemisphere without MO label (contralateral side) in that section, normalizing the average intensity value of the "contralateral side" to 100, and recalculating pixel intensity values for each individual ROI (contralateral and ipsilateral sides) within each brain section. Normalized values for six individual sections, each from an individual tadpole per treatment, obtained from two independent experiments were used for statistical comparison (Student t-test).

Visual avoidance task

Stage 45 tadpoles were placed in a 60 mm × 20 mm clear plastic petri dish, with darkened walls, filled to a depth of 1 cm with modified rearing solution at room temperature. The dish was placed on a CRT monitor screen and a solid, opaque box was placed over the monitor to eliminate outside light. A camera was affixed to the opening at the top of the box for video recording. Visual stimuli were produced by a

custom-written Matlab program (MathWorks, Natick, MA, USA) generously donated by Dr. Carlos Aizenman, Brown University. A black circle with radius 0.3 mm was projected in the center of a circle on a white background. This size was found to produce optimal responses to the stimulus as shown in [63]. The circle was then manually directed to collide with the path of the swimming tadpole every 30 s for six trials. The tadpole's responses to the circle, when the dot approached the tadpole and when the dot returned to the dish center, were analyzed blind to treatment with frame-by-frame replay of recorded responses. Tadpoles were observed to both freeze and swim away by altering their direction, speed, or both when presented with stimuli. These responses were counted as visual reactions to the stimuli. Failure to move away from the circle or a lack of freezing behavior prior to when the circle encountered the tadpole was considered a failure to respond. Experiments were performed during the 12-h light cycle. Treatments were identical to those of in vivo imaging studies with the exception that tadpoles were injected in the ventricle and laterally in the subpial space overlying both tectal hemispheres. Only tadpoles that responded to at least 50% of the visual stimuli at 0 h were included in the analysis. The behavior of a total of 16–26 tadpoles was analyzed per condition: 16 controls uninjected, 25 vehicle-injected, 14 Control MO-treated, 26 DSCAM MO-treated. Student's t-tests and one-way ANOVA with Tukey's multiple comparison tests were used for the statistical analysis of the data. Results of behavioral analysis were considered significant as follows: *$p \leq 0.05$, **$p \leq 0.005$, ***$p \leq 0.001$.

3.4. Results

Altered DSCAM expression in the optic tectum impacts visual avoidance behavior

To correlate structural changes in tectal neuron morphology mediated by DSCAM missexpression with potential functional changes, we used a modified avoidance task adapted to probe specific visual responses of tadpoles at stage 46. This behavioral assay assessed the effects of downregulating DSCAM levels bilaterally in the optic tectum by targeting the MO transfection specifically to the caudal midbrain (Fig. 3.1a). Between stages 44 and 47, tadpoles begin to show an avoidance response to moving visual stimuli that is mediated by the maturing retinotectal circuit, which correlates with changes in response properties of tectal neurons [27]. Tadpoles naturally freeze or swim away rapidly when presented with visual stimuli (Fig. 3.1b). Tadpoles with targeted DSCAM MO electroporation into the optic tectum at stage 45 showed significant deficits in visual responses at stage 46, 24 h after transfection (Fig. 3.1c). DSCAM MO knockdown significantly decreased the tadpoles' avoidance behavior when compared to tadpoles transfected with Control MO at the same stage, and with control uninjected or vehicle injected tadpoles (Fig. 3.1c). No change in swim time was observed for any of the groups tested (not shown). The altered response to visual stimuli therefore indicates that structural cell-autonomous changes in tectal neuron dendritic arbor morphology can impact their connectivity and in turn influence visual information processing in the developing retinotectal system.

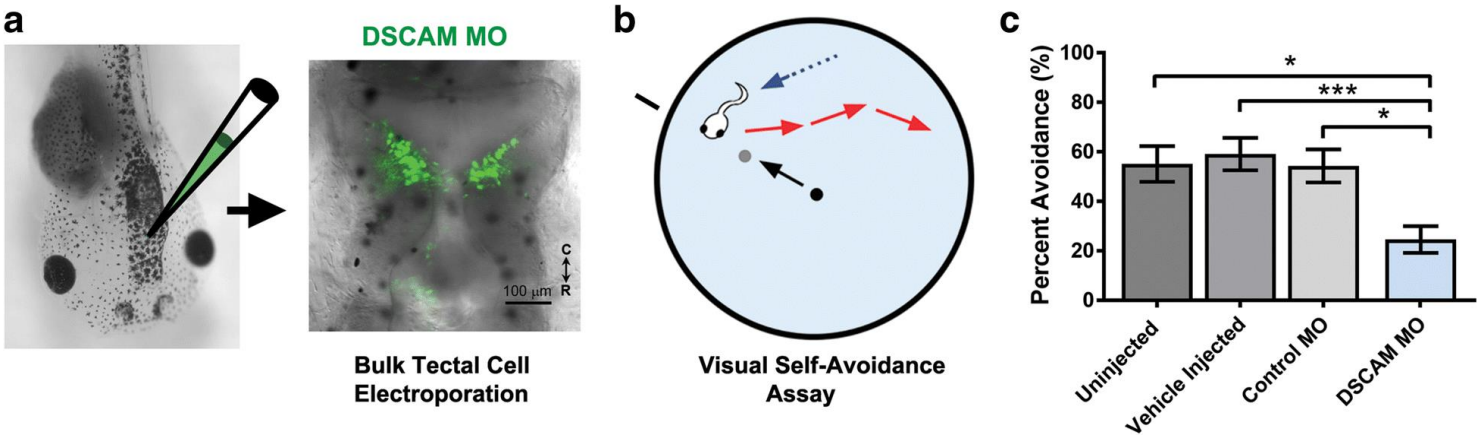

Fig 3.1. Downregulation of DSCAM expression in the optic tectum affects visually guided behavior. a Fluorescein-tagged Control MO or DSCAM MO was bulk electroporated into the caudal midbrain region of stage 43 tadpoles. Fluorescence microscopy imaging was used to confirm bilateral MO transfection into the optic tectum at stage 45. b Schematic of the visual avoidance task. The tadpole's response to the advancing stimuli (black to gray circle) results in the tadpole changing its swimming direction (red arrows). c Tadpoles electroporated with DSCAM MO had decreased avoidance responses to the presentation of the stimulus 24 h post-treatment when compared to uninjected controls, vehicle injected controls, and Control MO electroporated tadpoles (Student's t-test). Error bars indicate mean ± SEM. * $p \leq 0.05$, ** $p \leq 0.005$, *** $p \leq 0.001$. Scale bars: 100 µm (a)

To further analyze whether structural and functional changes in retinotectal connectivity caused by DSCAM dysregulation correlate with synaptic modifications in the circuit, we determined potential changes in excitatory and inhibitory inputs by immunostaining with antibodies to vesicular glutamate transporter 2 (VGLUT) and vesicular GABA transporter (VGAT) in stage 45 tadpoles. Knockdown of DSCAM expression in embryos at the four-cell stage resulted in a significant increase in VGLUT immunoreactivity in the stage 45 tectal hemisphere where the DSCAM MO fluorescein tag localized (20% relative increase in VGLUT immunofluorescence intensity in hemisphere ipsilateral to MO label

versus contralateral side, Control MO, Fig. 3.2a, c; DSCAM MO, Fig. 3.2b, d, f). Moreover, targeted DSCAM MO electroporation into the optic tectum at stage 42 resulted in a more significant increase in both VGLUT and in VGAT immunoreactivity in midbrain regions with DSCAM MO label when compared to the contralateral (non-transfected) side of the same tadpoles (Fig. 3.2e, g). These results indicate that synaptic alterations in excitatory and inhibitory inputs as well as in excitatory to inhibitory balance accompany the changes in tectal neuron dendritic arbor morphology. The observation that altered synaptic connectivity accompanies DSCAM downregulation supports the effects of single-cell MO treatment and indicates that MO-mediated knockdown results in rapid changes in connectivity that may be compensated, at least in part, as neurons and/or the circuits mature.

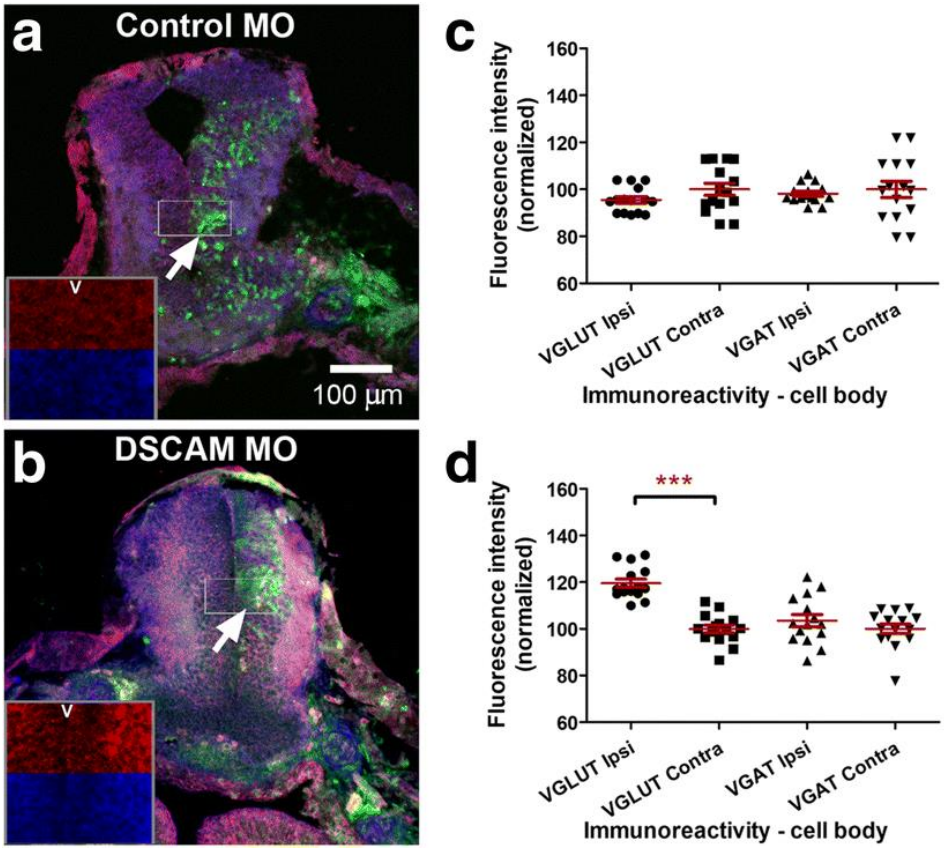

Fig 3.2. DSCAM downregulation alters excitatory to inhibitory synaptic ratios. Figure continued on next page. a, b Fluorescein-tagged Control MO or DSCAM MO (green) were injected into the light-shaded blastomeres of 4-cell stage embryos; animals were raised to Stage 45. Stage 45 morphant tectal tissues were immunostained with antibodies targeting vesicular glutamate transporter (VGLUT, red) and vesicular GABA transporter (VGAT, blue). Levels of VGLUT and VGAT immunoreactivity were quantified in midbrain regions with MO (right hemisphere-ipsilateral side; white arrows in (a and b) and were compared to the contralateral side (left hemisphere) where MO was not present. Fluorescence intensity for VGLUT (red, top) and VGAT (blue, bottom) immunoreactivities in both hemispheres is also illustrated by the magnified inserts where the ventricle (v) demarcates the separation between the ipsilateral and contralateral sides. c No significant differences in VGLUT or VGAT fluorescence intensity were detected between the ipsilateral side with control MO and the contralateral side without MO. d A significant increase in VGLUT intensity was observed along the cell body layer on the ipsilateral side of the tectum treated with DSCAM MO compared to the contralateral side without MO.

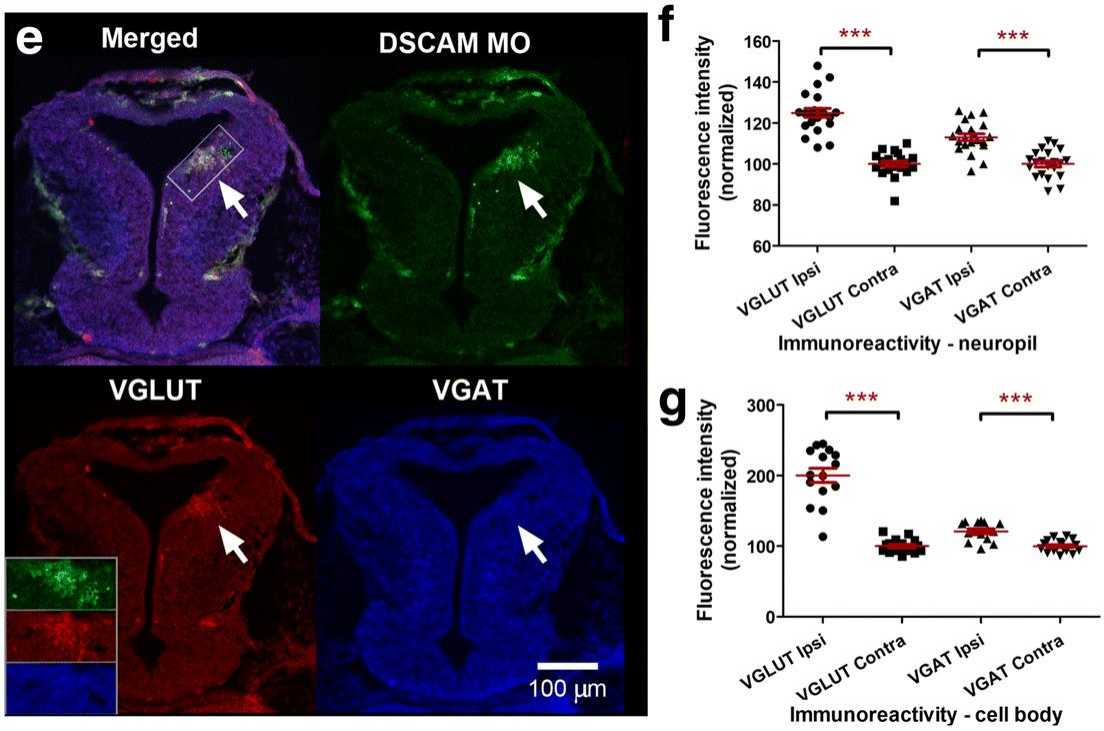

Fig 3.2. Continued. DSCAM downregulation alters excitatory to inhibitory synaptic ratios. f VGLUT and VGAT immunoreactivity was also increased in the neuropil ipsilateral to the DSCAM MO label. e Targeted bulk electroporation was used to focally transfect fluorescein-tagged Control MO or DSCAM MO into the tectum of stage 42 tadpoles; animals were then raised to stage 45 to compare levels of VGLUT and VGAT via immunohistochemistry. The difference in fluorescence intensity in VGLUT (red) and VGAT (blue) immunoreactivity in neighboring areas with and without the DSCAM MO fluorescein tag (green) is illustrated in the overlap and by separating the individual channels (see also the magnified insert; bottom left). g Note brain regions electroporated with DSCAM MO exhibited an increase in VGLUT and VGAT intensity relative to the contralateral non-MO side (Student's t-test). Error bars indicate mean ± SEM. *** $p \leq 0.001$. Scale bars: 100 µm in (a, b, e)

3.5. Discussion

Dysregulated DSCAM expression in the optic tectum resulted in changes in visual behavior of tadpoles that may not only be explained by the structural changes in tectal neurons but also by synaptic changes within the circuit. Proper synaptic transmission across circuits depends, at least in part, on the morphology of dendritic arbors [95, 96]. Studies investigating the physiology of circuits have demonstrated that structural dendritic arbor changes affect neuronal excitability [97-99]. In addition to assessing visually guided behavior in tadpoles with DSCAM knockdown, we indirectly correlated structural dendritic changes to synaptic changes by examining VGLUT/VGAT expression as a proxy of synaptic changes in tectal neurons. Our results demonstrate that synaptic changes in excitatory markers (VGLUT) in the optic tectum are more significant than the changes in inhibitory markers (VGAT) and accompany the exuberant changes in dendritic growth of tectal neurons when DSCAM expression is downregulated. Thus, reduction in DSCAM expression can alter synaptic balance and neuronal excitability of tectal neurons – either by directly modulating glutamate receptors or VGLUT/ VGAT transmission at the synapse, or indirectly by changing the structural pattern of dendritic arbors which can consequently affect visual responses corresponding to tectum-dependent visual behavior. It is possible that DSCAM signaling may also be acting on multiple mechanisms simultaneously, coordinating transmission at the synapses and patterning the structure of dendritic arbors at the cellular level, like in Aplysia, where DSCAM signaling can directly modulate neuronal activity at the

synapse by altering glutamate receptor expression during learning-related synapse formation [100].

A leading cause of abnormal cognitive and sensory disabilities in individuals with Down syndrome has been attributed to aberrant changes in neuronal wiring during human embryonic development. It is therefore possible that DSCAM overexpression may contribute to changes in early neuronal wiring at multiple levels along the visual pathway that significantly affect cognitive and sensory functions later in life [54]. Indeed, infants with Down syndrome show deficits in spatial visual acuity and contrast sensitivity that have been linked to abnormal wiring of visual circuitry [54, 101].

3.6. Conclusion

We found that decreasing DSCAM levels negatively affected the ability of tadpoles to react to an approaching visual stimulus without affecting the total time that tadpoles spent swimming, suggesting that DSCAM signaling is necessary for normal visual system function. We further correlate these visually-guided behavioral deficits with changes to excitatory to inhibitory synaptic ratios.

Chapter 4

DSCAM Differentially Shapes Dendritic and Axonal Arbor Morphology in the Xenopus Developing Visual System

4.1. Abstract

Retinal ganglion cells (RGCs) and bipolar cells (BCs) are two key cell types that process visual information in the vertebrate retina. Proper design of dendritic and axonal arbors from both cell types is critical for information to be efficiently carried throughout the visual circuitry. Developing neurons rely on an array of molecular cues to shape arbor morphology, but the underlying mechanisms guiding the differentiation of dendritic and axonal arbors from the same retinal neuron remains unclear. Here we explore how Down Syndrome cell adhesion molecule (DSCAM) differentially shapes the dendritic and axonal morphology of RGCs and BCs in the Xenopus visual system. In this chapter we showed that lowering DSCAM expression in RGCs impacts axon branching in the midbrain of Xenopus embryos. RGC axon arbors with DSCAM knockdown had a similar initial number of terminal axon branches as controls, but over 48 hrs of imaging failed to significantly increase their number of branches. Our results suggest that DSCAM has a cell-autonomous role in facilitating axonal arbor development. Because DSCAM also localizes to the dendrites of RGCs, altering DSCAM levels in RGCs may influence dendritic arbor development as well. To determine effects of DSCAM downregulation on dendritic arbor development in RGCs, we measured the total number of branches and branch length of RGCs electroporated with either control anti-sense oligonucleotide

morpholino (MO) or DSCAM MO. Confocal microscopy of retinal sections showed that the number of branches and the total length of the dendritic arbors of RGCs with DSCAM MO-mediated knockdown were not significantly different from those of control MO transfected RGCs. In contrast, analysis of BCs revealed that downregulation of DSCAM in retinal BCs resulted in significant morphological changes, with neurons possessing a significantly higher number of dendritic branches and longer total dendritic arbor length when compared to control MO transfected BCs. To further evaluate potential effects of DSCAM downregulation on dendritic arbor morphology on developing Xenopus retinal cells, we quantified the number of dendrite crossings and of dendrites that overlap in both RGCs and BCs with DSCAM MO-mediated knockdown. Only BCs showed deficits in dendrite self-avoidance, therefore demonstrating differential effects of DSCAM downregulation that depend on the cell type. Together, these results indicate that in the vertebrate visual system, endogenous DSCAM acts at multiple levels along the visual pathway and independently modulates dendrite and axon arborization, where cell-autonomous roles vary depending on the neuronal population.

4.2. Introduction

During retinotectal circuit wiring, retinal axons innervate and arborize at the optic tectum. Locally secreted factors found at the axon termination site can act as a growth-promoting signaling cues to initiate and facilitate axon branching along the main retinal arbor. Brain derived neurotrophic factor (BDNF) and its high affinity receptor TrkB has been established as key signaling molecules involved in stimulating axon branch growth

[48]. BDNF ligands are expressed uniformly throughout the tectum, with a sub-population of retinal axons expressing TrkB receptors. Studies from our lab have shown that injection of exogenous BDNF into the tectum increases the complexity and branching of retinal terminal arbor, while sequestering BDNF using neutralizing antibodies reduces axon arborization. Interestingly, not all RGC axons respond to BDNF growth-promoting effects due to a sub-population of axons not expressing the TrkB receptor [21, 102], implying that additional signaling cues are also involved in directing specific axonal arborization.

While growth-promoting factors are at work, local inhibitory signaling cues are also present during axon development. Inhibition provides an important regulatory mechanism that restricts branching to a topographic-specific site. Several key studies have shown that the same ephrin and Eph signaling used for retinotopic mapping is also used to control specific arborization by restricting RGC axon branching [49-51]. However, an important note to understand is that ephrin signaling alone does not exclusively generate branching of RGC axons at a specific anatomical site. Currents studies have suggested that ephrin signaling coordinates with BDNF to control retinal axon branching. Coupling of branch-promoting factors with regulatory mechanisms that restricts branching allow for precise retinotopic mapping.

Previous work from our lab have shown that netrin-1 signaling, mediated through its receptor Deleted in Colorectal Cancer (DCC), promote arborization of retinal axons in

the developing Xenopus tectum [52, 53]. The effects of netrin-1 are similar to BDNF, where both ligands increase arbor complexity of retinal axon arbors. Netrin-1, in contrast, is a prominent chemoattractant that works with several receptors. Crosstalk between netrin-1 and multiple receptors allows for different roles to be performed – including axon guidance, arborization, and synapse maturation. This is generally a reoccurring theme that emerges in development where different combinations of neurotrophins, chemoattractants, and local inhibitory cues are all at work guiding the developing circuit pathway. Important crosstalk among these signaling cues orchestrates connectivity, which allows a single molecule to contribute to multiple events in circuit development.

Several emerging studies have revealed DSCAM as a novel netrin receptor mediating axon development [10, 54-56]. Previous work has shown that DSCAM, in collaboration with DCC, directs turning responses of spinal commissural axons to netrin-1 signaling [54]. These studies, performed on mice, originally identified DSCAM as an axon guidance cue but never explored DSCAM's role in the differentiation and arborization of retinal axons, events that occur after axon pathfinding. This chapter explores this question on whether DSCAM modulates arborization of axons located in the central midbrain and cells in the retina.

4.3. Material and Methods

Animals

Xenopus laevis tadpoles were obtained by in vitro fertilization of oocytes from adult females primed with human chorionic gonadotropin and raised in rearing solution [60 mM NaCl, 0.67 mM KCl, 0.34 mM Ca(NO3)2, 0.83 mM MgSO4, 10 mM HEPES, pH 7.4, and 40 mg/l gentamycin] plus 0.001% phenylthiocarbamide to prevent melanocyte pigmentation. Tadpoles were anesthetized during experimental manipulations with 0.05% tricaine methanesulfonate (Finquel; Argent Laboratories, Redmond, WA, USA). Staging was performed according to Nieuwkoop and Faber [13]. Animal procedures were approved by the Institutional Animal Care and Use Committee of the University of California, Irvine (Animal Welfare Assurance Number A3416–01).

Transfection of Morpholinos in RGCs

Downregulation of DSCAM expression was performed using lissamine-tagged morpholino anti-sense oligonucleotides (300 nmol, Genetools, Philomath, OR, USA) to block protein translation. A morpholino (MO) against Xenopus laevis Dscam mRNA was designed with the sequence 5′-ACATATAAGACTTCGACAGAGACGT-3′. Targeted downregulation of DSCAM expression in RGCs was achieved using single-cell electroporation in developing Xenopus tadpoles [14]. Prior to electroporation, tadpoles were anesthetized with 0.05% tricaine methanesulfonate. A CUY-21 edit stimulator was used to electroporate and transfect individual RGCs of stage 43 tadpoles (20 V, 1 ms pulse duration on, 1 ms pulse duration off, set to repeat 99 times). RGCs were

electroporated with lissamine-tagged DSCAM MO (150 nM pipette concentration) and a cell-filling dye Alexa Fluor 488 Dextran, 3000 MW (2 mg/111 µl pipette concentration, Invitrogen, Eugene, OR, USA). Reagents were loaded onto an aluminosilicate capillary glass tube (AF100–64-10, 1.00 mm, 0.64 mm, 10 cm) with a pulled tapered-tip with an opening of about 0.5 µm. Neurons transfected with a standard lissamine-tagged control MO (150 nM pipette concentration) and 488 dextran were used as a control comparison with DSCAM MO transfected neurons. Co-transfections of lissamine-tagged morpholinos and Alexa 488 dextran was confirmed via fluorescence microscopy. For DSCAM downregulation in retina, Control or DSCAM MO was pressure injected into both the left and right eyes of anesthetized stage 42 tadpoles. Directly after the microinjection, tadpoles were electroporated with 20 V at both normal polarity and reversed polarity with the CUY-21 edit stimulator. Tadpoles were then left in a 12-h light-dark cycle at 22 °C until stage 45 (~ 2 days later).

In vivo confocal microscopy imaging

Stage 45 tadpoles were anesthetized with 0.05% tricaine methanesulfonate prior to imaging, were mounted in a custom-made sylgard chamber during imaging, and were then allowed to recover in fresh rearing solution immediately after imaging. Neurons co-transfected with lissamine-tagged morpholinos and Alexa 488 dextran were imaged in real time using an LSM780 confocal microscope (Zeiss) over the course of 3 days, at 24-h intervals. The LSM 780 confocal microscope is equipped with a MaiTai Ti:Sapphire multiphoton laser system. A two-photon wavelength of 760 to 780 was used to image the Alexa 488 cell-filling dye in RGC axons in the midbrain. For analysis of RGC and bipolar cell dendritic morphologies, tadpoles with retinal MO transfections were reared until stage 45 (48 h post-injection), euthanized with tricaine methanesulfonate, then fixed in 4% paraformaldehyde overnight at 4 °C and transferred to 30% sucrose for at least 1 h to overnight in 4 °C. Tadpoles were immersed in OCT embedding compound and 60 µm thick cryostat sections were obtained. Slides were then coverslipped with ProLong™ Gold Antifade Mountant with DAPI to label nuclei and differentiate between the retinal layers. For arbor analysis, images of the retina were taken with a 63× oil-immersion objective using a Zeiss Pascal laser scanning confocal microscope equipped with a HeNe laser. Images were collected in a 0.5 µm interval throughout the extent of the dendritic arbor (z-axis).

Neuronal arbor analysis for RGC axons

In brief, three-dimensional images of fluorescently-labeled axonal and dendritic arbors were manually reconstructed using a Neuromantic tracing software blind to treatment. Alexa 488 dextran-labeled RGC axon arbors were also reconstructed using Neuromantic. Each axonal arbor was reconstructed plane-by-plane from the image stack and was then analyzed using the Neuromantic software. Branch tips were identified as the terminal ends of primary axons and dendritic arbors. The total arbor lengths, branches, and branch tips of reconstructed arbors were thresholded, binarized, and skeletonized with the Neuromantic software so that the soma perimeter and dendrites were represented as a single pixel width. Processes of more than 5 μm in length were considered branches, while processes less than 5 μm were categorized as filopodia. Statistical analysis was performed as described [63]. Additionally, ImageJ was used for three-dimensional Sholl analysis of reconstructed arbors. A radius step size of 10 μm intervals were used for both dendritic and axonal arbor measurements. For axonal arbors of RGCs, Sholl analysis was quantified 5 μm from the main branch point of the primary axonal stem. Sholl branch-tip distributions were compared across experimental groups and two-way ANOVA statistical analysis of data was performed. Neuromantic data and Sholl analysis results were considered significant in comparison to control as follows: *$p \leq 0.05$, **$p \leq 0.005$, ***$p \leq 0.001$, unless otherwise indicated on the graph with bars marking additional significant comparisons.

4.4. Results

Retinal ganglion cells exhibit stunted axon branching in response to downregulation of DSCAM levels

DSCAM protein expression localizes to both the retina and optic tectum of developing Xenopus tadpoles (results from Ch. 2., Fig. 2.1) and could therefore also affect synaptic connectivity in the retinotectal system by acting presynaptically. To investigate whether DSCAM independently modulates the targeting and branching of developing presynaptic retinal axon arbors, we examined the effects of DSCAM downregulation in individual RGCs. Co-electroporation of DSCAM MO and Alexa 488 cell-filling dextran in single RGCs of anesthetized tadpoles was used to downregulate DSCAM expression at stage 43, when RGC axons target and begin to branch in the optic tectum. In vivo two-photon confocal microscopy imaging of individual RGC axons 24 h after MO transfection, at stage 45, showed no targeting errors in axons from either DSCAM MO or Control MO transfected RGCs. Axons from RGCs with DSCAM downregulation projected normally to the contralateral tectal neuropil (Fig. 4.1a). However, both qualitative and quantitative analyses of axons imaged over the course of 3 days showed limited axonal arbor growth in axons of RGCs with DSCAM MO-mediated knockdown. RGC axon arbors with DSCAM knockdown had similar number of terminal branches as control at the first imaging time point but over the course of the 48-h imaging period failed to significantly increase their number of branches (Fig. 4.1b). While axon arbors of RGCs with DSCAM knockdown continued to lengthen over the 48-h imaging period (Fig. 4.1a, c), axon arbors exhibited a significant slower growth rate relative to axons of RGCs

transfected with Control MO (Fig. 4.1d, change in branch number and length). Even though axons from RGCs with DSCAM knockdown extended fewer branches over the 48-imaging period, Sholl analysis revealed that the overall distribution of terminal branches of RGC axonal arbors treated with DSCAM MO did not differ from that of RGC axon arbors transfected with Control MO (Fig. 4.1e). Moreover, axon branches from RGCs transfected with DSCAM MO continued to self-avoid (not shown).

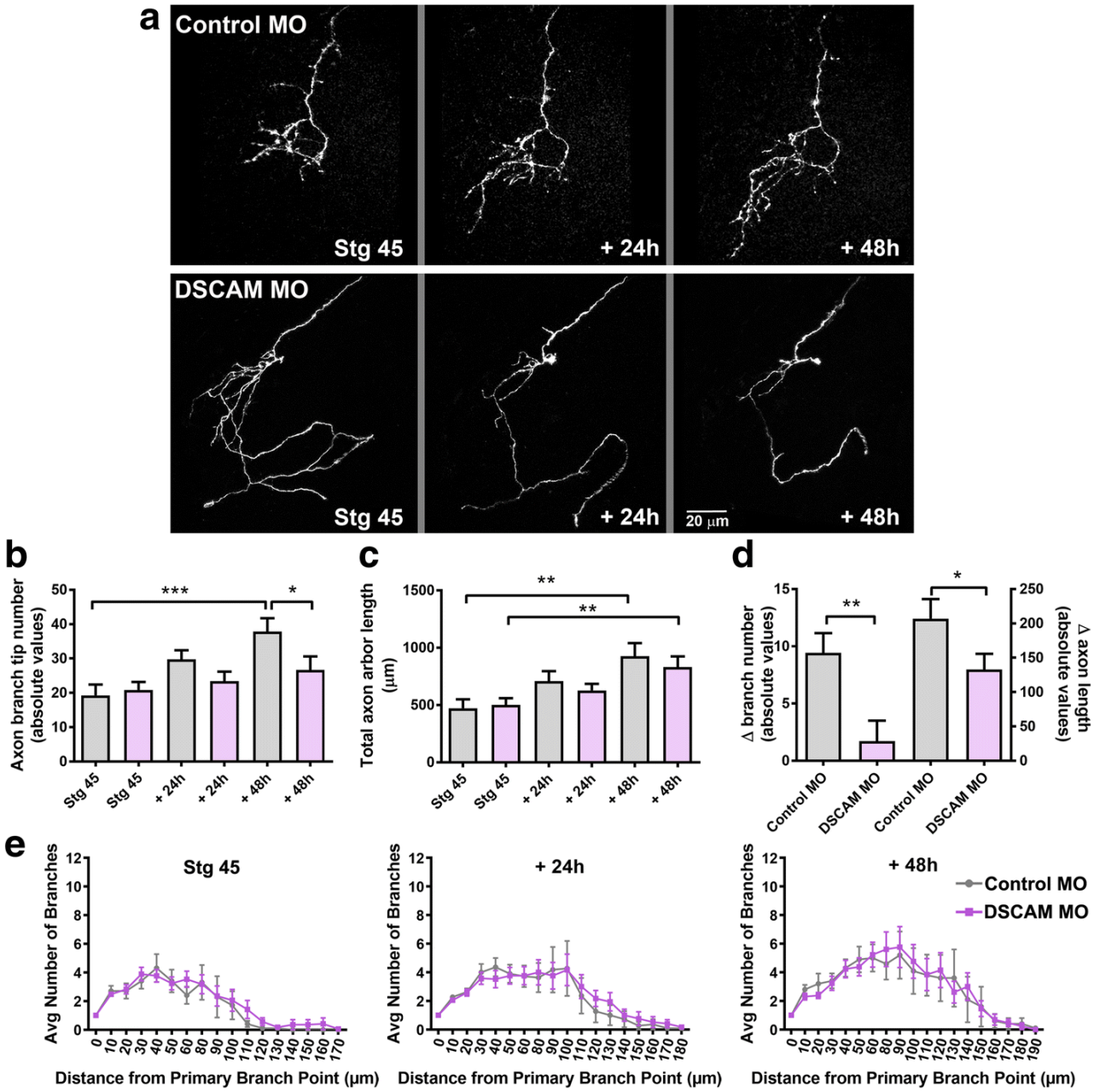

Fig 4.1. DSCAM downregulation decreases RGC axon arbor growth cell autonomously. a Sample of axon arbors from RGCs transfected with Control MO or DSCAM MO together with Alexa 488 dextran and imaged at stage 45, and 24 and 48 h after initial imaging. b-d Quantitative analysis of axon branch number (b) and total axon arbor length (c) demonstrate that in contrast Control MO transfected RGCs, axons from RGCs with DSCAM knockdown failed to increase their number of branches over time, an effect that significantly decreased axon arbor growth rate (d; change in branch number and length). e Sholl analysis revealed no significant differences in the branching patterns of RGC axons with DSCAM knockdown each imaging time point when compared to controls. Control MO (n = 15) or DSCAM MO (n = 18). Comparisons are by Two-way ANOVA and Student's-t-test. Error bars indicate mean ± SEM. * $p \leq 0.05$, ** $p \leq 0.005$, *** $p \leq 0.001$. Scale bars: 20 μm in (a)

To differentiate effects of DSCAM on dendritic differentiation versus axon arborization on the same population of neurons, namely RGCs, we performed bulk electroporation of either control MO or DSCAM MO in retina of stage 41 tadpoles and analyzed dendritic arbor morphology of sparsely labeled neurons 48 h after treatment. Multiphoton confocal microscopy of fixed stage 45 retinal sections showed that the number of branches and the total length of the dendritic arbors of RGCs with DSCAM MO-mediated knockdown were not significantly different from those of control MO transfected RGCs (Fig. 4.2a-c). Because electroporation of MO resulted in the sparse transfection and labeling of neurons in the same retinal tissue, we also analyzed bipolar cell dendritic morphologies to confirm the effectiveness of the treatment. This analysis revealed that downregulation of DSCAM in retinal bipolar cells results in significant morphological changes, with neurons possessing a significantly higher number of dendritic branches and longer total dendritic arbor length when compared to control MO transfected bipolar cells (Fig. 4.2d-g). These observations are consistent with findings on effects of targeted DSCAM knockout on a subpopulation of bipolar cells in the mature mouse retina [16]. To further evaluate potential effects of DSCAM downregulation on dendritic arbor morphology of retinal neurons, we quantified the numbers of dendrite crossings and the number of dendrites that overlap in both RGCs and bipolar cells with DSCAM MO-mediated knockdown. Only bipolar cells showed deficits in dendrite self-avoidance, therefore demonstrating differential effects of DSCAM downregulation that depend on the cell type (Fig. 4.2c, g). Together, these results indicate that in the Xenopus visual system, endogenous DSCAM acts at multiple

levels along the visual pathway and independently modulates dendrite and axon arborization of RGCs.

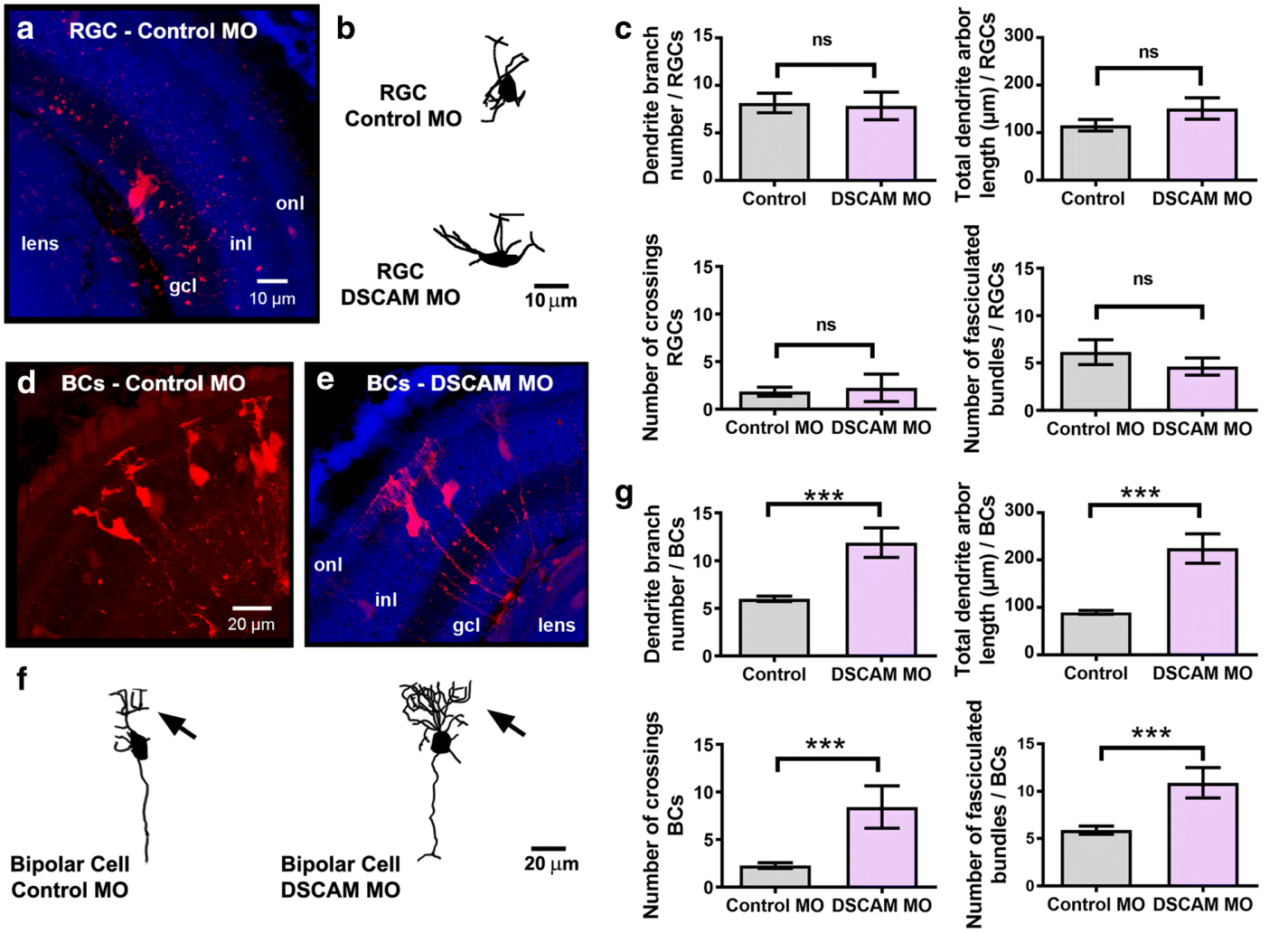

Fig 4.2. DSCAM downregulation differentially influences RGC and bipolar cell dendrite growth. Dendritic morphologies of fluorescently labeled (a-c) RGCs and (d-g) bipolar cells (BCs) transfected with Control MO or DSCAM MO are illustrated by the confocal projections of stage 45 retina cryostat sections (a, d, e) and sample three-dimensional tracings (b, f). Sections in (a and e) were counterstained with DAPI to reveal the retinal layers. Inl, inner nuclear layer; gcl, ganglion cell layer; onl, outer nuclear layer. c The number of dendritic branches, total dendritic arbor length, number of dendritic crossings, and number of fasciculated dendritic bundles of RGCs treated with DSCAM MO (n = 18) were compared to those treated with Control MO (n = 13). No significant differences were found across each category. g Morphological analysis of neurons traced three-dimensionally reveals a significant increase in the number of dendritic branches and total dendritic arbor length of bipolar cells in response to DSCAM downregulation. BCs treated with DSCAM MO also showed a significant increase in the number of dendritic crossings and fasciculated bundles compared to cells treated with control MO. DSCAM MO (n = 28), Control MO (n = 42). Error bars indicate mean ± SEM. ***p < 0.001, or ns for no significance. Scale bars: 10 µm in (a, b); 20 µm in (d-f)

4.5. Discussion

The observation that knockdown of DSCAM expression in Xenopus RGCs decreased axon terminal branching but did not alter dendrite number or induced dendrites to overlap may be due to cell-type and species-specificity of the effects, or alternatively due to the developmental stage of their dendritic arbors or the timing of DSCAM knockdown. Among its multiple functions in the retina of distinct vertebrate species, DSCAM has been implicated in modulating dendrite self-avoidance and in guiding dendrites to stratify in specific synaptic laminae. A role for DSCAM in synaptic lamination of RGC dendrites within the inner plexiform layer was first demonstrated in the developing chick retina through manipulations of Dscam expression, while in Dscam and DscamL1 knockout mice laminar specificity seemed to be preserved [14, 15]. More recent cell-type-specific analyses of DSCAM function have revealed some similarities in DSCAM's role in synaptic lamination of RGC dendrites among vertebrate species, as defects in lamination can be induced by non-autonomous changes in DSCAM expression in mice [103]. The influence of DSCAM in the spatial organization and fasciculation of dendrites of the same cell type has also been demonstrated for retinal neurons in mice through cell-type-specific loss and gain of DSCAM function [14, 104]. In mouse RGCs, the role of DSCAM in self-avoidance appears to be restricted to neurons of the same type, guiding them as they extend processes and encounter the distal processes of neighboring homotypic cells [14, 104]. In stage 45 Xenopus tadpoles, the dendritic arbors of RGCs are still quite immature, extending only a few short dendrites towards a developing inner plexiform layer, thus effects of DSCAM dysregulation on

dendrite fasciculation, branching or shape may not transpire within the short period of MO-mediated downregulation of DSCAM expression. In contrast to their dendrites being unaffected, downregulation of DSCAM expression in RGCs significantly impacted the arborization of their axons at the target at the same developmental stage.

Analysis of mutant mice has shown that both DSCAM and DSCAML1 are involved in dendrite self-avoidance in the retina, with DSCAM influencing bipolar cells, amacrine cells and RGCs [14, 16, 64]. In Xenopus, dendritic arbors of bipolar cells normally self-avoid and arborize compactly in three-dimensional space (Fig. 4.2d, average 8–10 μm in depth). DSCAM knockdown affected these two processes, increasing the number of branches that overlap as well as branch number. Therefore, the effects of targeted DSCAM downregulation in developing Xenopus bipolar cells are consistent with findings of effects of targeted DSCAM downregulation in mature mouse bipolar cells [16].

Several studies using mouse models have shown that DSCAM is implicated in several aspects of optic pathway development. DSCAM has been implicated in the growth of RGC axons from the chiasm to the dorsal thalamus, with axon arrival at the target site being delayed in DSCAM knockout mice [9]. Moreover, analysis of a mouse model of Down syndrome shows that DSCAM organizes the segregation of ipsilateral and contralateral retinal axons in the dorsal lateral geniculate nucleus [42]. These findings suggest that DSCAM promotes RGC axon growth and controls the timing of when RGC axons reach their visual brain target sites. Our studies demonstrate a novel, cell-

autonomous role for DSCAM during RGC axon growth and arborization at their target that is independent of its potential effects on their dendritic arbor. In Xenopus, RGC axons branched and grew at a slower rate within their target neuropil in response to DSCAM downregulation. These effects were opposite to those of DSCAM downregulation in tectal neurons, where dendritic arbors overgrow, and neurons extend multiple axon terminals. While no obvious targeting errors were observed in individual RGC axons with DSCAM knockdown, errors in axons being able to exit the eye were observed when overexpressing DSCAM in developing RGCs of young tadpoles (data not shown), consistent with observations of misdirected RGC axons within the retina of adult DSCAM mutant mice [105]. An instructive role for DSCAM on presynaptic arbor growth that is independent of its effects on dendrites has been demonstrated for Drosophila sensory neurons, where Dscam expression levels and homophilic interactions correlate with patterned presynaptic arbor branching and size [106, 107]. Thus, our findings in developing Xenopus embryos together with studies that analyzed more mature visual circuits in mice support the notion that DSCAM plays a multifaceted role in modulating the growth and timing at which RGC axons reach and arborize in brain targets for precise visual connections to form. These studies also demonstrate that the function of DSCAM on RGC axon terminals is separable from its dendritic functions, at least during early stages of dendritic and axon arbor development.

Multiple complementary molecular and signaling mechanisms are involved in dendrite differentiation and arborization that may vary depending on cell type [108-111]. DSCAM

has been implicated as a netrin receptor that collaborates with DCC and traffics commissural axons across the ventral portion of the spinal cord [54]. Moreover, studies have shown that DSCAM-netrin signaling is involved in mechanisms driving axon attraction towards their target site [54-57]. While DSCAM and DCC collaborate as co-receptors at the axon terminal in the spinal cord [54], roles for DSCAM during dendritic arbor development appear to be independent from netrin signaling, as shown by their differential effects on the targeting of dendrites in the Drosophila CNS [49, 50]. In the Xenopus visual system, netrin signaling is an important factor that modulates several aspects of retinotectal development [52, 53, 63, 112]. Previous work from our laboratory has shown that netrin influences not only pathfinding, branching, and synaptic differentiation of mature RGC axons at their target [52, 53], but also that acute alterations in netrin levels can rapidly induce postsynaptic remodeling of tectal neuron dendritic arbors, with tectal neuron dendrites remaining simple over time and redirecting their directionality of growth when netrin levels are increased or receptor signaling is altered [19]. Our current studies support the idea that DSCAM acts independent of netrin signaling during tectal neuron differentiation rather than as a canonical receptor for netrin-1. Cell-autonomous downregulation of DSCAM expression resulted in neurons with exuberant dendritic arbor growth, an effect that significantly differs from altered DCC-mediated netrin signaling. Downregulation of DCC levels in the optic tectum with function blocking antibodies to DCC [63], and knockdown of DCC expression in single tectal neurons through DCC MO transfection (A.N. Nagel and SCC, unpublished data) both result in altered directionality of dendrite arbor growth, an effect

that differs from the effects of either DSCAM downregulation and overexpression. Thus, our results demonstrate that in the retinotectal system DSCAM is required for proper arbor development of pre- and postsynaptic neurons that are themselves modulated by netrin-dependent signaling, but that DSCAM acts independently of DCC signaling. Whether in RGC axons DSCAM participates, at least in part, in netrin-mediated DCC signaling remains a possibility since downregulation of DSCAM expression in RGCs interfered with RGC axon branching, similarly to effects of altering DCC signaling at the optic tectal target [52, 53].

An emerging concept is that molecules that participate in neuronal wiring and that are aberrantly expressed in Down syndrome may differentially impact multiple cell-types, may affect each cell type at different times in development, and may continue to affect neuronal function even in the adult CNS [16, 105]. Our studies in Xenopus for the first time implicate DSCAM in the control of both pre- and postsynaptic structural and functional connectivity in the developing visual system, where it differentially guides postsynaptic dendrite growth of neurons in the central visual targets while it also facilitates presynaptic arborization of RGC axons acting cell-autonomously. Determining the cell-autonomous contribution of DSCAM to early aspects of neural circuit formation at a single population level in accessible vertebrate animal models can help better understand the pathophysiology of complex neurodevelopmental disorders that affect neural circuit formation and function.

4.6. Conclusion

Xenopus laevis was used as a model to examine developmental effects of DSCAM in vivo and to provide a unique temporal and spatial understanding of how visual circuits are dynamically shaped. In the Xenopus visual system, endogenous DSCAM acts at multiple levels along the visual pathway and independently modulates dendrite and axon arborization, where cell-autonomous roles vary depending on the cell type. Results from Chapter 2 and 4 implicate DSCAM in the control of both pre- and postsynaptic neuronal cytoarchitecture and functional connectivity in the retinotectal circuit, whereby it primarily acts as a neuronal brake to limit and guide tectal neuron dendrite growth. RGC axons at the target are differentially influenced by DSCAM, where DSCAM expression levels positively impact presynaptic arbor size. The cellular mechanisms mediated by DSCAM in shaping tectal neuron connectivity also play a key role in central visual processing. Thus, the wiring of functional neural circuits during embryonic development requires coordinated organization between developing axon and dendritic arbors, a process that is dependent on molecules that have been implicated in Down syndrome and autism, such as DSCAM.

Chapter 5

DSCAM Coordinates Retinal Topographic Order and Stabilizes Retinotectal Synapses

5.1. Abstract

The Xenopus retinotectal circuit is organized topographically, where the dorsal-ventral axis of the retina maps respectively on to the ventral-dorsal axis of the tectum; the nasal-temporal axis of the retina project respectively to the caudal-rostral axis of the tecum. Studies throughout the last two decades have shown that rudimentary mechanisms involving molecular recognition of proper termination domains are at work guiding topographic organization. Such studies have shown that gradient distribution of molecular cues is important for topographic mapping. However, the molecular cues organizing topography along the developing optic nerve tract, as retinal axons cross the chiasm, remains unknown. DSCAM has been thoroughly characterized as a key molecule in axon guidance, making it a strong candidate involved in the topographic organization of retinal fibers along the optic nerve. In this chapter, we traced the projection of ventral and dorsal retinal fibers starting from the eye, followed the optic nerve into the chiasm, and into the Xenopus tectum. We found that DSCAM expression is localized on the ventral posterior region of the optic nerve; this expression pattern coincides with ventral fibers derived from ventral RGCs. I also assessed the effects of DSCAM knockdown on the establishment of retinotopic maps. Knocking down DSCAM levels affects the segregation and proper sorting of medial axon fibers, derived from

ventral RGCs, in the neuropil, indicating that DSCAM plays a role in retinotopic organization. Additionally, we found that DSCAM co-localized post-synaptically to a subset of synapses marked by GFP-Synaptobrevin. When we elevated levels of DSCAM during retinotectal development, by acute exogenous DSCAM treatment, we observed a significant reduction of synaptic connections. Our work, for the first time, shows DSCAM having multiple direct roles in coordinating retinotopic order and establishing selective synapse connections in the developing vertebrate central nervous system.

5.2. Introduction

During embryonic eye development, connections from the retina to the brain are carefully arranged in a preserved spatial manner that creates a topographic map of the visual world. In the amphibian visual system, retinal ganglion cell (RGC) axons project to the tectum in a manner that mirrors the relative positioning of RGCs across the retina – effectively constructing a point-to-point representation of visual space in the brain [24-26]. The formation of precise topographic maps requires active molecular cues guiding specific axon targeting and establishing selective synaptic connections. Studies throughout the last two decades have shown that rudimentary mechanisms involving molecular recognition of proper termination domains are at work guiding topographic organization. Such studies have demonstrated that gradient distribution of molecular cues is important for topographic mapping. In mice, topographic mapping of retinal axons along the anterior-posterior axis of the superior colliculus (equivalent to the tectum in lower vertebrates) relies heavily on repulsive-mediated signaling between

EphA receptors and their Ephrin-A ligands [32-34]. Disrupting the signaling gradient either by knocking out the receptor or the ligand affects topographic ordering, but not entirely [32-34]. Disruption of ephrin signaling, only to a certain extent, shifts axonal fibers posteriorly and others anteriorly [35]. Furthermore, prior to reaching the tectum, retinal axon fibers are already topographically sorted along the optic nerve tract where gradient ephrin signaling has not been reported [36-40]. These findings suggest that graded ephrin signaling does not exclusively shape topography and additional key molecules are involved. The molecular cues organizing topography along the developing optic nerve tract, as retinal axons cross the chiasm, remain unknown.

Histology data gathered during my graduate work surprisingly shows specific Down Syndrome Cell Adhesion Molecule (DSCAM) expression along the ventral and posterior regions of the optic nerve, indicating that a subpopulation of retinal fibers express DSCAM as they navigate the optic tract. DSCAM's role as a receptor for axon growth is evident [8-11, 41], but whether the molecule is involved in the topographic organization of retinal fibers has yet to be investigated. Multiple studies have confirmed DSCAM expression in RGCs and retinal projections along the developing mouse optic nerve [9, 14, 42, 43]. Research done by Erskine and colleagues found that knocking out DSCAM disrupted the timing at which mouse retinal axons arrived at the thalamus, suggesting that DSCAM acts as a permissive signal and mediates growth-promoting interactions that help facilitate retinal axon growth towards their target [9]. In another relevant study, DSCAM was shown to be involved in segregating contralateral retinal projections from

ipsilateral fibers in the dLGN [42]. Though these two studies did not directly test DSCAM's involvement in retinal topography, the implication of their work is that DSCAM may contribute to the specificity of axonal wiring.

Once bundles of retinal axons innervate and target a specific part of the tectum, tightly tethered axon bundles defasciculate and allow individual axons to arborize and form synaptic connections with tectal partners. It is important to note that axon arborization and synaptic formation are closely interdependent events. Synaptic connections formed between interacting axons and dendritic arbors are a major contributing factor to the arbors' growth, size and complexity which, in turn, influences how precise topographic maps are established [61, 62]. Work done as part of my dissertation show that DSCAM acts as a permissive signal that facilitates RGC axon arbor growth into the optic tectum, but whether it is involved in the formation of retinotectal synapses is still unclear. What we know currently about DSCAM in synapse differentiation has mostly been derived from work done in Aplysia neuronal cultures. These studies have taught us that DSCAM interacts trans-synaptically and collaborates with AMPA-like receptors to not only facilitate synaptogenesis, but also maintain the transmission between synapses. It is apparent that such function is necessary in the proper development of dendritic spine growth as confirmed in cortical histology experiments done on mice modeling Down Syndrome.

In this present work, we use the Xenopus tadpole visual system as a model to study the effects of DSCAM knockdown on establishing retinotopic order and synaptic connections in the optic tectum. We trace the projection of ventral and dorsal retinal fibers starting from the tadpole eye, follow the optic nerve into the chiasm, and finally perform real-time confocal imaging of retinal axon arbors in the Xenopus optic tectum. We provide evidence revealing DSCAM expression coinciding with ventral axonal fibers along the optic nerve tract, at the midline of the optic chiasm, and in a gradient of expression that coincides with axonal arbors in the neuropil of the tectum. Downregulating DSCAM levels also affects the segregation and proper sorting of medial axon fibers, derived from ventral RGCs, in the neuropil, indicating that DSCAM plays a role in retinotopic organization. When we elevated levels of DSCAM during retinotectal development, by acute exogenous DSCAM treatment, we observed a significant reduction of synaptic connections. Our work, for the first time, shows DSCAM having multiple direct roles in coordinating retinotopic order and establishing selective synapse connections in the developing vertebrate central nervous system.

5.3. Methods

Animals

Xenopus laevis embryos were obtained via natural mating between adult male and female frogs. Both adult genders were primed with human chorionic gonadotropin (10,000 units; Millipore Sigma) before natural mating. Collected embryos were raised in rearing solution (60 mM NaCl, 0.67 mM KCl, 0.34 mM $Ca(NO_3)_2$, 0.83 mM $MgSO_4$, 10

mM HEPES, pH 7.4, and 40 mg/L gentamycin). Rearing solutions containing embryos was supplemented with 0.001% phenylthiocarbamide (PTU) to prevent melanocyte pigmentation. All embryos were anesthetized during experimental manipulations with 0.05% tricane methanesulfonate (Finquel; Argent Laboratories, Redmond, WA). Staging of embryos was performed according to Nieuwkoop and Faber [90]. Animal procedures were approved by the Institutional Animal Care and Use Committee of the University of California, Irvine (Animal Welfare Assurance Number A341601).

Immunohistochemistry

Stage 45 to 46 tadpoles were euthanized with tricaine methanesulfonate (Finquel MS-222) and fixed in 4% paraformaldehyde in 1x PBS, pH 7.5, for 4 hrs. Tadpoles were cryoprotected in 30% sucrose for 1 hr in room temp, and embedded in OCT compound (Sakura Finetek, Torrance, CA, USA). 40-μm cryostat sections were obtained for both coronal and horizontal tissue. Before primary antibody incubation, coronal and horizontal sections at the level of the optic chiasm were washed with 1x PBST 3 times, 5 minutes each. Sections were then blocked, for 1 hr, using 10% normal goat serum (Antibodies Incorporated), 10% DMSO, 1% Triton X-100 in 1x PBST. Blocking solution was removed and sections were incubated overnight with an antibody against the middle region of human DSCAM (rabbit polyclonal, 1:1000 dilution; Aviva System, San Diego, CA, USA) in staining solution (2% normal goat serum, 10% DMSO, 0.1%Triton X-100, 0.05% sodium azide, in PBST). Brain tissues were washed then incubated in goat

anti-rabbit Alexa 568 secondary antibodies (1:500 dilution; Invitrogen, Eugene, OR, USA) in staining solution. Sections were washed prior to being coated with DAPI.

Whole Brain Clearing

Xenopus-Fast Clearing Technique (X-FaCT) was performed as described in the protocol by Affaticati and colleagues [113]. In brief summary, stage 45 to 46 tadpoles were euthanized with Finquel and fixed in 4% paraformaldehyde in 1x PBST overnight. Tadpoles were washed in 1x PBST and whole heads were dissected. Tissues were first placed in pre-incubation solution 0.5× SSC (150 mM NaCl, 15 mM sodium citrate, pH 7.2), 0.1% Tween 20, and were then incubated in depigmentation solution (5% formamide, 0.5× SSC, 3% H_2O_2) to remove melanocyte pigmentation. Samples were transferred into a 2 mL glass vial and were blocked for 4 hrs at room temp. For localizing DSCAM expression and retinal axons throughout the whole head, tissues were incubated in DSCAM rabbit polyclonal (1:500; Aviva System) and 3A10 mouse anti-neurofilament-associated protein antibody (1:500 Developmental Studies Hybridoma Bank). Goat anti-rabbit Alexa 568 and goat anti-mouse 488 secondary antibodies (both at 1:500; Invitrogen) were used as secondary antibodies, respectively. Tissues were cleared using a fructose–based high–refractive index solution at room temp overnight. Cleared samples were imaged using a LSM780 confocal microscope (Zeiss).

Labeling Retinal Ganglion Cell Axons

To visualize retinotopic organization, ventral and dorsal RGCs axons were labeled by electroporation following a similar protocol developed by Kurt Haas and colleagues [82]. Tadpoles at stage 46 were anesthetized in diluted tricaine methanesulfonate. A custom-made trench, to hold the head of a stage 46 tadpole, was carved out in sylgard (Silicone Elastomer Kit). In the trench, a single embryo was placed laterally on their side and a standard size harp slice grid (ALA Scientific Instruments) was used to hold the embryo in place. The tadpole's right eye was positioned and made available for electroporation. Standard control oligonucleotide morpholinos lissamine-tagged (Gene Tools) were used to label ventral retinal axons, while flouresceinated control morpholinos or 488 Alexa fixable dextran (10,000 MW, Invitrogen) were used to label dorsal axon fibers. Flouresceinated control morpholinos were used for histology work because they labeled axon fibers better; 488 Alexa fixable dextran labeled axon arbors better for in vivo imaging. To alter DSCAM levels in ventral RGCs, a morpholino (MO) targeting Xenopus laevis *Dscam* mRNA was designed with the sequence 5′-ACATATAAGACTTCGACAGAGACGT-3′. Individual reagents were loaded into an aluminosilicate glass electrode (with filament; AF100–64-10, 1.00 mm, 0.64 mm, 10 cm) equipped with a silver wire connected to a Grass SD9 electrical stimulator. An external ground wire, connected to the stimulator, was placed in the sylgard trench dish holding the anesthetized tadpole. For lissamine-tagged morpholino, repeated currents were delivered at 200 Hz, 2 ms delay, 2 ms duration, 20 V until ventral or dorsal RGCs were stained (flouresceinated control morpholinos and 488 Alexa fixable dextran were

delivered at 200 Hz, 4 ms delay, 4 ms duration, 40 V). tadpoles with axons that were labeled properly were used for histology or in vivo imaging.

To assess the effects of exogenous DSCAM treatment on synapse development, retinal ganglion cells axons were electroporated with tdTomato and GFP- synaptobrevin DNA plasmids following a protocol by Falk and colleagues (Electroporation of cDNA/Morpholinos to targeted areas of embryonic CNS in Xenopus). Tadpoles at stage 30-34 were anesthetized in diluted tricaine methanesulfonate. The tadpole's right eye was positioned and made available for pressure injection of DNA reagents and electroporation. GFP-synaptobrevin and tdTomato plasmid DNA (both controlled by CMV promoters) were prepared at a stock concentration of 5-8 µg/µl dissolved in TE buffer using an Endrofree Maxi Prep Kit (Qiagen). Equimolar amounts of both DNA plasmids were loaded into an aluminosilicate glass pipette pulled to a relatively light tapered-tip. Using forceps, the tapered-tip was snipped open. Repeated injections of about 100 nl volume of DNA were pressure-injected into the embryo retina (20 psi, 15 ms duration, Picospritzer). Concurrently, as DNA is being pressure-injected, the surface of the eye was electroporated with a pair of anode and cathode copper electrodes connected to a Grass SD9 electrical stimulator (single currents were delivered at 200 Hz, 2 ms delay, 2 ms duration, 40 V; polarity was reversed after every 5 currents). A total of 15 pressure-injection pulses and single current pulses were delivered simultaneously into the eye. After transfection, tadpoles were raised to stage 45 for in vivo manipulation. Tadpoles with sparse RGC labeling were treated either with

recombinant human DSCAM protein (reconstituted at 500 ng/ul in 0.1% BSA ml 1x PBS sterile, 3666-DS, R&D System) or in 1x PBS. Prior to recombinant DSCAM treatment, axons innervating the contralateral side of the tectum were imaged at a baseline timepoint using a Nikon Confocal microscope. After recombinant DSCAM treatment, tadpoles were further imaged 6, 12, and 24 hours later *in vivo*.

Neuronal arbor analysis

Three-dimensional images of axon arbors labeled with tdTomato were manually reconstructed using a Neuromantic tracing software blind to treatment. Axonal arbors were traced plane-by-plane from the image z-stacks. Traced axonal arbor were represented as a single pixel width. Branch tips were identified as the terminal ends of primary axons. Total arbor length and total branch tips of RGC axon tracings were quantified using the Neuromantic software. To characterize the distribution of synapses across RGC axons we traced, GFP-synaptobrevin puncta were counted plane-by-plane from the confocal image z-stacks. A subset of axons that we traced clearly expressed GFP-Syb for quantitative analysis. The total number of synapses and synapse density per total branch length were quantified from the 4 time points (0, 6, 12, 24 hrs) we gathered for each individual axon arbor. Un-paired t-tests were used for statistical analysis as described previously [63]. Data results were considered significant in comparison to control as follows: *$p \leq 0.05$, **$p \leq 0.005$, ***$p \leq 0.001$, unless otherwise indicated on the graph with bars marking additional significant comparisons.

5.3. Results

5.3.1. Specific Expression of DSCAM in the Xenopus Optic Nerve

Previous work from our lab has shown Xenopus DSCAM expression in the cell body (soma) membrane surface of RGCs in the retina and in tectal cells in the optic tectum of stage 45 tadpoles [114]. In that past study, we detected DSCAM punctate expression in the neuropil of the optic tectum where retinotectal axons and dendrites establish functional synaptic connections, but we had yet to confirm if DSCAM was localized specifically in pre- or post-synaptic arbors in the retinotectal circuits. For this current study, we co-stained stage 45 to 46 tadpole brain tissue with a 3A10 anti-neurofilament protein antibody, to label retinal axons, and used the same DSCAM antibody we applied in our previous study [114]. Surprisingly, we found specific DSCAM expression along the ventral region of the optic nerve bundle (Fig 5.1a). 3A10 staining labeled axons in what appears to be a complementary manner localizing to the dorsal region of the optic nerve. We continued to see this distribution of DSCAM expression in the optic chiasm where retinal axon bundles cross the midbrain. By the time retinal axons cross the chiasm and project contralaterally to the tectum (white arrow, Fig 5.1b), DSCAM expression does not follow 3A10 staining and sits at the ventral base of the optic chiasm. In horizontal tissue sections, we found specific DSCAM expression in the posterior region of the axon bundle in the optic chiasm (Fig 5.1c). We observed that several fibers with DSCAM staining co-localizes with 3A10, confirming that our DSCAM antibody stains axon fibers (Fig 5.1d). These results indicate that a sub-population of RGC axons express DSCAM as they navigate the optic nerve pathway and to the point of the optic chiasm.

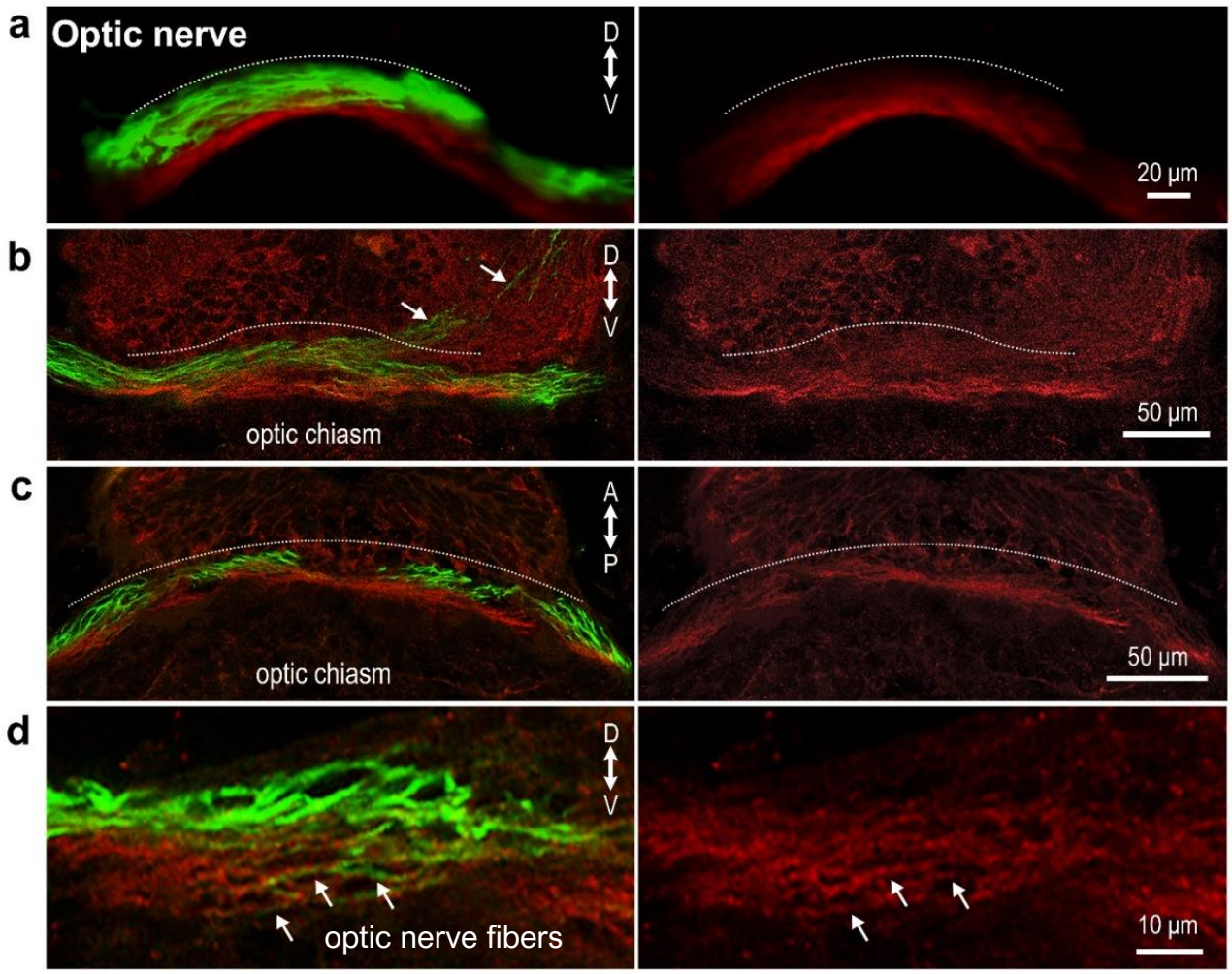

Figure 5.1. The visualization of stage 45 to 46 DSCAM treated tadpole optic nerve, optic chiasm, tectum, and eye using a DSCAM anti-body (red) and a 3A10 anti-neurofilament protein antibody (green). (a) Expression of DSCAM was observed along the ventral region of the optic nerve bundle. While 3A10 staining was expressed on the dorsal region of the optic nerve bundle. **(b)** In the coronal section of the optic chiasm, DSCAM was not expressed and 3A10 staining was observed at the ventral base. The projections of retinal axons (annotated as white arrows) are seen to cross the optic chiasm contralaterally to the tectum. **(c)** In the horizontal section of the optic chiasm, DSCAM was detected in the posterior region of the axon bundle. **(d)** We observed that several fibers with DSCAM staining co-localizes with 3A10, confirming that our DSCAM antibody stains axon fibers.

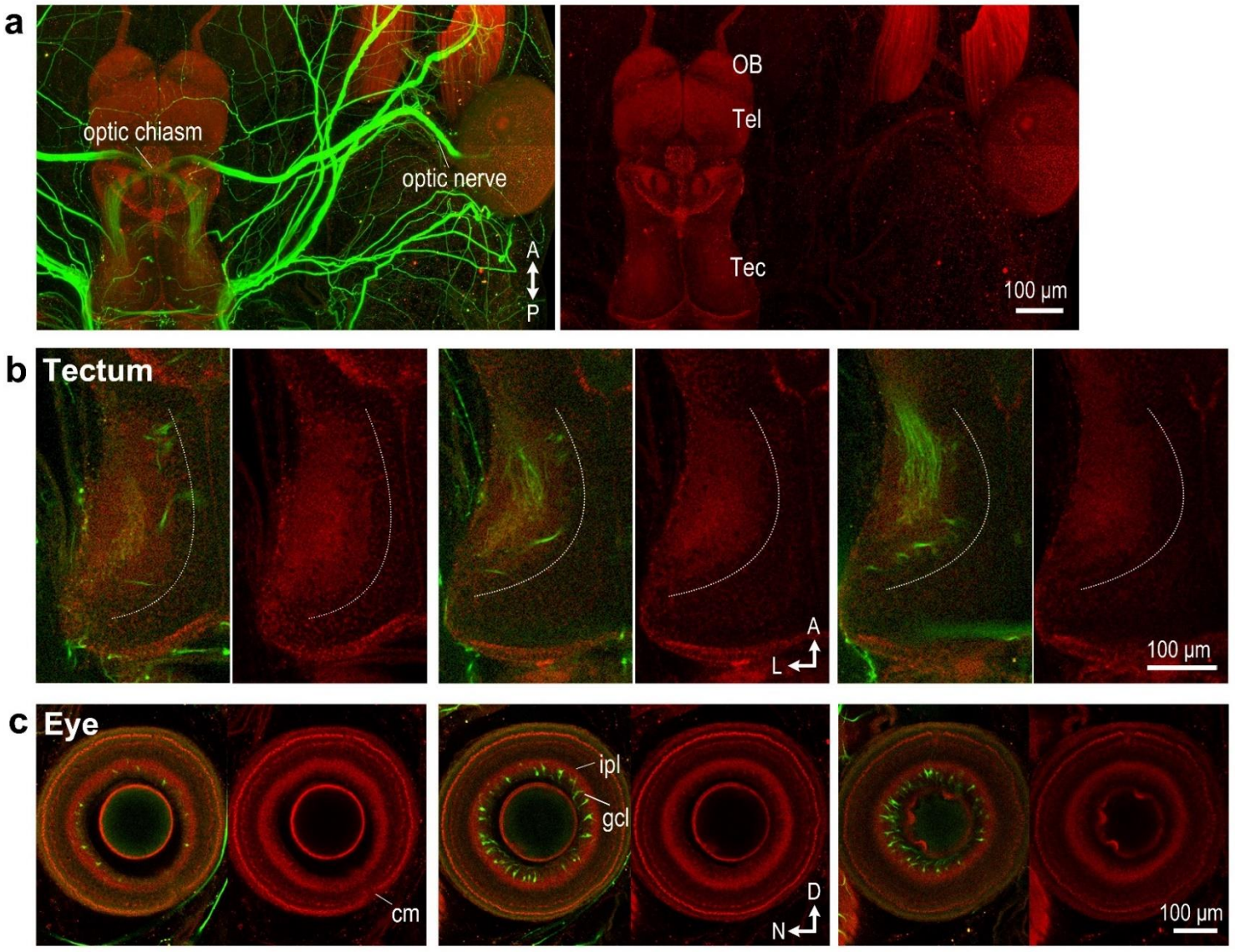

Figure 5.2. The visualization of stage 45 to 46 DSCAM expression using whole brain clearing (a) Whole brain clearing of tadpole head treated with DSCAM and 3A10 protein antibodies. 3A10 antibody expression was observed in the sensory and motor cranial nerves. The olfactory bulb and telencephalon regions of the forebrain contained a large expression of DSCAM. Within the tectum, the neutrophil exhibited a lighter expression of DSCAM along with 3A10 staining. **(b)** The optic tectum was observed in dorsal to ventral horizontal z-stacks. DSCAM expression was largely prevalent on the dorsal plane of the tectum compared to the most ventral plane. Planes are arranged from dorsal to ventral. **(c)** Arbors of retinal axons innervated the neuropil containing expressions of DSCAM and 3A10 protein antibodies. The dorsal and ventral regions of the retina did not contain traceable amounts of DSCAM expression. Planes are arranged along the lateral to medial axis.

If a specific subpopulation of retinal fibers is expressing DSCAM, we questioned whether a gradient pattern would be detected on axonal arbors in the optic tectum and/or throughout the whole eye. We decided to do whole brain clearing to preserve the integrity of the tissue and bypass the translucent epidermis of tadpoles. Compared to brain sectioning, brain clearing is powerful technique that allows us to gain a novel perspective of any gradient pattern of DSCAM throughout the whole tectum and the intact eye tissue.

Normally, the opacity of brain tissue is a result of light scattering and a mismatch of refractive index (RI). Cellular lipids and proteins are at high RI values at about 1.44 to 1.43, respectively [115]. Whereas in the cytosol of the cell, the RI value is much lower at 1.35 [116-118]. Through osmotic pressure, the cell cytosol can be passively replaced by immersing fixed tissue with a high RI solution as a clearing reagent. The cytosolic content in our sample, dissected heads of stage 45 to 46 tadpoles, were replaced with a high-refractive fructose solution (about 1.45) to homogenize the average refractive index and reduce light scattering throughout brain tissue. We were able to clear dissected tadpole heads labeled with DSCAM and 3A10 protein antibodies (Fig 5.2a). In addition to the optic nerve being labeled (Fig 5.2a), sensory and motor cranial nerves throughout the tadpole head were marked by the 3A10 antibody. Noticeably, a strong uniform expression of DSCAM was found in the olfactory bulb and telencephalon regions of the forebrain where spiny neurons are located [119]. The neuropil of the tectum exhibited a

lighter pattern of DSCAM that coincided with 3A10 staining (Fig 5.2a). When we examined individual horizontal z-stacks at the level of the optic tectum, from dorsal to ventral planes, DSCAM expression was strongest and widespread at the dorsal plane compared to the more ventral plane (planes arranged from dorsal to ventral, Fig 5.2b). DSCAM expression pattern coincided with 3A10 retinal axons as arbors innervated the neuropil, confirming that DSCAM localizes to pre-synaptic axon arbors in the tectum. However, in the eye, we did not encounter differential expression of DSCAM in ventral and dorsal regions of the retina (planes arranged along the lateral to medial axis, Fig 5.2c).

In my results, we discovered a unique pattern of DSCAM expression never before seen in the developing vertebrate visual system. Because graded distribution of molecular cues has largely been implicated in topographic mapping, we next questioned whether DSCAM played a specific role in organizing the topography of ventral retinal fibers as they cross the optic chasm and enter the tectum. Prior work done on a mouse model of Down syndrome has proposed that DSCAM regulates eye-specific segregation of retinogeniculate projections into the dLGN [42]. Based on current and previous findings, our experiments set out to explore whether DSCAM is a strong candidate involved in retinotopic organization.

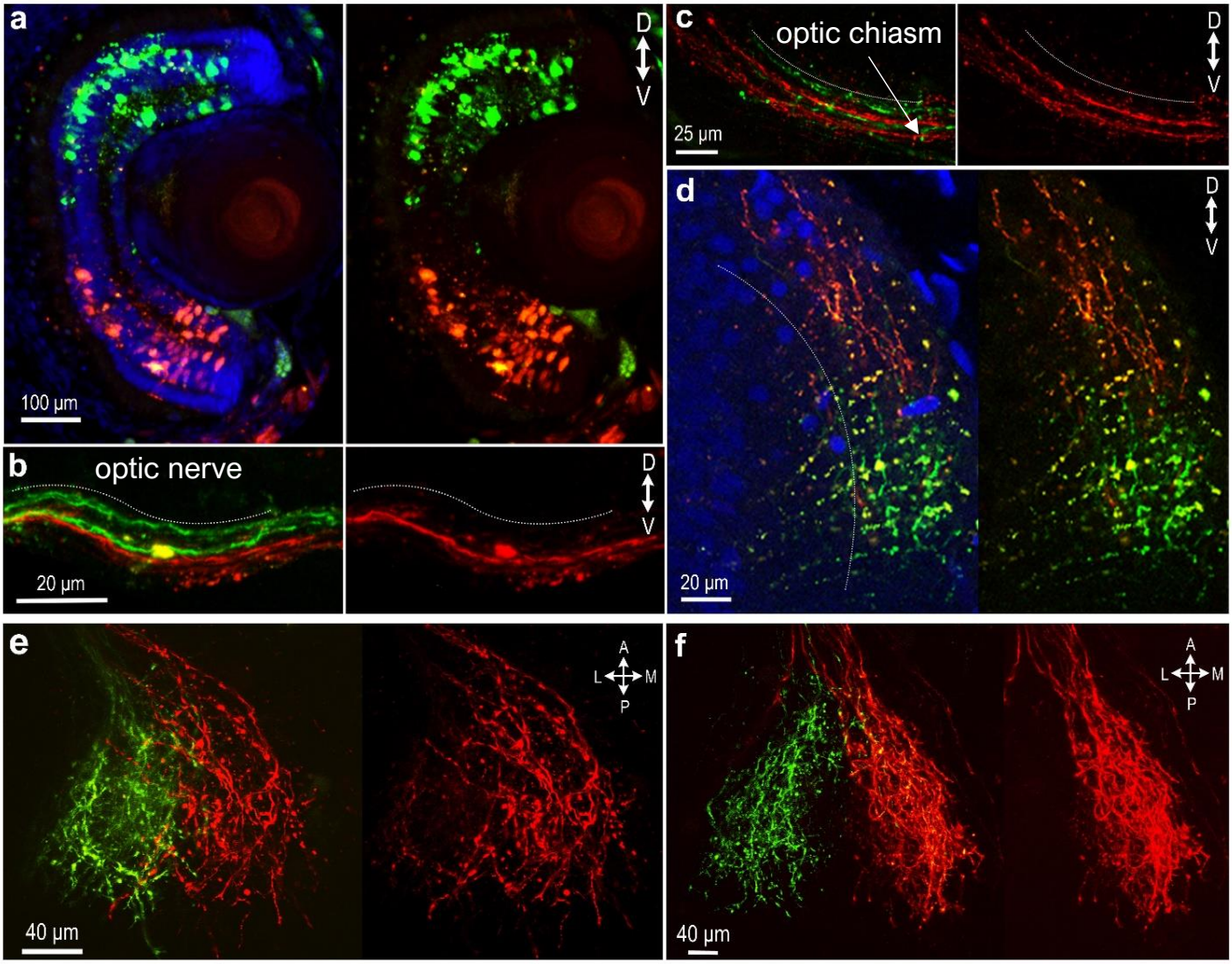

Fig 5.3. Rearrangement of Dorsoventral Axon Fibers Entering the Xenopus Tectum. **(a)** At stage 46, dorsal RGCs were labeled using standard control oligonucleotide lissamine-tagged morpholinos (red) while ventral RGCs were labeled using Alexa Fluor 488 dextran (green). **(b)** RGCs labeled with lissamine projected axon fibers located primarily along the ventral side of the optic nerve while the RGCs labeled with 488 dextran projected fibers located along the dorsal side of the optic nerve. **(c)** Lissamine labeled RGCs, entering the tectum, were located on the dorsal region of the optic pathway while the 488-labeled RGCs were found on the ventral region. (d)Inside the tectum, the lissamine-labeled axon fibers were found on the dorsal branch while the 488-labeled axon fibers were located ventrally. (e)In-vivo imaging at early stage 46, along the lateral-medial axis revealed lissamine-labeled axon fibers along the lateraly side of the tectum, while the 488-labaled axon fibers predominated the medial side. There was a degree of arbor overlap (average 20 µm) between the medial and lateral branch arbors, indicated by the with line. (f) At stage 47, there was a clear separation between medial and lateral arbors.

5.3.2. Dorsoventral Axon Sorting in the Xenopus Retinotectal System

During zebrafish development (which closely resembles Xenopus), dorsal retinal fibers normally reach the optic tectum via the lateral branch, while ventral axons project via the medial branch [36]. Disrupting mechanisms dependent on RNA-binding proteins, such as Hermes, causes an aberrant shift in topographic ordering and results in lateral dorsal axons projecting ectopically into the medial branch arbor [36]. We created a similar experimental design in the Xenopus embryo to assess the effects of DSCAM knockdown on the formation of retinotopic organization. But beforehand, we first sought to thoroughly characterize the projection and ordering of ventral and dorsal fibers starting from the retina and following their trajectory as they cross the chiasm and enter into the tectum. Standard control oligonucleotide lissamine-tagged morpholinos (red dye) and Alexa Fluor 488 dextran (green dye) were electroporated separately to label ventral and dorsal RGCs (Fig 5.3a). Our results reveal that lissamine-labeled RGCs project fibers that are positioned along the ventral portion of the optic nerve, while 488-labeled RGCs send axon fibers along the dorsal region of the optic nerve (Fig 5.3b). As soon as lissamine- and 488-labeled axons enter and cross the chiasm, turning contralaterally into the tectum, we observed a reshuffling of fiber arrangement; lissamine-fibers that were originally positioned on the ventral side of the optic nerve, were intermixing and positioning more dorsally in the optic chiasm (Fig 5.3c). This also occurred for 488-labeled fibers that were originally flanked on the dorsal side, which shifted more ventrally. By the time axon fibers innervate the tectum, we see a complete

inverted arrangement; lissamine-labeled axons enter the tectum through the dorsal branch, while 488-labeled fibers are found ventrally in the tectum (Fig 5.3d) which is confirmed in the literature [18, 120]. Based on the results presented so far, specific DSCAM expression along the ventral portion of the optic nerve would, to some extent, coincide with ventral RGCs traveling through the ventral side of the optic nerve pathway prior to crossing at the tectum (Fig 5.1a and Fig 5.3b). It is still unclear whether subgroups of axons, derived either from ventral or dorsal RGCs, correspond to the widespread DSCAM expression we observed in our cleared whole brain staining, specifically in the dorsal planes of the tectum (Fig 1e).

Along the lateral-medial axis, lissamine-labeled axons ventral RGC innervate the tectum laterally, while 488-labeled dorsal RGC axons travel more medially (Fig 5.3e), which has been previously confirmed [121]. The arrangement of arbors we observed is also similar to the anatomical pattern seen in zebrafish larvae [36]. When we labeled axons at early stage 46 and imaged axon arbors 48 hrs afterwards, we noticed that medial branch arbors (ventral RGC, labeled with lissamine) share a degree of arbor overlap (average 20 μm) with lateral branch arbors (dorsal RGC, 488-labeled) Fig 5.3e. When we labeled axons at a later age, around stage 47, medial arbors are visibly separated from lateral arbors (Fig 2f). This separation between lateral and medial arbors in *Xenopus* tadpole is consistent with zebrafish larvae at 5 days postfertilization (dpf), when the optic tectum is first fully innervated [36]. From our in vivo imaging studies, we have observed that *Xenopus* dorsal RGC axons projecting through the lateral branch initially overlap with

ventral RGC axons traveling through the medial branch; then at later stages, as the tectum expands and arbors become more complex, lateral and medial arbors diverge and clearly separate along the *Xenopus* neuropil.

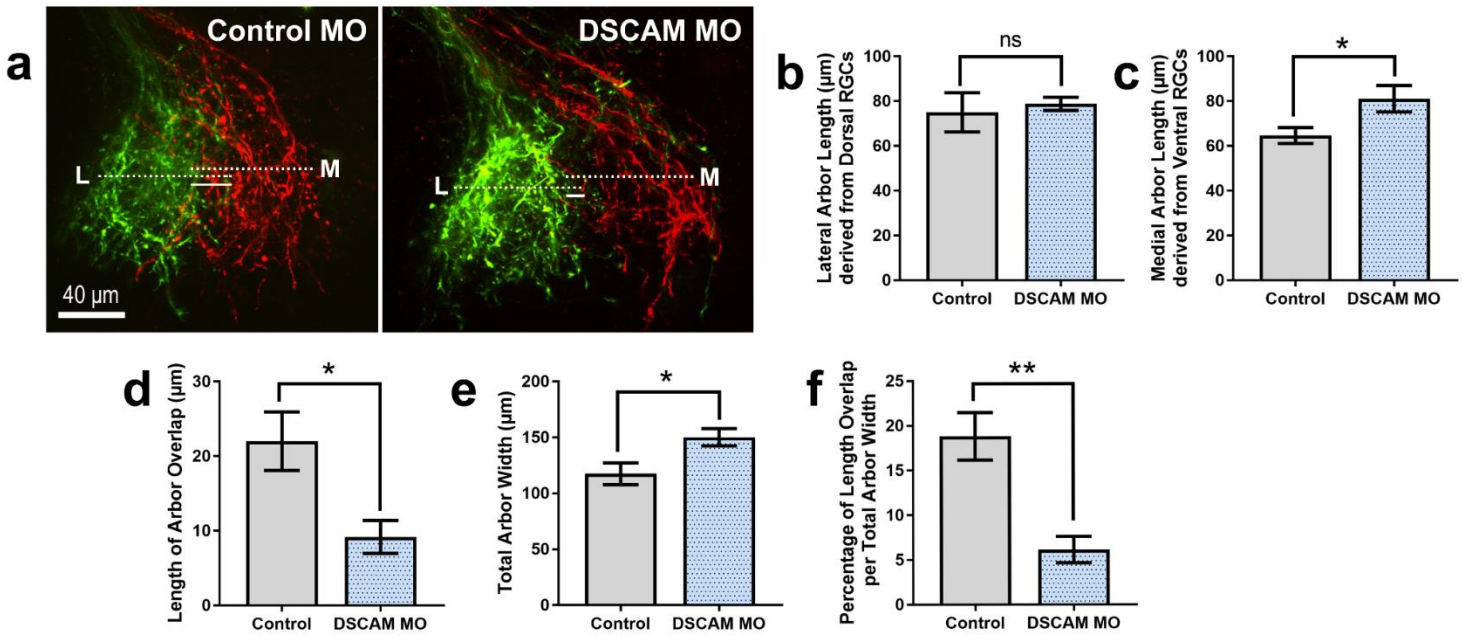

Figure 5.4. Statistical analysis of the degree of overlap between medial and lateral arbors labeled in early stage 46 embryos treated with either DSCAM MO or left as the control. **(a)** All subsequent data significance was determined using an unpaired, two-tailed t test with equal sample sizes for both control and DSCAM MO groups, n = 6. **(b)** When comparing the lateral arbor lengths (dorsal RGCs) of each group, it was determined that their difference in widths were not significant, p = 0.6875, NS. **(c)** There was, however, an observable significant difference when comparing the medial arbor lengths (ventral RGCs). DSCAM MO treated animals were shown to have longer axon arbor width than the control group, *p = 0.0377. **(d)** Analysis of the length of overlap between the medial and lateral arbors showed that there was a significant difference between the groups, with the DSCAM MO animals demonstrating a smaller amount of overlap compared to the control, *p = 0.0169. **(e)** When looking at the overall total arbor width of each group, DSCAM MO animals were shown to have a greater total length than the control group, *p = 0.0257. **(f)** Further tests also confirmed and supported significant reduction in overlap with the DSCAM MO group when illustrating measurements as a percentage of length overlap per total arbor width, **p = 0.0019. (*p ≤ 0.05, ** p ≤ 0.005).

5.3.3. Knockdown of DSCAM Disrupts Proper Topographic Segregation

To identify specific cellular actions of DSCAM in directing retinotopy in the tectum, we electroporated a morpholino (MO) targeting Xenopus laevis *Dscam* mRNA to block translation and downregulate endogenous DSCAM levels in medial axon arbors. We specifically introduced DSCAM MO into ventral RGCs in embryos at stage 46, when majority of medial axons have already arborized in the tectum. Therefore, the effects we see largely involves the arborization mechanics in the tectum, instead of mechanisms concerning axon pathfinding. We targeted whole bundles of axon arbors to visualize the innervation pattern and topographic organization of axon arbors in the neuropil. As we have seen in the previous data set, when arbors reach the tectum, axons derived from ventral and dorsal RGCs are sorted along the medial-lateral axis (Fig 2e). Ventral RGCs axons dominantly arborize in the medial portion of the neuropil, while dorsal RGCs axons arborize in the lateral section close to the lateral ventricle. 48 hours after we introduced DSCAM MO into ventral RGCs of stage 46 embryos, we noticed that medial axon arbors were positioned more medially compared to controls (Fig 5.4a). To quantify this, we measured the total arbor width of medial axons treated with DSCAM MO and compared the width to medial axons treated with control MO. The average arbor width (μm) of axons treated with DSCAM MO were significantly more extended than controls (Controls 117.5 ± 9.73, n = 6; DSCAM MO 150.2 ± 7.81, n = 6, p = 0.0257, Fig 5.4c). Lateral arbors, both labeled with Alexa 488 dextran, had the same arbor width regardless of either treatment (Controls 75.03 ± 8.723, n = 6; DSCAM MO 78.85 ± 2.95, n = 6, p = 0.6875, not significant, Fig 5.4b). As mentioned earlier, labeling axons arbors

at early stage 46 embryos, produced medial and lateral axon arbors that share a degree of overlap in the neuropil, about an average arbor width of 20 μm. Axons treated with DSCAM MO showed a significant reduction in lateral and medial arbor overlap width compared to control arbors (Controls 22.02 ± 3.915, n = 6; DSCAM MO 9.185 ± 2.193, n = 6, *p = 0.0169, Fig 5.4d). When looking at the overall total arbor width of each group, DSCAM MO animals were shown to have a greater total length than the control group, (Controls 117.5 ± 9.733, n = 6; DSCAM MO 150.2 ± 7.808, n = 6, *p = 0.0257, Fig 5.4e). Further tests also confirmed and supported significant reduction in overlap with the DSCAM MO group when illustrating measurements as a percentage of length overlap per total arbor width (Controls 18.82 ± 2.685, n = 6; DSCAM MO 6.135 ± 1.482, n = 6, **p = 0.0019, Fig 5.4f). This effect resulted in dorsal and ventral RGC axon arbors with less overlap in the optic tecum than control axons at the same stage. Together, these findings suggest that medial axons extend more medially, away from lateral arbors, therefore, increased segregation of medial and lateral occurred in response to lowered endogenous DSCAM levels.

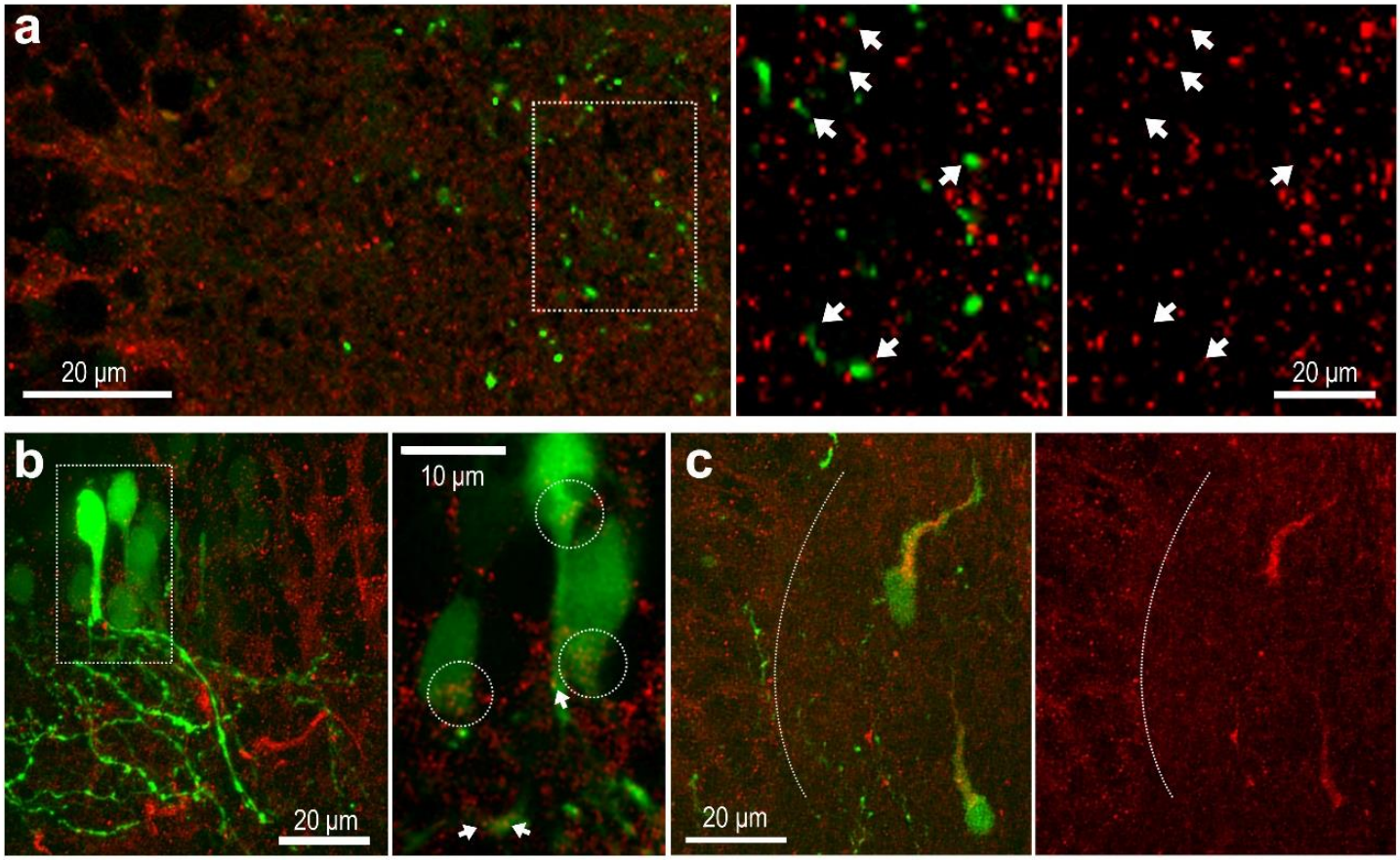

Figure 5.5. Characterization of DSCAM in retinotectal synapses in neuropil. (a) GFP-Synaptobrevin plasmids were electroporated at stage 30-34 embryo retinas. Embryos were raised to stage 45 for confocal imaging with DSCAM antibody staining. Horizontal tissue sections indicate co-localization of DSCAM in a sub-set of retinotectal synapses (annotated as white arrows) and located post-synaptically to synapses marked by GFP-Syn. (b) Electroporation of tectal cells with CMV-driven plasmid expressing GFP. GFP positive embryonic tadpoles were fixed and stained with DSCAM antibody. DSCAM expression was observed on the cell surfaces of tectal cells along with expression on primary dendrites and dendritic branches (annotated as white arrows). (c) Primary processes of cells positioned in the neuropil show strong expression of DSCAM.

5.3.4. DSCAM Localizes Post-synaptically on Retinotectal Synapses and on Tectal Neurons

We previously demonstrated that knocking down DSCAM levels stunted arbor development of individual RGCs axons, indicating that endogenous DSCAM, under normal conditions, acts as permissive cue that facilitates RGC axon growth. In contrast, DSCAM acts as a restrictive cue to regulate the size and complexity of dendritic arbors of tectal neurons [114]. It is apparent that DSCAM plays a role in guiding axons and directing the formation of dendrites in developing circuits, but whether the molecule plays a key role in vertebrate synapse formation remains unexplored *in vivo*. We know that homophilic binding between DSCAM proteins mediate neurite adhesion, which helps facilitate precise synaptic targeting within a specific sub-lamina in the retina [15]; and according to the work done in Aplysia cell cultures, DSCAM acts trans-synaptically and in collaboration with AMPA-like receptors to promote synapse formation [100]. In comparison to these studies, we wanted to directly explore *in vivo* how DSCAM influences the formation of retinotectal synapses as axons and dendritic arbors form in the *Xenopus* tectum.

We first characterized the location of DSCAM expression at retinotectal synapses in the neuropil. A GFP- Synaptobrevin (GFP-Syb) DNA plasmid, which serves as a marker to visualize pre-synaptic sites, was electroporated in the retina of stage 30-34 embryos. Tadpoles labeled with positive GFP-Syb expression were raised to stage 45 and were fixed for histology. Horizontal tissue sections were further immunostained with the

DSCAM antibody. We found that DSCAM puncta localized adjacently to a sub-population of pre-synaptic GFP-Syb markers, suggesting that DSCAM is selectively positioned post-synaptically at some, but not all, retinotectal synapses (white arrows Fig 4a). If DSCAM is expressed on post-synaptic tectal cells, we would expect DSCAM expression localized on dendritic arbors of tectal neurons. To test this, we electroporated tectal cells with a CMV-driven plasmid expressing GFP. Embryos with GFP-positive tectal cells were fixed and stained for DSCAM expression. We found that DSCAM is not only expressed along the cell body surface of tectal neurons, as previously shown in our past work [114](Santos RA, 2018), but is also expressed along primary dendrites and dendritic branches (white arrows Fig 4b). Interestingly, we found strong DSCAM expression along the primary processes of cells that were positioned in the neuropil (Fig 4c). We do not know the identity of these cells, but these cells share similar morphology and features to tegmental projection neurons characterized by Robles and colleagues using id2b transgenic zebrafish larvae [122]; both cells are found exclusively in the neuropil and have a prominent primary process that protrudes apically. Further experiments would need to confirm whether these cells are the same cell-type.

5.3.5. Abrupt Elevated Levels of DSCAM Disrupt Retinotectal Synapses

DSCAM initiates signaling functions through homophilic and heterophilic interactions to execute a combination of key events in vertebrate circuit wiring [123]. Drosophila DSCAM isoforms are well known for their homophilic binding and their ability to recognize DSCAMs of the same isoforms. Even though vertebrate animals lack the

DSCAM isoform diversity seen in fruit flies, vertebrate DSCAM and DSCAML1s can also bind homophilically, and have been shown to mediate neurite adhesion during synaptic targeting [15]. Vertebrate DSCAM has also been shown to act as a heterophilic receptor and bind to diffusible netrin ligands, specifically directing the turning of axons toward netrin-1 source in explant cultures [54]. Motivated by these findings, we questioned whether elevating DSCAM levels during retinotectal circuit development would abruptly affect RGC axon arborization and the formation of retinotectal synapses by interfering with endogenous DSCAM functions that are operating homophilically and/or heterophilically with key developmental signaling molecules in the tectum.

RGCs were electroporated with CMV-driven plasmids expressing tdTomato and GFP-Syn. We imaged axons starting at stage 45, when RGC axons actively branch and form synaptic connections with tectal partners [46, 61]. Axon arbors, clearly labeled with tdTomato and GFP-Syn, were treated with either exogenous recombinant DSCAM (reconstituted at 500 ng/ul in 0.1% BSA ml 1x PBS sterile) or vehicle solution (1x PBS). For quantitative analysis, axons were followed 6, 12, and 24 hours after treatment (Fig 5a, b). Our time-lapse imaging studies showed that axon arbors, from both treatments, grew and extended normally over time. Elevated DSCAM levels did not significantly alter total RGC axon arbor length and total branch tips when compared to controls (Controls n = 17; DSCAM n = 12; un-paired t-test showed no significance, Fig 5c, d). When evaluating the effects of recombinant DSCAM treatment on retinotectal synapses, we quantified the total number of GFP-Syb markers per axon arbor at each individual time

point. As noted in the methods, we had a lower sample size for this analysis because not all axon arbors labeled with tdTomato expressed GFP-Syb to mark synapses (as shown in our control axons on fig 5.5a). When we quantified the total number of synapses of retinal axon arbors at each individual timepoint, our analysis showed no significant difference between treatments. We did note that there was a subtle drop in the number of synapses between the 6 and 12-hour timepoint in response to recombinant DSCAM (Controls n = 17; DSCAM n = 12; un-paired t-test showed no significance, Fig 5.5g). When we took into account the arbor length of each individual axon arbor, we found that the number of synapses per branch length was significantly reduced between the 6 and 12-hr timepoints (Controls 115.5 ± 20.42 n = 6; DSCAM 67.38 ± 9.265 recombinant n = 8, Fig 5.5f, h) in comparison to control arbors; this was a result of synapses being eliminated, on average, hours after recombinant treatment (white arrows Fig 5.5h). Together, these findings suggest that treating RGC axons with exogenous recombinant DSCAM did not affect the arborization of axons, but rather the stability of retinotectal synapses. Our histology data showed that a subset of synapses localize with endogenous DSCAM protein; therefore, if acting directly, our recombinant DSCAM treatment would not have a global effect on all synapses but only on a subset of synapses specifically expressing DSCAM. It is possible that the effect we see here, a subtle decrease in synapses, is likely a reflection of homophilic interference between our exogenous DSCAM treatment and endogenous DSCAM that is potentially needed for maintaining and anchoring synaptic connections.

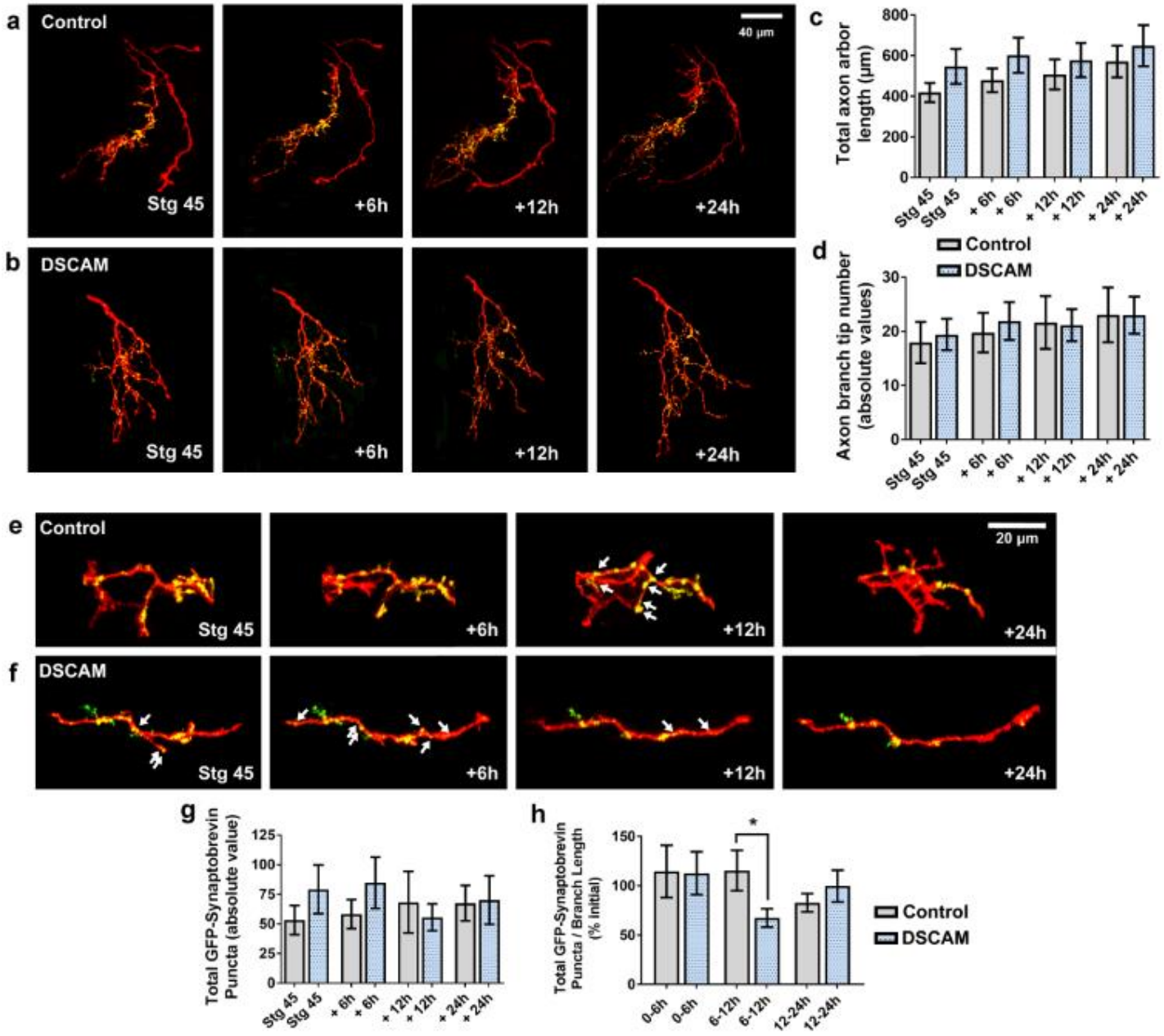

Figure 5.5. Treatment of exogenous recombinant DSCAM on RGC axons create stability in retinotectal synapses, but no effect on the arborization of axons. Caption on next page.

Figure 5.5. Treatment of exogenous recombinant DSCAM on RGC axons create stability in retinotectal synapses, but no effect on the arborization of axons. (**a, b**) Sample RGC axons were treated with either vehicle solution (1x PBS) or DSCAM at stage 45 and imaged at 0h, 6h, 12h, and 24h after initial treatment. RGC axons visualized using CMV-driven plasmids expressing tdTomato and GFP-Synaptobrevin using a confocal microscope in vivo **(c, d)** The total axon arbor length and axon branch tip number were measured for RGC at Stage 45, 6h, 12h, and 24h after DSCAM (n=17) and vehicle solution (n=12) treatment. Both treatments did not significantly affect the total axon arbor length and axon branch tip number. **(e, f)** Retinotectal synapses treated with DSCAM or vehicle solution were imaged to quantify the total number of GFP-Syb markers per axon arbor at Stage 45, 6h, 12h, and 24h after initial treatment. White arrows are annotated at time points where retinotectal synapses disappear from RGC axons. **(g)** When we quantified the total number of synapses of retinal axon arbors at each individual timepoint, our analysis showed no significant difference between treatments. We did note that there was a subtle drop in the number of synapses between the 6 and 12-hour timepoint in response to recombinant DSCAM. **(h)** A significant reduction of GFP-Synaptobrevin puncta/branch length was observed between the 6h and 12h timepoints in DSCAM treated axons (n=6) with a p value of 0.37 compared to control (n=8). Comparisons analyzed by unpaired t-test. (*$p \leq 0.05$)

5.4. Discussion

In summary, we discovered a ventral specific pattern of DSCAM expression along the Xenopus optic nerve and correlated this expression pattern to how optic nerve fibers are topographically organized. Fasciculated bundles of ventral fibers derived from ventral RGCs normally navigate the optic nerve along the ventral side, which coincides with strong DSCAM expression. As soon as fibers cross the optic chiasm, DSCAM expression is decreased. This coincides with ventral and dorsal retinal axons rearranging topographically as fibers pass the chiasm and project contralaterally into the tectum. Based on previous studies, DSCAM has been well characterized as a homophilic binding molecule mediating intracellular adhesion and the fasciculation of axon bundles [9, 91]. The site and timing of expression suggests that DSCAM is

involved, to some degree, in maintaining the ventrodorsal topography of optic nerve fibers in the spatial arrangement that mirrors how axons exit the optic disk. There is a possibility that the adhesive properties of DSCAM, through homophilic interactions, anchors ventral fibers together, preventing any rearrangement or interchange with dorsal axons as fibers navigate the optic pathway from the optic disk to the chiasm. Differential fasciculation of fibers along the optic nerve may be an underlying mechanism to traffic axons in an orderly manner to the chiasm. Organized arrival of axons at the site of the chiasm would allow axons to respond to the next set of guidance cues, including ephrins, chemoattractant cues, and neurotrophic factors [21, 52, 53, 102, 124], which all prepare for the subsequent stage of morphological trajectory into the tectum. For this study, we mostly characterized the expression of DSCAM along the ventrodorsal axis of the optic nerve, and we followed the navigation of ventral and dorsal retinal axons corresponding to this expression. We did detect DSCAM expression along the posterior region of the Xenopus optic chiasm as well (Fig 5.1c), and it has also been noted that DSCAM expression has been detected in the posterior region of the mouse optic chiasm [9]. Future experiments exploring DSCAM expression along the anteroposterior axis of the optic nerve would give us a thorough understanding of how DSCAM organizes the full topographic organization of retinal fibers throughout the entire optic nerve.

In addition to mechanisms organizing the topography and spatial arrangement of fibers, it is important to note that there are also time-based mechanisms involved that indirectly

contribute to the topographic wiring of circuits. During Xenopus eye development, new retinal ganglion cells are generated at the ciliary margin located at the peripheral edges of the eye [29, 30]. Older cells are pushed towards the central portion of the retina and a gradient of maturing cells is created along the retina radius. Because of the temporal pattern of early eye development, the deployment of emerging RGC axons via the optic tract is set to a defined temporal sequence. Dorsal retinal fibers exit the eye first, navigate the optic pathway, and reach the tectum 6 hours ahead of ventral retinal axons. The newer set of axon fibers exiting the eye travel along the most ventral portion of the optic nerve as innervation takes place [29, 31]. It is possible that fasciculation of retinal fibers by DSCAM indirectly modulates the pacing of ventral axons along the optic nerve – perpetuating a difference in timing at which ventral and dorsal axons reach their target sites. In our previous published work using time-lapse imaging, we showed that DSCAM is important in promoting the growth rate of retinal axons into the tectum in vivo, which supports the idea that DSCAM is involved in a temporal aspect of axon development.

Differential timing of retinotectal projections was initially thought to be the mechanism that generates topographic mapping in the optic tectum, with the argument that pioneering dorsal fibers innervate ventral areas in the tectum simply for arriving first at the available sites. This hypothesis stated that ventral fibers of the retina would later follow and would be forced to occupy the next available sites at the dorsal area of the tectum, due to the constraints of existing dorsal axons [29]. Studies, however, have shown that disrupting the timing of retinal axon deployment, by heterochronic

transplantation of early age RGCs into older embryos, does not seem to affect the topographic mapping formed during development, indicating that other mechanisms are at work [29]. It is becoming increasingly evident, based on a number of studies, that sub-populations of RGCs employ different molecular and cellular strategies to achieve axon-target specificity [125, 126]. For example, it is apparent that sub-populations of RGCs heavily rely on repellant and attractive cues for precise axon targeting. In amphibians, populations of RGCs differentially express ephrin-Bs in a high dorsal to low ventral gradient in the retina [127, 128]. This gradient pattern in the retina complements EphB1 receptors expression along the Xenopus tectum which is distributed in a high ventral to low dorsal gradient. Signaling between EphB1 receptors and ephrin-B ligands have been suggested to be the underlying mechanism that attracts dorsal retinal axons into the ventral portion of the tectum [127]. The work we present in this study adds DSCAM to a growing of list of molecular strategies retinal axons use to self-organize topographically along the optic nerve.

We observed that DSCAM expression diminishes following the site of the chiasm, but then reemerges gradually at the neuropil of the tectum where retinal axons arborize and form connections with post-synaptic tectal partners. At this spatial gap where DSCAM is withdrawn, axons fibers are rearranged, most likely by pre- and post-synaptic molecular interaction mediated by Ephs/ephrin signaling, to reorient the topography of axons in an inverted manner, while also distributing their projection along the mediolateral axis in the neuropil. Here we tested specifically whether DSCAM, expressed in the neuropil,

played a role in sorting the arrangement of arbors across the mediolateral plane. We found that knocking down DSCAM in arbors terminating medially in the tectum caused an aberrant shift and extension away from lateral arbors, suggesting that DSCAM guides the directionality of arbors derived from ventral RGCs. In our previous published research, we explored the cell-autonomous role of DSCAM and how it directed both pre- and postsynaptic structural and functional connectivity in the developing retinotectal circuit. We saw that DSCAM primarily acts as a neuronal brake to limit and guide postsynaptic dendrite growth of tectal neurons while it also facilitates arborization of presynaptic RGC axons cell autonomously. The retinal axons we so happen to target in our previous published study were ventral RGCs, which project arbors medially in the neuropil. We targeted the ventral RGCs in the retina because, according to the literature [29], ventral RGCs project axons to the most dorsal part of the tectum, close to the epidermis, which was an accessible window for in vivo confocal imaging. Findings from this current work and in our previous study clearly establish important cell-autonomous roles mediated by DSCAM at multiple levels of retinotectal circuit assembly. It is possible that the non-cell-autonomous role of DSCAM, referring to the trans-arbor interactions of DSCAM between retinal axons and the dendrites of tectal neurons, may also contribute to the structural development of retinotectal arbors, and can also influence how axonal and dendritic arbors are sorted along the neuropil.

During the events of RGC axon arborization, coordinated addition and retraction of axon branches and dendritic neurites of tectal cells allow gradual recognition between pre-

and postsynaptic partners which, subsequently, allows synaptic connections to be formed [61, 62]. Additionally, bi-directional communication at the molecular level are also at work facilitating synaptogenesis. For instance, neurotrophins, including brain-derived neurotrophic factor (BDNF), can act as a retrograde signal to influence presynaptic neurons, while also acting as an anterograde factor on postsynaptic cells [61, 129]. This type of bi-directional signaling can generally induce the development and maturation of synapses, or even modify the structure of existing synapses. Here in this paper, we show that endogenous DSCAM, localized post-synaptically, is implicated in the stability and maintenance of synapse function. Though, we found that DSCAM localizes only to a sub-set of retinotectal synapses, which might explain the moderate reduction in synapse density shortly after exogenous recombinant DSCAM treatment. Neurotrophins and cell-adhesion molecules, like DSCAM, are perhaps the general underlying mechanisms that modulate synaptogenesis and synapse function, but whether they are also involved in additional mechanisms for precise topographic mapping at the synaptic level have not been explored. During development, an excess amount of connections is formed. It is through activity-dependent refinement and sculpting of connection through physiological competition that establishes the main working functional synapses. Several key studies, however, have shown that topographic arrangement of axons is also precisely organized at the synapse level. In both the mouse hippocampus and neuronal networks throughout C. elegans, graded inhibitory cues for synapse formation and maintenance are used to restrict synapses distribution and create synapse topographic maps [130]. In the developing Xenopus

tadpole, visually driven Ca^{2+} signals are topographically organized at the subcellular dendritic scale in tectal neurons [121]. Characterizing the spatial distribution of molecules, such as DSCAM, at either pre- and post-synaptic arbors and match their anatomical location along synapses remains open to investigation.

Our work demonstrates how DSCAM is involved in multiple events during development, including topographic organization of axon fibers and synapse maintenance. A caveat to our analysis testing exogenous recombinant DSCAM on retinotectal synapses is that it may not be able to substitute or effectively outcompete endogenous DSCAM. Further experiments using a dominant negative ligand to block DSCAM signaling, while being able to image synapses in vivo, would be a stronger alternative to the current experiments done in this study. Nonetheless, findings across several published research articles provide us insight to how cell surface molecules, such as DSCAM, mediate neurite avoidance, while facilitating physical contact between pre- and postsynaptic sites. Work done by Dr. Robert Burgess and colleagues has found that DSCAM can functionally interact with other CAMs, specifically cadherins and protocadherins, and "mask" their adhesive properties that, consequently, prevent neurite collision and fasciculation [75]. Their results, obtained in the mouse retina, reveal that DSCAM works in collaboration with other CAMs to modulate cell adhesion by acting as a "non-stick" signal. In comparison, studies have shown that DSCAM co-localizes with AMPA-like receptors during *de novo* synapse formation in Aplysia circuits. Blocking Aplysia DSCAM terminates synaptic transmission and clustering of AMPA-like receptors,

suggesting that DSCAM mediates trans-synaptic interactions during developmental synapse formation [100]. It is also been suggested that DSCAM collaborates with NMDA receptors to facilitate dendritic spine and synapse formation [93]. Based on the studies discussed, it is possible that developing neurites use DSCAM, in collaboration with specific cell surface receptors, as a mechanism to distinguish areas that need to be avoided and recognize specific areas where synapses can be established.

5.5. Conclusion

Across a number of studies, DSCAM has been implicated in many various aspects of vertebrate circuit assembly. Our understanding of DSCAM's extraordinary ability to help construct different features of circuit formation is due to its collaborative nature to interact with an array of signaling molecules. Precise wiring of neural circuits in the vertebrate visual system is orchestrated through a series of carefully constructed events. In the developing tadpole, axons exit the retina via the optic nerve tract, cross the optic chiasm, and project contralaterally to the optic tectum where axons arborize and form selective synaptic connections with tectal partners. Each step underlying vertebrate visual circuit assembly depends on a wide variety of molecular guidance cues to be properly executed. But interestingly, a single type of molecule, such as DSCAM, can be reused taking on reoccurring roles throughout development. Here we show that DSCAM plays an important role in directing the topographic organization of retinal fibers as they travel the optic nerve, sort axon arbors along the mediolateral axis in the neuropil and are also important in maintaining retinotectal synapses.

Chapter 6

General Discussion

6.1. Summary and Current State of Knowledge

The overarching goal of my dissertation is to explore DSCAM's role in the assembly of neuronal circuits in the vertebrate CNS. This main goal has taken me through a journey exploring multiple aspects of neuronal circuit development and uncovering how DSCAM can play a multifaceted role throughout circuit assembly. I primarily examined the development of the retinotectal circuit in Xenopus tadpoles, using an array of methods including in vivo time-lapse confocal imaging and whole brain clearing, to examine key events of circuit assembly. Using the Xenopus tadpole model allowed me to investigate DSCAM's role in vivo and discover novel spatial and temporal details that furthers our knowledge of how DSCAM operates throughout development. I specifically explored three primary events that shape neuronal circuit connectivity: (1) guiding axons to correct target sites, (2) axons and dendrites arborizing into a defined zone, and finally (3) axons forming functional synaptic connections at distinct regions on post-synaptic neurons.

In summary, I found that DSCAM plays an important role in mediating the control of both pre- and postsynaptic structural and functional connectivity in the developing retinotectal circuit, where it primarily acts as a neuronal brake to limit and guide postsynaptic dendrite growth of tectal neurons while it also facilitates arborization of

presynaptic RGC axons cell autonomously; this occurs independently of RGC dendritic arbor development and at the same stage. (Fig. 6.1a, b). Additionally, DSCAM plays an important role in directing the topographic organization of retinal fibers as they travel the optic nerve (Fig 6.1e), sort axon arbors along the mediolateral axis in the neuropil and participate in the formation and/or stabilization of retinotectal synapses (Fig 6.1f). Although my dissertation work focuses on the developmental mechanisms shaping the retinotectal circuit, the same general mechanisms uncovered here can translate and help us understand similar mechanisms that are used throughout the nervous system during the formation of specific connections.

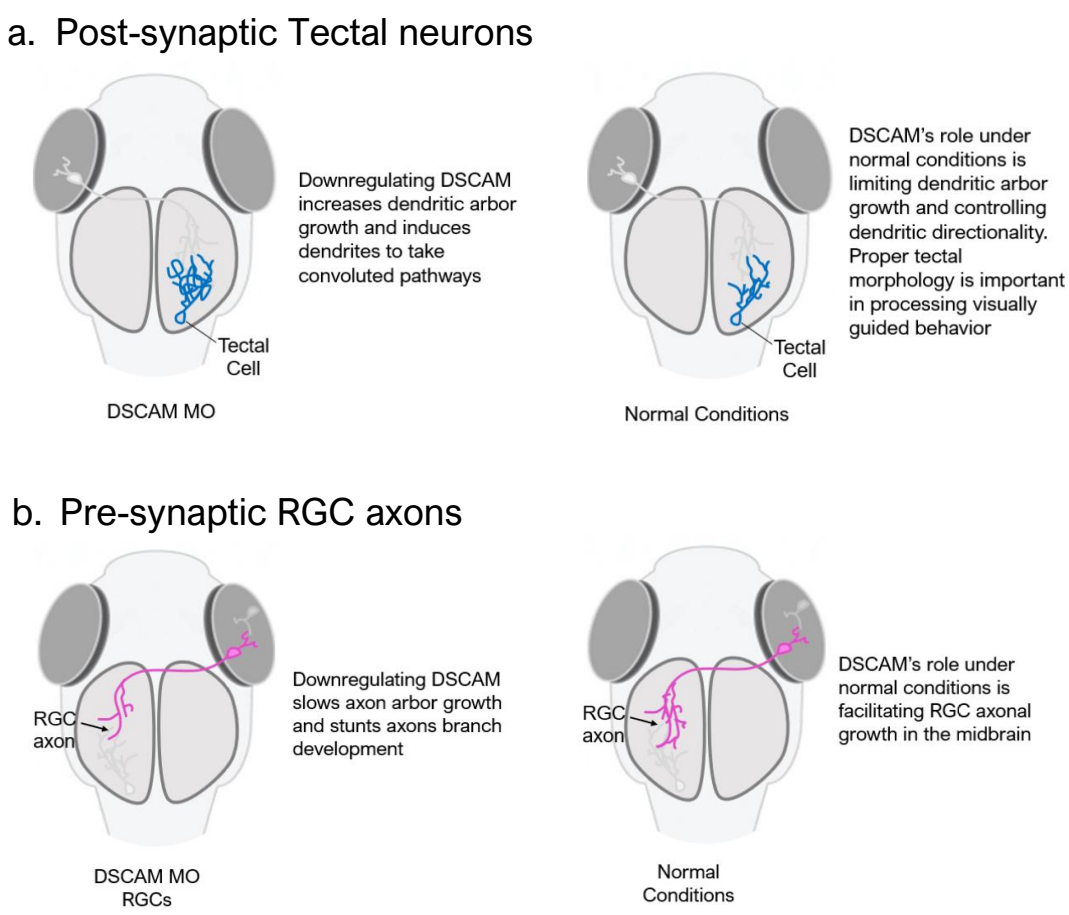

Figure 6.1. Schematic summarizing the effects of manipulating DSCAM levels in the retinotectal circuits. Caption on next page.

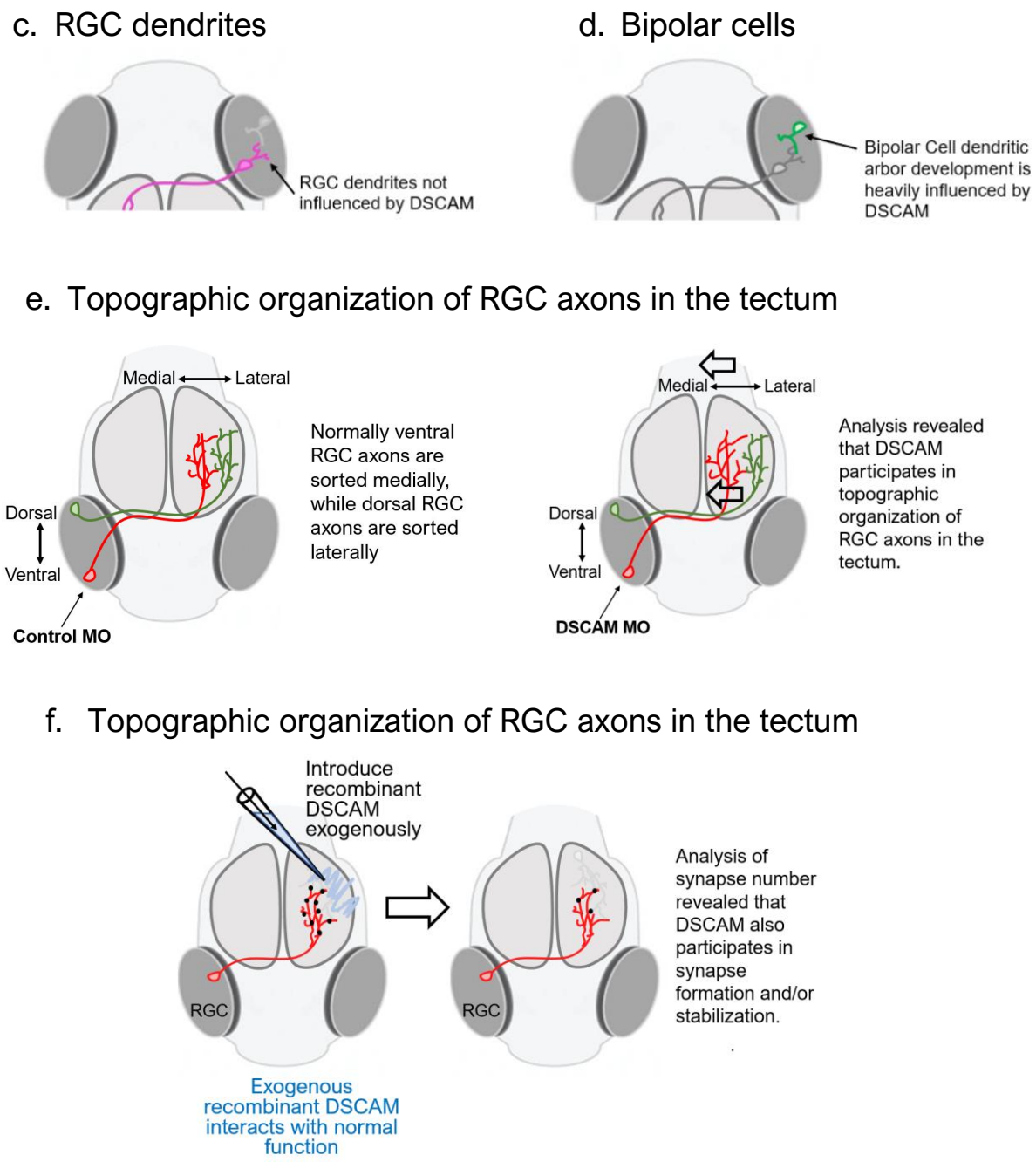

Figure 6.1. Schematic summarizing the effects of manipulating DSCAM levels in the retinotectal circuits. (**a**) DSCAM limits dendrite branching and growth of tectal neurons but does not regulate dendritic self-avoidant patterning. Dendritic development of tectal neurons is important in processing visually guided behavior. (**b, c, d, e**) DSCAM facilitates branching, stabilization, and topographic organization of RGC axons at their target in the midbrain; this occurs independently of RGC dendritic arbor development and at the same stage. (**f**) DSCAM also participates in synapse formation and/or stabilization.

6.2. Future Directions

It is important to mention that there are many events and different types of circuits forming in development that I have yet to explore, and that DSCAM may possibly be in implicated in. For example, based on our whole brain clearing work that I present in chapter 5, we detected strong DSCAM expression along the forebrain where spiny neurons are located. Spiny neurons exhibit a complex dendritic arbor morphology with prominent synapses (referred as dendritic spines) distributed along dendrite branches. Whether DSCAM is implicated in shaping the morphological pattern of dendritic arbors of spiny neurons or in the formation of dendritic spines is novel avenue of research. Additionally, the olfactory circuits in the forebrain are accessible for manipulation. One could target olfactory receptor neurons and/or their postsynaptic spiny neurons in the forebrain and asses how DSCAM directs the assembly of olfactory circuits.

Based on my result from chapter 5, I show that endogenous DSCAM, localized post-synaptically, is implicated in the stability and/or maintenance of synapse function. Key experiments are still needed to understand the molecular mechanism underlying the changes in synapse density in response to recombinant DSCAM from chapter 5 (recombinant DSCAM treatment on retinotectal synapses, Fig. 5.5a–h, Fig. 6.1f). Understanding how recombinant DSCAM is interacting with endogenous DSCAM function still remains unclear. Based on the literature, we know that vertebrate DSCAM can function homophilically and/or heterophilically as a receptor. Determining the

molecular mechanisms mediated by DCSAM signaling that are involved in shaping the formation of retinotectal circuits would be insightful.

Additionally, we found that DSCAM localizes only to a sub-set of retinotectal synapses, which might explain the moderate reduction in synapse density shortly after recombinant DSCAM treatment on RGC axon arbors. Doing similar experiments to see the effects of recombinant DSCAM treatment on the dendritic morphology of tectal neurons could be the primary effect driving a decrease in synapse density because structural changes in dendrites can affect synaptic connections. If no effect is observed on the dendritic development of tectal neurons based on this hypothetical experimental design, then these potential results would further confirm that the recombinant DSCAM treatment we performed in Fig 5.5a–h had a direct effect on synapses labeled with GFP-Syb.

In the discussion section of chapter 5, I mention that neurotrophins and cell-adhesion molecules, like DSCAM, are generally the underlying mechanisms that modulate synaptogenesis and synapse function. Whether these guidance cues are involved in mechanisms directing precise topographic mapping at the synaptic level remain unexplored. During development, an excess amount of connections is formed. It is through activity-dependent refinement and sculpting of connection through physiological competition that establishes the main working functional synapses. Several key studies, however, have shown that topographic arrangement of axons is also

precisely organized at the synapse level. In both the mouse hippocampus and neuronal networks throughout C. elegans, graded inhibitory cues for synapse formation and maintenance are used to restrict synapses distribution and create synapse topographic maps [130]. In the developing Xenopus tadpole, visually driven Ca^{2+} signals are topographically organized at the subcellular scale along the dendritic arbor of tectal neurons [121]. Characterizing the spatial distribution of molecules, such as DSCAM, at post-synaptic arbors and mapping their anatomical location according to how their cell bodies are placed along the tectum would potentially reveal that the topography of connections is organized even at the synaptic level. This will demonstrate how precise connections are established throughout visual circuits.

6.3. Closing Statement

In summary, it is absolutely astonishing to observe the many emerging events that occur during neuronal circuit development. Selective pressure by natural selection has led to the evolution of robust developmental mechanism that have given rise to complex circuits throughout the vertebrate brain. These circuits are built with unique structural pattern and functional modality which greatly aids in the animal's survival. The work from my dissertation largely explores how one molecule, such as DSCAM, serves its role in shaping neuronal circuits, but its apparent how DSCAM-mediated mechanisms are intertwined with a vast array of molecular and cellular mechanisms that are at work throughout the events of development.

Bibliography

1. Sargent, P.B., *What distinguishes axons from dendrites? Neurons know more than we do.* Trends in Neurosciences, 1989. **12**(6): p. 203-205.
2. Kolodkin, A.L. and M. Tessier-Lavigne, *Mechanisms and molecules of neuronal wiring: a primer.* Cold Spring Harbor perspectives in biology, 2011. **3**(6): p. a001727.
3. Williams, M.E., J. de Wit, and A. Ghosh, *Molecular mechanisms of synaptic specificity in developing neural circuits.* Neuron, 2010. **68**(1): p. 9-18.
4. Cragg, B.G., *The development of synapses in the visual system of the cat.* Journal of Comparative Neurology, 1975. **160**(2): p. 147-166.
5. Attardi, D.G. and R.W. Sperry, *Preferential selection of central pathways by regenerating optic fibers.* Experimental Neurology, 1963. **7**(1): p. 46-64.
6. de Wit, J. and A. Ghosh, *Specification of synaptic connectivity by cell surface interactions.* Nature Reviews Neuroscience, 2016. **17**(1): p. 4-4.
7. Weiner, J.A., J.D. Jontes, and R.W. Burgess, *Introduction to mechanisms of neural circuit formation.* Frontiers in molecular neuroscience, 2013. **6**: p. 12-12.
8. Zhan, X.-L., et al., *Analysis of Dscam Diversity in Regulating Axon Guidance in Drosophila Mushroom Bodies.* Neuron, 2004. **43**(5): p. 673-686.
9. Bruce, F.M., et al., *DSCAM promotes axon fasciculation and growth in the developing optic pathway.* Proceedings of the National Academy of Sciences, 2017. **114**(7): p. 1702.
10. Liu, G., et al., *DSCAM functions as a netrin receptor in commissural axon pathfinding.* Proceedings of the National Academy of Sciences, 2009. **106**(8): p. 2951.
11. Schmucker, D., et al., *Drosophila Dscam Is an Axon Guidance Receptor Exhibiting Extraordinary Molecular Diversity.* Cell, 2000. **101**(6): p. 671-684.
12. Hattori, D., et al., *Dscam-Mediated Cell Recognition Regulates Neural Circuit Formation.* Annual Review of Cell and Developmental Biology, 2008. **24**(1): p. 597-620.
13. Zhu, H., et al., *Dendritic patterning by Dscam and synaptic partner matching in the Drosophila antennal lobe.* Nature Neuroscience, 2006. **9**(3): p. 349-355.
14. Fuerst, P.G., et al., *DSCAM and DSCAML1 function in self-avoidance in multiple cell types in the developing mouse retina.* Neuron, 2009. **64**(4): p. 484-497.
15. Yamagata, M. and J.R. Sanes, *Dscam and Sidekick proteins direct lamina-specific synaptic connections in vertebrate retina.* Nature, 2008. **451**(7177): p. 465-469.
16. Simmons, A.B., et al., *DSCAM-mediated control of dendritic and axonal arbor outgrowth enforces tiling and inhibits synaptic plasticity.* Proceedings of the National Academy of Sciences, 2017. **114**(47): p. E10224.
17. Huberman, A.D., M.B. Feller, and B. Chapman, *Mechanisms Underlying Development of Visual Maps and Receptive Fields.* Annual Review of Neuroscience, 2008. **31**(1): p. 479-509.

18. Liu, Z., A.S. Hamodi, and K.G. Pratt, *Early development and function of the Xenopus tadpole retinotectal circuit.* Current Opinion in Neurobiology, 2016. **41**: p. 17-23.
19. Pratt, K.G. and A.S. Khakhalin, *Modeling human neurodevelopmental disorders in the Xenopus tadpole: from mechanisms to therapeutic targets.* Disease Models & Mechanisms, 2013. **6**(5): p. 1057.
20. Cline, H.T. and D. Kelly, *Xenopus as an experimental system for developmental neuroscience: Introduction to a special issue.* Developmental Neurobiology, 2012. **72**(4): p. 463-464.
21. Cohen-Cory, S. and S.E. Fraser, *Effects of brain-derived neurotrophic factor on optic axon branching and remodelling in vivo.* Nature, 1995. **378**(6553): p. 192-196.
22. Raper, J. and C. Mason, *Cellular strategies of axonal pathfinding.* Cold Spring Harbor perspectives in biology, 2010. **2**(9): p. a001933-a001933.
23. van Horck, F.P.G., C. Weinl, and C.E. Holt, *Retinal axon guidance: novel mechanisms for steering.* Current Opinion in Neurobiology, 2004. **14**(1): p. 61-66.
24. Wang, L. and T. Marquardt, *What axons tell each other: axon–axon signaling in nerve and circuit assembly.* Current Opinion in Neurobiology, 2013. **23**(6): p. 974-982.
25. Feldheim, D.A. and D.D.M. O'Leary, *Visual Map Development: Bidirectional Signaling, Bifunctional Guidance Molecules, and Competition.* Cold Spring Harbor Perspectives in Biology, 2010. **2**(11).
26. Luo, L. and J.G. Flanagan, *Development of Continuous and Discrete Neural Maps.* Neuron, 2007. **56**(2): p. 284-300.
27. Sakaguchi, D.S. and R.K. Murphey, *Map formation in the developing Xenopus retinotectal system: an examination of ganglion cell terminal arborizations.* The Journal of Neuroscience, 1985. **5**(12): p. 3228.
28. Lin, A.C. and C.E. Holt, *Topographic Maps: Molecular Mechanisms*, in *Encyclopedia of Neuroscience*, L.R. Squire, Editor. 2009, Academic Press: Oxford. p. 1019-1027.
29. Holt, C.E., *Does timing of axon outgrowth influence initial retinotectal topography in Xenopus?* The Journal of Neuroscience, 1984. **4**(4): p. 1130.
30. Hollyfield, J.G., *Differential growth of the neural retina inXenopus laevis larvae.* Developmental Biology, 1971. **24**(2): p. 264-286.
31. Cima, C. and P. Grant, *Development of the optic nerve in Xenopus laevis</em&gt.* Journal of Embryology and Experimental Morphology, 1982. **72**(1): p. 251.
32. Dickson, B.J., *Molecular Mechanisms of Axon Guidance.* Science, 2002. **298**(5600): p. 1959.
33. Feldheim, D.A., et al., *Genetic Analysis of Ephrin-A2 and Ephrin-A5 Shows Their Requirement in Multiple Aspects of Retinocollicular Mapping.* Neuron, 2000. **25**(3): p. 563-574.
34. Cang, J. and D.A. Feldheim, *Developmental Mechanisms of Topographic Map Formation and Alignment.* Annual Review of Neuroscience, 2013. **36**(1): p. 51-77.

35. Demyanenko, G.P. and P.F. Maness, *The L1 Cell Adhesion Molecule Is Essential for Topographic Mapping of Retinal Axons.* The Journal of Neuroscience, 2003. **23**(2): p. 530.
36. Hörnberg, H., et al., *Hermes Regulates Axon Sorting in the Optic Tract by Post-Trancriptional Regulation of Neuropilin 1.* The Journal of Neuroscience, 2016. **36**(50): p. 12697.
37. Scholes, J.H., *Nerve fibre topography in the retinal projection to the tectum.* Nature, 1979. **278**(5705): p. 620-624.
38. Fawcett, J.W., et al., *Fibre order in the normal Xenopus optic tract, near the chiasma.* Journal of Embryology and Experimental Morphology, 1984. **83**(1): p. 1.
39. Stuermer, C.A., *Retinotopic organization of the developing retinotectal projection in the zebrafish embryo.* The Journal of Neuroscience, 1988. **8**(12): p. 4513.
40. Plas, D.T., J.E. Lopez, and M.C. Crair, *Pretarget sorting of retinocollicular axons in the mouse.* Journal of Comparative Neurology, 2005. **491**(4): p. 305-319.
41. Wojtowicz, W.M., et al., *Alternative Splicing of Drosophila Dscam Generates Axon Guidance Receptors that Exhibit Isoform-Specific Homophilic Binding.* Cell, 2004. **118**(5): p. 619-633.
42. Blank, M., et al., *The Down Syndrome Critical Region Regulates Retinogeniculate Refinement.* The Journal of Neuroscience, 2011. **31**(15): p. 5764.
43. Barlow, G.M., et al., *Mammalian DSCAMs: roles in the development of the spinal cord, cortex, and cerebellum?* Biochemical and Biophysical Research Communications, 2002. **293**(3): p. 881-891.
44. Aberle, H., *Axon Guidance and Collective Cell Migration by Substrate-Derived Attractants.* Frontiers in molecular neuroscience, 2019. **12**: p. 148-148.
45. Katow, H., et al., *Regulation of axon arborization pattern in the developing chick ciliary ganglion: Possible involvement of caspase 3.* Development, Growth & Differentiation, 2017. **59**(3): p. 115-128.
46. O'Rourke, N.A. and S.E. Fraser, *Dynamic changes in optic fiber terminal arbors lead to retinotopic map formation: An in vivo confocal microscopic study.* Neuron, 1990. **5**(2): p. 159-171.
47. Ruthazer, E.S., C.J. Akerman, and H.T. Cline, *Control of Axon Branch Dynamics by Correlated Activity in Vivo.* Science, 2003. **301**(5629): p. 66.
48. Lom, B., et al., *Local and Target-Derived Brain-Derived Neurotrophic Factor Exert Opposing Effects on the Dendritic Arborization of Retinal Ganglion Cells In Vivo.* The Journal of Neuroscience, 2002. **22**(17): p. 7639.
49. Gibson, D.A. and L. Ma, *Developmental regulation of axon branching in the vertebrate nervous system.* Development, 2011. **138**(2): p. 183.
50. Yates, P.A., et al., *Topographic-Specific Axon Branching Controlled by Ephrin-As Is the Critical Event in Retinotectal Map Development.* The Journal of Neuroscience, 2001. **21**(21): p. 8548.
51. Rashid, T., et al., *Opposing Gradients of Ephrin-As and EphA7 in the Superior Colliculus Are Essential for Topographic Mapping in the Mammalian Visual System.* Neuron, 2005. **47**(1): p. 57-69.

52. Shirkey, N.J., et al., *Dynamic responses of Xenopus retinal ganglion cell axon growth cones to netrin-1 as they innervate their in vivo target.* Developmental Neurobiology, 2012. **72**(4): p. 628-648.
53. Manitt, C., et al., *Netrin Participates in the Development of Retinotectal Synaptic Connectivity by Modulating Axon Arborization and Synapse Formation in the Developing Brain.* The Journal of Neuroscience, 2009. **29**(36): p. 11065.
54. Ly, A., et al., *DSCAM Is a Netrin Receptor that Collaborates with DCC in Mediating Turning Responses to Netrin-1.* Cell, 2008. **133**(7): p. 1241-1254.
55. Andrews, G.L., et al., *Dscam guides embryonic axons by Netrin-dependent and -independent functions.* Development, 2008. **135**(23): p. 3839.
56. Purohit, A.A., et al., *Down Syndrome Cell Adhesion Molecule (DSCAM) Associates with Uncoordinated-5C (UNC5C) in Netrin-1-mediated Growth Cone Collapse.* Journal of Biological Chemistry, 2012. **287**(32): p. 27126-27138.
57. Palmesino, E., et al., *Genetic Analysis of DSCAM's Role as a Netrin-1 Receptor in Vertebrates.* The Journal of Neuroscience, 2012. **32**(2): p. 411.
58. Arikkath, J., *Molecular mechanisms of dendrite morphogenesis.* Frontiers in cellular neuroscience, 2012. **6**: p. 61-61.
59. Emoto, K., *Signaling mechanisms that coordinate the development and maintenance of dendritic fields.* Current Opinion in Neurobiology, 2012. **22**(5): p. 805-811.
60. Jan, Y.-N. and L.Y. Jan, *Branching out: mechanisms of dendritic arborization.* Nature Reviews Neuroscience, 2010. **11**(5): p. 316-328.
61. Alsina, B., T. Vu, and S. Cohen-Cory, *Visualizing synapse formation in arborizing optic axons in vivo: dynamics and modulation by BDNF.* Nature Neuroscience, 2001. **4**(11): p. 1093-1101.
62. Cline, H.T., *Dendritic arbor development and synaptogenesis.* Current Opinion in Neurobiology, 2001. **11**(1): p. 118-126.
63. Nagel, A.N., et al., *Netrin-1 directs dendritic growth and connectivity of vertebrate central neurons in vivo.* Neural Development, 2015. **10**(1): p. 14.
64. Lawrence Zipursky, S. and W.B. Grueber, *The Molecular Basis of Self-Avoidance.* Annual Review of Neuroscience, 2013. **36**(1): p. 547-568.
65. Millard, S.S. and S.L. Zipursky, *Dscam-mediated repulsion controls tiling and self-avoidance.* Current Opinion in Neurobiology, 2008. **18**(1): p. 84-89.
66. Grueber, W.B. and A. Sagasti, *Self-avoidance and Tiling: Mechanisms of Dendrite and Axon Spacing.* Cold Spring Harbor Perspectives in Biology, 2010. **2**(9).
67. Millard, S.S., et al., *Dscam2 mediates axonal tiling in the Drosophila visual system.* Nature, 2007. **447**(7145): p. 720-724.
68. Kimura, H., et al., *Potential dual molecular interaction of the Drosophila 7-pass transmembrane cadherin Flamingo in dendritic morphogenesis.* Journal of Cell Science, 2006. **119**(6): p. 1118.
69. Hattori, D., et al., *Dscam diversity is essential for neuronal wiring and self-recognition.* Nature, 2007. **449**(7159): p. 223-227.
70. Matthews, B.J., et al., *Dendrite Self-Avoidance Is Controlled by Dscam.* Cell, 2007. **129**(3): p. 593-604.

71. Meijers, R., et al., *Structural basis of Dscam isoform specificity.* Nature, 2007. **449**(7161): p. 487-491.
72. Wojtowicz, W.M., et al., *A Vast Repertoire of Dscam Binding Specificities Arises from Modular Interactions of Variable Ig Domains.* Cell, 2007. **130**(6): p. 1134-1145.
73. Soba, P., et al., *Drosophila sensory neurons require Dscam for dendritic self-avoidance and proper dendritic field organization.* Neuron, 2007. **54**(3): p. 403-416.
74. Agarwala, K.L., et al., *Dscam is associated with axonal and dendritic features of neuronal cells.* Journal of Neuroscience Research, 2001. **66**(3): p. 337-346.
75. Garrett, A.M., et al., *DSCAM promotes self-avoidance in the developing mouse retina by masking the functions of cadherin superfamily members.* Proceedings of the National Academy of Sciences, 2018. **115**(43): p. E10216.
76. Robles, E., S. Smith, and H. Baier, *Characterization of Genetically Targeted Neuron Types in the Zebrafish Optic Tectum.* Frontiers in Neural Circuits, 2011. **5**(1).
77. Robles, E., A. Filosa, and H. Baier, *Precise Lamination of Retinal Axons Generates Multiple Parallel Input Pathways in the Tectum.* The Journal of Neuroscience, 2013. **33**(11): p. 5027.
78. Giagtzoglou, N., C.V. Ly, and H.J. Bellen, *Cell Adhesion, the Backbone of the Synapse: "Vertebrate" and "Invertebrate" Perspectives.* Cold Spring Harbor Perspectives in Biology, 2009. **1**(4).
79. Robles, E., E. Laurell, and H. Baier, *The Retinal Projectome Reveals Brain-Area-Specific Visual Representations Generated by Ganglion Cell Diversity.* Current Biology, 2014. **24**(18): p. 2085-2096.
80. Dong, W., et al., *Visual avoidance in Xenopus tadpoles is correlated with the maturation of visual responses in the optic tectum.* Journal of neurophysiology, 2009. **101**(2): p. 803-815.
81. Gurdon, J.B., *Normal table of Xenopus laevis (Daudin): edited by P.D. Nieuwkoop and J. Faber Garland Publishing, 1994. $55.00 pbk (252 pages) ISBN 0 8153 1896 0.* Trends in Genetics, 1995. **11**(10): p. 418.
82. Haas, K., et al., *Targeted electroporation in Xenopus tadpoles in vivo – from single cells to the entire brain.* Differentiation, 2002. **70**(4): p. 148-154.
83. Marshak, S., et al., *Cell-Autonomous Alterations in Dendritic Arbor Morphology and Connectivity Induced by Overexpression of MeCP2 in Xenopus Central Neurons In Vivo.* PLOS ONE, 2012. **7**(3): p. e33153.
84. Marshak, S., et al., *Cell-Autonomous TrkB Signaling in Presynaptic Retinal Ganglion Cells Mediates Axon Arbor Growth and Synapse Maturation during the Establishment of Retinotectal Synaptic Connectivity.* The Journal of Neuroscience, 2007. **27**(10): p. 2444.
85. Fuerst, P.G., et al., *Neurite arborization and mosaic spacing in the mouse retina require DSCAM.* Nature, 2008. **451**(7177): p. 470-474.

86. McGinn, T.E., et al., *Restoration of Dendritic Complexity, Functional Connectivity, and Diversity of Regenerated Retinal Bipolar Neurons in Adult Zebrafish.* The Journal of Neuroscience, 2018. **38**(1): p. 120.
87. Sholl, D.A., *Dendritic organization in the neurons of the visual and motor cortices of the cat.* Journal of anatomy, 1953. **87**(4): p. 387-406.
88. Hughes, M.E., et al., *Homophilic Dscam Interactions Control Complex Dendrite Morphogenesis.* Neuron, 2007. **54**(3): p. 417-427.
89. Myatt, D.R., et al., *Neuromantic - from semi-manual to semi-automatic reconstruction of neuron morphology.* Frontiers in neuroinformatics, 2012. **6**: p. 4-4.
90. Lal Agarwala, K., et al., *Cloning and Functional Characterization of DSCAML1, a Novel DSCAM-like Cell Adhesion Molecule That Mediates Homophilic Intercellular Adhesion.* Biochemical and Biophysical Research Communications, 2001. **285**(3): p. 760-772.
91. Agarwala, K.L., et al., *Down syndrome cell adhesion molecule DSCAM mediates homophilic intercellular adhesion.* Molecular Brain Research, 2000. **79**(1): p. 118-126.
92. Cameron, S. and Y. Rao, *Molecular mechanisms of tiling and self-avoidance in neural development.* Molecular Brain, 2010. **3**(1): p. 28.
93. Alves-Sampaio, A., J.A. Troca-Marín, and M.L. Montesinos, *NMDA-Mediated Regulation of DSCAM Dendritic Local Translation Is Lost in a Mouse Model of Down's Syndrome.* The Journal of Neuroscience, 2010. **30**(40): p. 13537.
94. Chakrabarti, L., et al., *Olig1 and Olig2 triplication causes developmental brain defects in Down syndrome.* Nature Neuroscience, 2010. **13**(8): p. 927-934.
95. Sjöström, P.J., et al., *Dendritic Excitability and Synaptic Plasticity.* Physiological Reviews, 2008. **88**(2): p. 769-840.
96. Komendantov, A.O. and G.A. Ascoli, *Dendritic Excitability and Neuronal Morphology as Determinants of Synaptic Efficacy.* Journal of Neurophysiology, 2009. **101**(4): p. 1847-1866.
97. Gunnersen, J.M., et al., *Sez-6 Proteins Affect Dendritic Arborization Patterns and Excitability of Cortical Pyramidal Neurons.* Neuron, 2007. **56**(4): p. 621-639.
98. Reid, C.A., et al., *Reduced dendritic arborization and hyperexcitability of pyramidal neurons in a Scn1b-based model of Dravet syndrome.* Brain, 2014. **137**(6): p. 1701-1715.
99. Peng, Y.-R., et al., *Coordinated Changes in Dendritic Arborization and Synaptic Strength during Neural Circuit Development.* Neuron, 2009. **61**(1): p. 71-84.
100. Li, H.-L., et al., *Dscam Mediates Remodeling of Glutamate Receptors in Aplysia during De Novo and Learning-Related Synapse Formation.* Neuron, 2009. **61**(4): p. 527-540.
101. Souchet, B., et al., *Pharmacological correction of excitation/inhibition imbalance in Down syndrome mouse models.* Frontiers in Behavioral Neuroscience, 2015. **9**(267).

102. Cohen-Cory, S. and S.E. Fraser, *BDNF in the development of the visual system of Xenopus.* Neuron, 1994. **12**(4): p. 747-761.
103. Fuerst, P.G., et al., *Cell autonomy of DSCAM function in retinal development.* Developmental Biology, 2012. **361**(2): p. 326-337.
104. Li, S., et al., *DSCAM Promotes Refinement in the Mouse Retina through Cell Death and Restriction of Exploring Dendrites.* The Journal of Neuroscience, 2015. **35**(14): p. 5640.
105. Fernandes, K.A., et al., *Novel axon projection after stress and degeneration in the Dscam mutant retina.* Molecular and Cellular Neuroscience, 2016. **71**: p. 1-12.
106. Kim, Jung H., et al., *Dscam Expression Levels Determine Presynaptic Arbor Sizes in Drosophila Sensory Neurons.* Neuron, 2013. **78**(5): p. 827-838.
107. He, H., et al., *Cell-intrinsic requirement of Dscam1 isoform diversity for axon collateral formation.* Science, 2014. **344**(6188): p. 1182.
108. Corty, M.M., B.J. Matthews, and W.B. Grueber, *Molecules and mechanisms of dendrite development in <em>Drosophila</em&gt.* Development, 2009. **136**(7): p. 1049.
109. McAllister, A.K., *Cellular and Molecular Mechanisms of Dendrite Growth.* Cerebral Cortex, 2000. **10**(10): p. 963-973.
110. Puram, S.V. and A. Bonni, *Cell-intrinsic drivers of dendrite morphogenesis.* Development, 2013. **140**(23): p. 4657.
111. Jan, Y.-N. and L.Y. Jan, *The Control of Dendrite Development.* Neuron, 2003. **40**(2): p. 229-242.
112. Shewan, D., et al., *Age-related changes underlie switch in netrin-1 responsiveness as growth cones advance along visual pathway.* Nature Neuroscience, 2002. **5**(10): p. 955-962.
113. Affaticati, P., et al., *X-FaCT: Xenopus-Fast Clearing Technique*, in *Xenopus: Methods and Protocols*, K. Vleminckx, Editor. 2018, Springer New York: New York, NY. p. 233-241.
114. Santos, R.A., et al., *DSCAM differentially modulates pre- and postsynaptic structural and functional central connectivity during visual system wiring.* Neural development, 2018. **13**(1): p. 22-22.
115. Costa, E.C., et al., *Optical clearing methods: An overview of the techniques used for the imaging of 3D spheroids.* Biotechnology and Bioengineering, 2019. **116**(10): p. 2742-2763.
116. Feuchtinger, A., A. Walch, and M. Dobosz, *Deep tissue imaging: a review from a preclinical cancer research perspective.* Histochemistry and Cell Biology, 2016. **146**(6): p. 781-806.
117. Jinyoung, S., et al., *Clearing and Labeling Techniques for Large-Scale Biological Tissues.* Molecules and Cells, 2016. **39**(6): p. 439-446.
118. Susaki, Etsuo A. and Hiroki R. Ueda, *Whole-body and Whole-Organ Clearing and Imaging Techniques with Single-Cell Resolution: Toward Organism-Level Systems Biology in Mammals.* Cell Chemical Biology, 2016. **23**(1): p. 137-157.

119. Huang, Y.-B., et al., *In Vivo Study of Dynamics and Stability of Dendritic Spines on Olfactory Bulb Interneurons in Xenopus laevis Tadpoles.* PLOS ONE, 2015. **10**(10): p. e0140752.
120. Erdogan, B., P.T. Ebbert, and L.A. Lowery, *Using Xenopus laevis retinal and spinal neurons to study mechanisms of axon guidance in vivo and in vitro.* Seminars in cell & developmental biology, 2016. **51**: p. 64-72.
121. Bollmann, J.H. and F. Engert, *Subcellular topography of visually driven dendritic activity in the vertebrate visual system.* Neuron, 2009. **61**(6): p. 895-905.
122. DeMarco, E., et al., *Neuron types in the zebrafish optic tectum labeled by an id2b transgene.* Journal of Comparative Neurology, 2020. **528**(7): p. 1173-1188.
123. Schmucker, D. and B. Chen, *Dscam and DSCAM: complex genes in simple animals, complex animals yet simple genes.* Genes & Development, 2009. **23**(2): p. 147-156.
124. Mann, F., et al., *B-type Eph receptors and ephrins induce growth cone collapse through distinct intracellular pathways.* Journal of neurobiology, 2003. **57**(3): p. 323-336.
125. Osterhout, Jessica A., et al., *Birthdate and Outgrowth Timing Predict Cellular Mechanisms of Axon Target Matching in the Developing Visual Pathway.* Cell Reports, 2014. **8**(4): p. 1006-1017.
126. Osterhout, Jessica A., et al., *Cadherin-6 Mediates Axon-Target Matching in a Non-Image-Forming Visual Circuit.* Neuron, 2011. **71**(4): p. 632-639.
127. Mann, F., et al., *Ephrins regulate the formation of terminal axonal arbors during the development of thalamocortical projections.* Development, 2002. **129**(16): p. 3945.
128. Scalia, F., J.R. Currie, and D.A. Feldheim, *Eph/ephrin gradients in the retinotectal system of Rana pipiens: Developmental and adult expression patterns.* Journal of Comparative Neurology, 2009. **514**(1): p. 30-48.
129. Cohen-Cory, S., *The Developing Synapse: Construction and Modulation of Synaptic Structures and Circuits.* Science, 2002. **298**(5594): p. 770.
130. Mizumoto, K. and K. Shen, *Two Wnts instruct topographic synaptic innervation in C. elegans.* Cell reports, 2013. **5**(2): p. 389-396.
131. Bahr, B.A., et al., *Targeting the endocannabinoid system in treating brain disorders.* Expert Opinion on Investigational Drugs, 2006. **15**(4): p. 351-365.
132. Shohami, E., et al., *Endocannabinoids and traumatic brain injury.* British journal of pharmacology, 2011. **163**(7): p. 1402-1410.
133. Tanaka, M., S. Sackett, and Y. Zhang, *Endocannabinoid Modulation of Microglial Phenotypes in Neuropathology.* Frontiers in Neurology, 2020. **11**(87).
134. Hájos, N., et al., *Cannabinoids inhibit hippocampal GABAergic transmission and network oscillations.* European Journal of Neuroscience, 2000. **12**(9): p. 3239-3249.
135. Katona, I., et al., *Distribution of CB1 Cannabinoid Receptors in the Amygdala and their Role in the Control of GABAergic Transmission.* The Journal of Neuroscience, 2001. **21**(23): p. 9506.

136. Hájos, N., C. Ledent, and T.F. Freund, *Novel cannabinoid-sensitive receptor mediates inhibition of glutamatergic synaptic transmission in the hippocampus.* Neuroscience, 2001. **106**(1): p. 1-4.
137. Pertwee, R.G., *Ligands that target cannabinoid receptors in the brain: from THC to anandamide and beyond.* Addiction Biology, 2008. **13**(2): p. 147-159.
138. Maresz, K., et al., *Modulation of the cannabinoid CB2 receptor in microglial cells in response to inflammatory stimuli.* Journal of Neurochemistry, 2005. **95**(2): p. 437-445.
139. Cherry, J.D., J.A. Olschowka, and M.K. O'Banion, *Neuroinflammation and M2 microglia: the good, the bad, and the inflamed.* Journal of Neuroinflammation, 2014. **11**(1): p. 98.
140. Gordon, S., *Alternative activation of macrophages.* Nature Reviews Immunology, 2003. **3**(1): p. 23-35.
141. Paredes, R., et al., *Xenopus: An in vivo model for imaging the inflammatory response following injury and bacterial infection.* Developmental biology, 2015. **408**(2): p. 213-228.
142. Goodbrand, I.A. and R.M. Gaze, *Microglia in tadpoles ofXenopus laevis: Normal distribution and the response to optic nerve injury.* Anatomy and Embryology, 1991. **184**(1): p. 71-82.
143. Pastuhov, S.I., et al., *Endocannabinoid-Goα signalling inhibits axon regeneration in Caenorhabditis elegans by antagonizing Gqα-PKC-JNK signalling.* Nature Communications, 2012. **3**(1): p. 1136.
144. Kha, C.X., et al., *A model for investigating developmental eye repair in Xenopus laevis.* Experimental Eye Research, 2018. **169**: p. 38-47.
145. Kha, C.X., D.J. Guerin, and K.A.-S. Tseng, *Using the Xenopus Developmental Eye Regrowth System to Distinguish the Role of Developmental Versus Regenerative Mechanisms.* Frontiers in Physiology, 2019. **10**(502).

Appendix

7.1. Modulation of Microglial States by Endocannabinoid Signaling

The formation of precise connections throughout the CNS requires many diverse developmental processes that are constructed through a carefully scheduled temporal sequence of events. What were to happen when one of these carefully timed events is perturbed during development? As we have seen in the developing visual system of the Xenopus tadpole, axons exit the retina via the optic nerve, cross the optic chiasm, and project contralaterally to the optic tectum where axons arborize and form selective synaptic connections with tectal partners. Overtime, newer connections are formed and layered over older connections in the tectum [29]. Each step underlying vertebrate visual circuit assembly depends heavily on an array of molecular signals to execute proper construction. Clearly, there is a defined temporal sequence in the construction of neuronal circuits precisely mediated by molecular cues and cellular interactions. Once the events of circuit formation have finished, it would be nearly impossible to recapitulate the temporal and spatial sequence of events that have unfolded throughout development. For these reasons, it becomes apparent how perturbation of these developmental events can be catastrophic and costly by impacting the construction and, most importantly, the overall function of circuits being assembled. The mechanisms underlying self-repair and re-wiring do occur during circuit damage, but these self-repairing mechanisms are not well understood and damaged circuits in the CNS never fully recover. It remains unclear which developmental components are required for

successful repair and whether endogenous developmental mechanisms act similarly or different during self-repair.

Interestingly, endocannabinoids (eCB) have emerged as a compensatory signaling system that responds promptly to acute or chronic injury in the adult brain, which may give us insight to how damaged circuits are self-repaired during development. Traumatic brain injury (TBI) studies have shown that endocannabinoids are elevated in response to brain damage, thus representing a potential compensatory repair mechanism [131]. The effects of TBI results in an accumulation of harmful factors that induces neuronal cell death, neuro-inflammation, and constriction of the cerebral microvasculature system – all of which leads to further secondary damage to the injured tissue (reviewed in Endocannabinoids and traumatic brain injury). The production of eCBs, during the time of injury, are synthesized ‘on-demand’, which subsequently inhibit excitotoxicity that causes cell death, reduce inflammatory cytokines, and counteract vasoconstriction [132]. Endocannabinoid-mediated signaling can also modulate different states of microglial phenotype which, if polarized to the alternative M2 activation state, can further promote anti-inflammatory effects on neuropathological injury [133]. There has been a growing interest in the field to enhance this on-demand action of eCBs for its ability to modulate microglial M2 activation and mitigate brain damage after TBI. Exploiting this signaling pathway has been thought of as a strategy to promote neuroprotective mechanisms and endogenous repair signaling during the events of injury. Active research involving TBI has given us insight to eCB signaling functions in

the damaged adult vertebrate brain, but many key questions still remain unanswered. Surprisingly, there is currently only one study published using C. elegans as a regenerative model to explore eCB signaling functions in circuit injury and repair. By using more robust developmental models such as the vertebrate Xenopus tadpole, we can further understand in vivo the underlying molecular and cellular mechanisms driven by eCB signaling that not only mediates neuroprotective effects on damaged circuits, but also examine and interweave eCB signaling across multiple physiological functions involving microglia activation states and regenerative processes. For future directions, I will explain in the following sections the current projects we are working on in the lab addressing (1) how eCB modulates microglial phenotypes during circuit injury and (2) how eCB signaling modulates re-wiring and regeneration of damaged circuits.

The eCB system is comprised of two canonical G-protein-coupled receptors, referred as cannabinoid receptors type 1 (CB1) and type 2 (CB2). Neuronal CB1 receptor are largely localized pre-synaptically on GABAergic interneurons and glutamatergic neurons [132, 134-136], whereas CB2 receptors are abundantly expressed on resident inflammatory cells within the CNS, mostly on microglia and dendritic cells [137, 138]. The primary endogenous ligands produced in the brain are N-arachidonoyl-ethanolamine (anandamide) and 2-arachidonoyl-glycerol (2-AG); these are the most studied ligands and are known to activate both CB1 and CB2 receptors [132]. Anabolic and catabolic enzymes are also present and are key mediators that regulate anandamide and 2-AG levels. Throughout the last two decades, research has studied

the expression and function of eCBs and their respective receptors on neurons, astrocytes, microglia and the cerebrovasculature throughout the brain. These studies have given us detailed insight to the role of eCBs in multiple physiological functions, but several mechanisms remain unclear specifically in the context of neuronal injury and how eCB signaling modulates microglial activation states.

In response to external factors produced from neuropathological injury, homeostatic (M0) microglia undergo morphological and functional changes either into two different states: the classical (M1) activation state which secretes pro-inflammatory cytokines and reactive oxygen species, while the second is the state of alternative (M2) activation which presumably takes on an anti-inflammatory phenotype involved in clearing debris, repairing neuronal tissue, and resolving neuroinflammation [139, 140]. Typically, the role of M1 microglial cells is to recognize foreign antigens and produce reactive oxygen species to eliminate intracellular pathogens. However, during the events of traumatic injury or neurodegenerative diseases, prolonged production of pro-inflammatory factors by M1 microglia, that are used normally to eliminate invasive pathogens, can cause detrimental damage on neuronal cells. Dying cells, subsequently, release more toxic stimulatory factors, which further exacerbates pro-inflammatory effects. It has been suggested that in order to halt chronic pathological conditions caused by injury, modulating and polarizing microglia towards the alternative activation (M2) state is absolutely crucial. The molecular mechanisms controlling the polarization of microglia activation states have yet to be established. A comprehensive review by Yumin Zhang

and colleagues has hypothesized that CB2 receptor mediated signaling polarizes the expression of microglia genes from neuroinflammatory genes to neuroprotective (M2-type) and homeostatic (M0-type) genes – which can facilitate therapeutic functionality (reviewed in emerging functions of endocannabinoid signaling during CNS development). The authors note that current research has been limited to gene or protein analyses and immunohistology work that provide a brief “snapshot” of microglial activation state. Tracking individual microglia in vivo and in real time as activation states are alternated during injury, while characterizing eCB signaling, would be a powerful approach to observe underlying events that were not seen in prior studies.

For current on-going projects in the lab, I have been using *Xenopus* transgenic larvae that express GFP under the control of a *mpeg1* promoter, which is normally a transgene that directs macrophage-lineage expression in zebrafish [141]. Using this transgenic model with in-vivo confocal time-lapse imaging allows our lab to investigate the behavior of macrophage-type cells in response to injury throughout the whole brain of the Xenopus tadpole (Fig 6.1D), while also characterizing the effects of eCB signaling manipulation. We can analyze the distribution, motility and migratory behavior in response to neuronal injury. I have been performing an optic nerve injury on Xenopus tadpoles that models a previous experimental study performed by Goodbrand and Gaze [142]. The authors found that microglia, stained with a monoclonal antibody, are sparsely but widely distributed throughout the retina, optic nerve, diencephalon and mesencephalon in uninjured pre-metamorphic Xenopus tadpoles staged at 54/56. After

optic nerve injury (either by crushing or cutting the optic nerve, or removing the eye), an extensive microglial response is observed along the optic pathway. Within 18 hours, the authors observed a drastic increase in microglial cells in the optic tract and the affected tectum. We performed the same optic nerve injury on *mpeg1* developing younger transgenic tadpoles to reiterate findings from the previous study. 24 hours in response to our injury model, we cleared the whole heads of injured tadpoles. We saw an increase in the number of GFP-labeled macrophage-type cells at the tectum contralateral to where the optic nerve was injured (as shown in Fig 6.1B, C) compared to uninjured controls (Fig 6.1A)

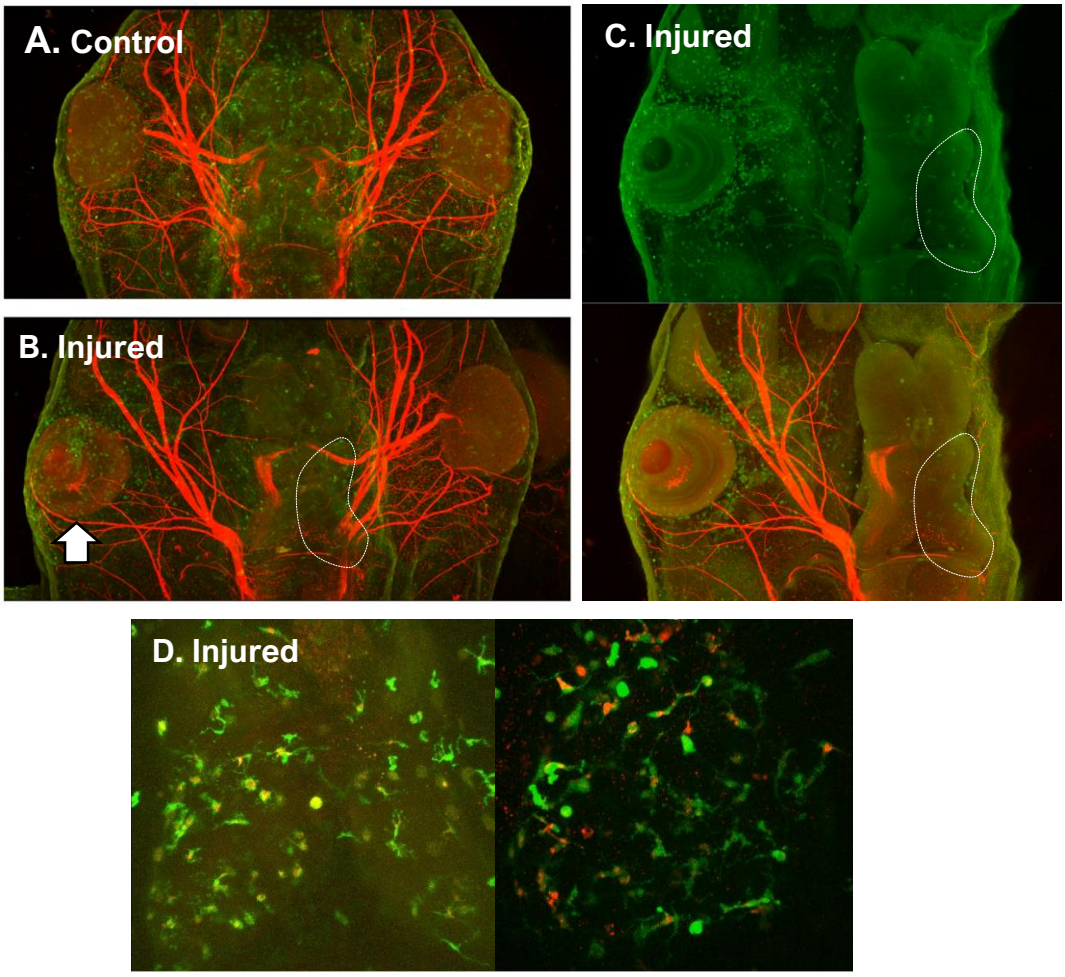

Figure 7.1. Transgenic Xenopus embryos expressing GFP under the control of a mpeg1 promoter, a transgene that is exclusively expressed in zebrafish, were cleared using X-Fact and stained with anti-GFP (green) and 3A10 anti-neurofilament (red). A. Control (uninjured): retinal axons from both eyes project to both hemispheres of the tectum. B. Injured: retinal axons from the injured eye (white arrow) are missing and do not project to the contralateral tectum (white dashed line). C. Injured: Individual z-stack of injured animals. The tectal hemisphere contralateral to the injured eye shows an increase macrophage-type cells (white dashed line) relative to the uninjured ipsilateral tectal side. Note that the contralateral side is also missing retinal axon arbors (bottom panel). D. In Vivo imaging of macrophage-cell types using confocal microscopy, at different magnifications (20x left) and (40x right). We can observe the motility of cells in response to injury.

Future experiments in the lab are working to confirm the identity of these cells labeled in these transgenic lines. For current ongoing projects in the lab, we are in the process of characterizing the activation states of these cells in response to injury and manipulation of eCB signaling. We are manipulating eCB signaling in the developing tadpoles by supplementing tadpole rearing solutions with exogenous eCB ligands, or with anabolic or catabolic enzymes that alter endogenous eCB ligands or using antagonists block CB1 or CB2 receptors. Alternatively, we can treat tadpoles with these drugs by directly injecting the drug solution into the tectum and observe direct changes on macrophage morphology, but direct acute treatments can be misleading since the act of delivering the drug directly into the tectum is an invasive injury that could partly activate an inflammatory response in and of itself. It is interesting to note that Goodbrand and Gaze observed that microglia respond promptly to optic nerve injury in *Xenopus* tadpoles and this response peaks just before regenerating optic nerve axons enter the brain. By the time retinotectal projections are re-established, microglial response is diminished. The authors suggest that the timing of microglial response could play a major factor in facilitating regeneration. I will explain in the next section how injury and self-repair/ regeneration are intertwining events that are closely mediated by eCB signaling and microglial state activation.

7.2. Endocannabinoid Signaling in Circuit Rewiring and Regeneration

In mammals, anandamide is produced locally and transiently in response to pathological conditions during injury. Elevated anandamide levels in TBI models have been

characterized as a mechanism to protect nerve cells and alleviate neuroinflammation. Interestingly, one published research using C. elegans to study neuronal regeneration, showed that damaging axons elevated anandamide levels which, in turn, transiently inhibits axon regeneration during the primary stage of healing [143]. The authors of this particular paper found that AEA regulates axon regeneration via Goα-dependent signaling and suggest that G-protein coupled anandamide receptors could be another mechanism mediating neuronal regeneration. Based on these findings, it is possible to further test how eCB signaling, specifically with great interest focused on anandamide, modulates axon regeneration in vertebrate models. The current optic nerve injury model we are using in the Xenopus tadpole can also be used to explore axon regeneration and tissue repair. Remarkable findings published from the lab of Dr. Kelly Ai-sun Tseng have demonstrated that Xenopus embryos, at a specific stage, can successfully regrow a functional eye that is morphologically indistinguishable from an age-matched control eye [144, 145]. Their model establishes a platform to define molecular mechanisms mediating axon repair and further characterize eCB signaling during tissue regeneration. Potential findings from this new avenue of research can provide novel mechanisms of CNS regeneration, which is quite limited compared to the regenerative capacity of the peripheral nervous system. Nonetheless, this new aspect of research would greatly aid in the development of therapeutic interventions to enhance regeneration and modulate plasticity following the events of CNS injury.